This is to certify that the

dissertation entitled

The Application of Singular Perturbation Methods to Optimal Control Problems in Flight Mechanics

presented by

Yung-Nam, Hu

has been accepted towards fulfillment
of the requirements for

Ph.D. degree in Systems Science

Hassan Khalil
Major professor

Date September 17, 1986

THE APPLICATION OF SINGULAR PERTURBATION METHODS TO OPTIMAL CONTROL PROBLEMS IN FLIGHT MECHANICS

BY

YUNG-NAN HU

A DISSERTATION

Submitted to
Michigan State Uinversity
in partial fulfillment of the requirements
for the degree of

DOCTOR OF PHILOSOPHY

Department of Electrical Engineering and
Systems Science

1986

ABSTRACT

THE APPLICATION OF SINGULAR PERTURBATION METHODS
TO OPTIMAL CONTROL PROBLEMS
IN FLIGHT MECHANICS

BY

YUNG-NAN HU

The use of singular perturbation methods in performance optimization problems in flight mechanics is investigated. The thesis addresses three fundamental issues: modeling of flight mechanics models in the singularly perturbed form, boundary-layer instability associated with the use of open-loop control, and the steering control problem of moving the state of the system from a given initial state to a given final state while minimizing a cost functional.

A normalization scheme for identifying the time-scale properties of flight mechanics models is presented. Time-scale properties must be identified before solutions can be obtained using the singular perturbation method. It is shown that this new scheme can rationalize identifying the flight vehicle's dynamic equations in a singularly perturbed form.

The use of singular perturbation methods in airplane performance optimization is evaluated. The evaluation is based on a study of the minimum time interception problem using F-4 aerodynamic and propulsion data as a base line. Emphasis is placed on the boundary-layer instability problem for real-time, auto-pilot implementation. A feedback stabilization scheme is

proposed to circumvent this instability problem.

In order to steer the state of a singularly perturbed system from a given initial state to a given final state, while minimizing a cost functional, a composite control strategy is developed. The composite control comprises three components: a reduced control and two boundary-layer controls. The boundary-layer controls do not optimize cost functionals. It is shown that application of this composite control results in a final state which is $O(\epsilon)$ close to the desired state. Moreover, the cost under the composite control is $O(\epsilon)$ close to the optimal cost of the reduced control problem. Particular attention is given to the minimum time-to-climb problem of an aircraft in a vertical plane.

ACKNOWLEDGEMENTS

I want to express my deep gratitudes to Dr. Hassan Khalil, my thesis advisor, for all his patience, guidance, and encourgement during the course of my research. His expert advice, useful insight, and stimulating discussions made this work possible.

I would like to thank my committee members, Dr. R. Schlueter, Dr. R. O. Barr, Dr. L. Tummala and Dr. R. O. Hill for their help and valuable suggestions.

To my wife who has constantly supported me with her love through my research period, I would like to express my deep appreciation.

TABLE OF CONTENTS

page

LIST OF SYMBOLS

Only basic conventional symbols are listed. Other symbols used in the monograph are defined during the presentation of the material.

c	Specific fuel consumption
C_D	Drag coefficient
C_{D_0}	Zeroth-lift drag coefficient
C_L	Lift coefficient
$C_{L\alpha}$	Lift curve slope
D	Drag force
D_L	Drag due to lift divided by weight
D_0	Zero-lift drag divided by weight
E	Specific energy
g	Acceleration of the gravity
h	Altitude
H	Hamiltonian function
J	Performance index; Jacobian matrix

L Lift force

m Mass of the vehicle

M Mach no.

n Load factor

r Radial distance from center of the earth; turning radius

s Reference area

t time, sec

u Control

T Thrust

V Speed

W Weight of vehicle

X, Y, Z Cartesian coordinate

x, y, z Cartesian coordinate

GREEK SYMBOLS

α	Angle of attack
α_1	Thrust angle of attack
β	Bank angle
γ	Flight path angle
θ	Longitude; dimensionless time
λ	Costate function
ς	Difference between thrust and drag per unit weight
ρ	Density of atmosphere, slug/ft^3
τ	Initial time stretch transformation
σ	Terminal time stretch transformation
ϕ	Latitude
ψ	Heading angle
ω	Angular velocity
Ω	Angular velocity
ϵ	Small "parastic" parameter
η	Induced drag parameter, rad^{-1}
α_L	Linear feedback stabilization control
α_N	Nonlinear feedback stabilization control
χ	Azimuth angle

SUBSCRIPTS

app Approximate solution by singular perturbation methods (SPT)

N Normalizing reference data

max Normalizing reference data (maximum reference data); maximum value

typ Normalizing reference data (typical reference data); region of interest

o Initial condition

f Terminal condition

SUPERSCRIPTS

o Reduced (slow) solution

~ Normalized variable

il Inner (left) boundary layer

ir Inner (right) boundary layer

LIST OF TABLES

LIST OF FIGURES

page

I. INTRODUCTION

Many problems in science and technology require choosing the best (or the optimal) solution among all the possible solutions. In this second half of our present century one of the most challenging and fascinating optimization problems is the analysis of optimal space trajectories. It consists of finding the best trajectory, in some sense, for the motion of a vehicle in a three-dimensional space. A general optimization problem in three-dimensional atmospheric flight is a difficult problem to solve. Realistic description of physical plants to be controlled usually result in high-order mathematical models. A straightforward application of the maximum principle always leads to a two-point boundary value problem involving several arbitrary parameters. Optimal control design for high-order systems is computationally cumbersome not only because of high-order but also because such systems invariably exhibit simultaneous slow and fast dynamics which are described by "stiff" differential equations. Many of the quasi-steady-state approximations made in the analysis of transport aircraft and other low-performance vehicles are not valid for the highly dynamic maneuvers typical of high-performance military aircraft. Up to a recent time, to display explicity the characteristics of the optimal controls, the different optimization problems considered were reduced order problems. A reduced order model involves less variables and renders the solution to the problem more manageable. Any high order problem would require pure numerical technique for its solution and the results obtained were restricted to a particular set of end conditions for a specified aircraft model.

Experience in actual flights, as well as comparison between various solutions in the analysis of the optimal control problem considered, often display the fact that the improvement in performance is minimal when the exact optimal trajectory is compared with a suboptimal one obtained by a simple analysis. A simple analysis, if properly carried out, has the added advantage that the resulting solution obtained is close to the optimal solution and hence can be used as a first guess reference solution in any iterative procedure. A simple analysis for a complex problem can be obtained in various ways depending on the physical characteristics of the problem, but the ultimate objective is always to reduce the order of the problem. If, in a problem, a certain variable x varies slowly, then the steady-state approximation $dx/dt=0$ will provide an equilibrium relation which can be used to eliminate one component of the state vector or one component of the control vector. A more sophisticated approximation would involve a combination of different state variables and the elimination of variables that are insensitive to the optimization process. One such efficient technique is the singular perturbation method and it is the subject of analysis in this thesis.

Singularly perturbed systems and, more generally, multi-time-scale systems, often occur naturally due to the presence of small "parastic" parameters, typically small time constants, masses, etc., multiplying time derivatives or, in more disguised form, due to the presence of large feedback gains and weak coupling. The chief purpose of singular perturbation approach to analysis and design is the alleviation of the high dimensionality and ill-conditioning resulting from the interaction of slow and fast dynamics. The multi-time-scale approach is asymptotic, that is, exact in the limit as the ratio ϵ of the speeds of the slow versus the fast dynamics tends to zero. When ϵ is small, approximations are obtained from reduced-order models in separate time scales.

While singular perturbation methods, a traditional tool of fluid dynamics and nonlinear mechanics, embraces a wide variety of dynamic phenomena possessing slow and fast modes, its assimilation in control theory is recent and rapidly developing. The methods of singular perturbations for initial and boundary value problem approximations and stability were already largely established in the 1960s, when they first became a means for simplified computation of optimal trajectories. Singular perturbation methods also proved useful for the analysis of high-gain feedback systems and the interpretation of other model order reduction techniques. More recently they have been applied to modeling and control of dynamic networks and certain classes of large-scale systems. This versatility of singular perturbation methods is due to their use of time-scale properties which are common to both linear and nonlinear dynamic systems.

The motivation for this thesis has been to deal with trajectory optimization of singularly perturbed systems in atmospheric flight. Time-scale properties must be identified before solutions can be obtained by using singular perturbation methods. The first objective of the present effort is to develop a systematic procedure to obtain a singularly perturbed models in flight mechanics. Auto-pilot implementation of the approximate open loop control obtained using singular perturbations may cause boundary-layer instability when unstable modes are present in the uncontrolled system. The second objective of this thesis is to demonstrate this fact and emphasis is placed on deriving a feedback stabilization scheme to circumvent this instability problem. For the sake of steering the state of a singularly perturbed system from a given initial state to a given final state while minimizing a cost functional, a composite control approach is developed. The composite control is calculated using reduced-order models in different time scales. Thus, a great reduction in the on-board computations is achieved.

A systematic procedure for the identification of time-scale properties of a nonlinear flight mechanics model is first introduced in Chapter II. A normalization scheme is developed; based on this scheme a singularly perturbed flight mechanics model is proposed. This scheme does not require that an "exact" optimal trajectory to be known, the dynamic state equations and the normalizing reference data are the only information required. The application of singular perturbation methods to trajectory optimization problems in flight mechanics is presented in Chapter III. The use of singular perturbation methods for airplane performance optimization is applied to a minimum time-to-climb problem. In this chapter, attention is focused on the boundary-layer instability problem for on-line, auto-pilot implementation. A feedback stabilization scheme is proposed to circumvent this boundary-layer instability problem. In Chapter IV, we develop a composite control approach to steer the state of a singularly perturbed system from a given initial state to a given final state; while minimizing a cost functional. The composite control comprises three components; a reduced control and two boundary-layer control components. The boundary-layer controls do not optimize cost functional as in earlier work. Asymptotic validity of the composite control is established by showing that its application to the singularly perturbed systems results in a final state which is $O(\epsilon)$ close to the desired state, and the cost under this composite control is $O(\epsilon)$ close to the optimal cost of the reduced control problem. Finally, in Chapter V, we apply the composite control strategy to the optimal maneuvers of an aircraft in a vertical plane. The objective of this chapter is to demonstrate the performance of the composite control on a typical problem of interest, namely, the minimum time-to-climb problem.

In this chapter, we present a systematic procedure for the identification time-scale properties of a nonlinear flight mechanics model. A normalization scheme is developed in order to improve the methods currently in use. Based on this scheme, a singularly perturbed flight mechanics model is proposed. The model agrees, generally, with previous time-scale studies of flight mechanics models.

II.1 HISTORICAL SURVEY

Many authors have discussed and illustrated the application of singular perturbation methods [1-7] to the solution of high performance trajectory optimization problems in flight mechanics. The principal advantage cited is that they reduced the order of individual integrations, so the computational burden is significantly reduced. However, several authors like Kelley [2] and Washburn, et al. [7] have observed that there is presently no rigorous and practical method that can cast this complex nonlinear trajectory optimization problem in a singularly perturbed form. For linear systems, analysis of time-scale separation has been discussed by Chow and Kokotovic [8], and by Syrcos and Sannuti [9]. The time-scale analysis of linear systems can be applied to nonlinear systems but the determined properties will only be valid locally. Moreover, linear analysis assumes that an optimal trajectory of the "exact" system is known (about which the linearization is to be performed). For nonlinear systems, Kelley [2] has considered transformations of state variables that reduce system's coupling and expose time-scale characteristics. The transformations involved, however, are given by partial differential equations, making this approach generally impractical for complex systems. Because of the difficulties in the above approaches, almost all singular perturbation analyses of aircraft trajectory optimization have relied on ad hoc methods for the selection of time-scales, based on physical insight and past experience. This procedure has been termed "forced singular perturbations" by Shinar [10].

In order to improve the ad hoc methods, Ardema and Rajan [11] have proposed two methods for the time-scale separation analysis. Both methods require knowledge of the state equations, bounds on the state and control variables and what control problems are of interest.

We develop a new normalization scheme that can rationalize identifying the flight vehicle's dynamic equations in a time-scale separation form, using only normalizing reference data.

II.2 DEVELOPMENT OF THE SEVENTH-ORDER AIRCRAFT MODEL

In this section, we give a brief account of the derivation of the equations of motion that are essential in the study of singularly perturbed models in the next section. We follows Vinh's book [12], where more details can be found. The motion of a vehicle considered as a point mass flying over a sphreical, rotating earth, is defined by [12-14]

$\vec{r}(t)$ - position vector (2.1a)

$\vec{V}(t)$ - velocity vector (2.1b)

$m(t)$ - mass (2.1c)

II. SINGULARLY PERTURBED MODELS IN FLIGHT MECHANICS

The total force of the flight vehicle is

$$\vec{F} = \vec{T} + \vec{A} + m\vec{g} \tag{2.2}$$

where $\vec{T}$ is thrusting force, $\vec{A}$ is aerodynamic force and $m\vec{g}$ is gravitational force. The aerodynamic force can be decomposed into a drag force $\vec{D}$ opposite to the velocity vector $\vec{V}$ and a lift force $\vec{L}$ orthogonal to it.

By Newton's second law, with respect to an inertial system, we obtain the vector equation

$$m \frac{d\vec{V}}{dt} = \vec{F} \tag{2.3}$$

In writing equation (2.3) it is implicitly assumed that the rate of change of mass with time is negligible. This assumption is not explicitly stated in [12]. As it will be seen later on, it is justified since m is much slower than V.

Consider a fixed coordinate system $OX_1Y_1Z_1$ and another system oxyz which is rotating with respect to the fixed system with angular velocity ω. Let B be any arbitrary vector with components B_x, B_y, and B_z along the rotating axes. Then, the time derivative of $\vec{B}$, taken with respect to the fixed system is

$$\frac{d\vec{B}}{dt} = \frac{dB_x}{dt}\vec{i} + \frac{dB_y}{dt}\vec{j} + \frac{dB_z}{dt}\vec{k} + B_x\frac{d\vec{i}}{dt} + B_y\frac{d\vec{j}}{dt} + B_z\frac{d\vec{k}}{dt} \tag{2.4}$$

By Possion's formula, the last three terms on the right-hand side of (2.4) are

$$B_x \frac{d\vec{i}}{dt} + B_y \frac{d\vec{j}}{dt} + B_z \frac{d\vec{k}}{dt} = \vec{\omega} \times \vec{B} \tag{2.5}$$

The first three terms on the right-hand side of(2.4) can be interpreted as the time derivative of the vector $\vec{B}$ if the vector $\vec{i}$, $\vec{j}$, and $\vec{k}$ were constant unit vectors. Hence, it is the time derivative of $\vec{B}$ with respect to the rotating system oxyz. We denote it by

$$\frac{\partial \vec{B}}{\partial t} = \frac{dB_x}{dt} \vec{i} + \frac{dB_y}{dt} \vec{j} + \frac{dB_z}{dt} \vec{k} \tag{2.6}$$

and write (2.4) as

$$\frac{d\vec{B}}{dt} = \frac{\partial \vec{B}}{\partial t} + \vec{\omega} \times \vec{B} \tag{2.7}$$

This is the formula for transforming the time derivative from fixed system to rotating system.

The inertial reference frame $OX_1Y_1Z_1$ is taken such that O is the center of the gravitational field of the spherical earth and the OX_1Y_1 plane is the equatorial plane. The OXYZ reference is fixed with respect to the earth with OZ coinciding with OZ_1. It is assumed that the earth is rotating with constant angular velocity $\vec{\omega}$ directed along the Z-axis.

The vector equation (2.3) is written with respect to the inertial frame. In deriving the equations of motion, we should use the earth-fixed axes OXYZ as the reference frame since it is a convenient base to follow the motion of the vehicle. Hence, putting $\vec{B} = \vec{r}$ in (2.7) and taking its derivative, we have

$$\frac{d\vec{r}}{dt} = \frac{\partial\vec{r}}{\partial t} + \vec{\omega} \times \vec{r} \tag{2.8}$$

and

$$\frac{d\vec{V}}{dt} = \frac{\partial^2\vec{r}}{\partial t^2} + 2\vec{\omega} \times \frac{\partial\vec{r}}{\partial t} + \vec{\omega} \times (\vec{\omega} \times \vec{r}) \tag{2.9}$$

where $\vec{\omega}$ is constant

The vector equation (2.3) now becomes

$$m \frac{\partial^2\vec{r}}{\partial t^2} = \vec{F} - 2m\vec{\omega} \times \frac{\partial\vec{r}}{\partial t} - m\vec{\omega} \times (\vec{\omega} \times \vec{r}) \tag{2.10}$$

For convenience, we change the notation for the time derivative and write this equation as

$$m \frac{d\vec{V}}{dt} = \vec{F} - 2m\vec{\omega} \times \vec{V} - m\vec{\omega} \times (\vec{\omega} \times \vec{r}) \tag{2.11}$$

In this equation, $\vec{V}$ is the velocity of the vehicle with respect to the earth-fixed axes and the time derivative is taken with respect to these axes.

Now, (2.11) and the kinematic equation

$$\frac{d\vec{r}}{dt} = \vec{V} \tag{2.12}$$

constitute the vector equations for the position vector $\vec{r}$ and the velocity vector $\vec{V}$. They are equivalent to six scalar equations, three of which are the kinematic equations and the other three are force equations.

With respect to the earth fixed system OXYZ (Fig.2.1), the position vector $\vec{r}$ is defined by its magnitude r, its longitude θ, measured from X-axis, in the equatorial plane, positively eastward, and it latitude ϕ, measured from the equatorial plane, along a meridian positively northward.

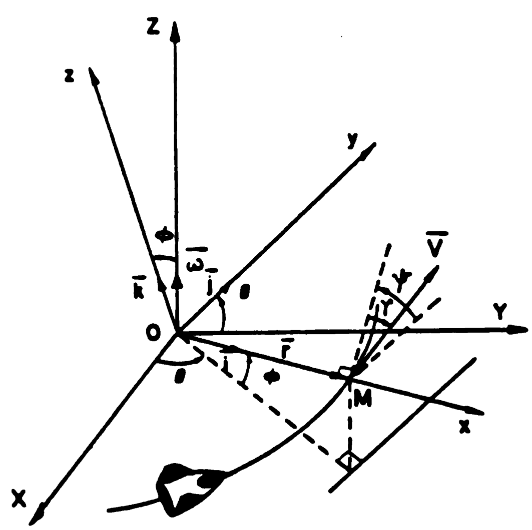

Fig.2. 1 Coordinate systems

Let γ be the angle between the local horizontal plane, that is the plane passing through the vehicle located at the point M and orthogonal to the position vector $\vec{r}$, and the velocity vector $\vec{V}$. The angle γ is termed the flight path angle and is positive when V is above the horizontal plane (Fig.2.2) . Let ψ be the angle between the local parallel of the latitude and the projection of $\vec{V}$ on the horizontal plane (Fig.2.2) . The angle ψ is termed the heading angle and is measured positively in the right handed direction about the X-axis.

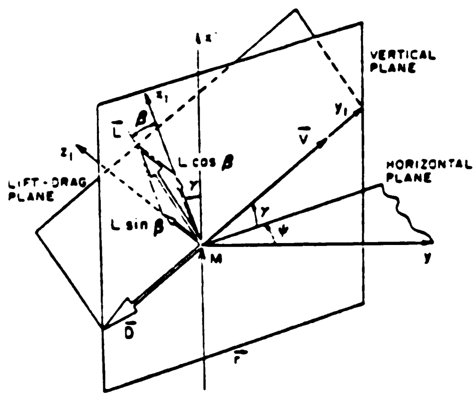

Fig.2.2 Coordinate systems with aerodynamic forces

Let $\vec{i}$, $\vec{j}$, and $\vec{k}$ be the unit vectors along the axes of a rotating system oxyz such that the x-axis is along the position vector (Fig.2.2). We then have

$$\vec{r} = r\vec{i} \tag{2.13}$$

and

$$\vec{V} = (V\mathrm{SIN}\gamma)\vec{i} + (V\mathrm{COS}\gamma\mathrm{COS}\psi)\vec{j} + (V\mathrm{COS}\gamma\mathrm{SIN}\psi)\vec{k} \tag{2.14}$$

We resolve all the vector terms in (2.11) and (2.12) into components along the rotating axes oxyz. In order to take the time derivative of the vectors $\vec{r}$ and $\vec{V}$ in (2.11) and (2.12) with respect to the earth-fixed system OXYZ using their components along the rotating system oxyz, we need to evaluate the angular velocity $\vec{\Omega}$ of the rotating axes. The system Oxyz is obtained from the system OXYZ by a rotation θ about the positive z-axis, followed by a rotation ϕ about the negative y-axis. Hence, the angular velocity $\vec{\Omega}$ of the rotating system Oxyz is given by

$$\vec{\Omega} = (\mathrm{SIN}\phi \frac{d\theta}{dt})\vec{i} - (\frac{d\phi}{dt})\vec{j} + (\mathrm{COS}\phi \frac{d\theta}{dt})\vec{k}$$

We take the derivative of $\vec{r}$ as given by (2.13). Using the Possion's formula for the derivative of $\vec{i}$, and the above expression of $\vec{\Omega}$, we have .

$$\vec{V} = \frac{d\vec{r}}{dt}$$

$$= (\frac{d\gamma}{dt})\vec{i} + \vec{\Omega} \times \vec{i}$$

$$= (\frac{dr}{dt})\vec{i} + (r\mathrm{COS}\phi \ \frac{d\theta}{dt})\vec{j} + (r \ \frac{d\phi}{dt})\vec{k} \tag{2.15}$$

Identifying this equation with (2.14) yields three scalar equations

$$\frac{dr}{dt} = VSIN\gamma \tag{2.16a}$$

$$\frac{d\theta}{dt} = \frac{VCOS\gamma COS\psi}{rCOS\phi} \tag{2.16b}$$

$$\frac{d\phi}{dt} = \frac{VCOS\gamma SIN\psi}{r} \tag{2.16c}$$

These equations are the kinematic equations.

On the other hand, taking the derivative of the velocity vector given by (2.12) and substituting it into the basic vector equation (2.11) yields, after lengthy manipulation and some simplifications [12], the three force equations

$$\frac{dV}{dt} = \frac{1}{m} F_T - gSIN\gamma \tag{2.17a}$$

$$V \frac{d\gamma}{dt} = \frac{1}{m} F_N COS\beta - gCOS\gamma + \frac{V^2}{r} COS\gamma \tag{2.17b}$$

$$V \frac{d\psi}{dt} = \frac{1}{m} \frac{F_N SIN\beta}{COS\gamma} - \frac{V^2}{r} COS\gamma COS\psi \tan\phi \tag{2.17c}$$

where the angle β, which is the angle between the vector $\vec{L}$ and $(\vec{r},\vec{V})$ plane, will be refered to as the roll, or bank angle (Fig.2.2). The term F_T is the component of the combined aerodynamic and propulsive force along the velocity vector and F_N is its component orthogonal to the velocity in the lift-drag plane (Fig.2.3) which are

$$F_T = TCOS(\alpha_1) - D \simeq T - D \tag{2.18a}$$

$$F_N = TSIN(\alpha_1) + L \simeq L \tag{2.18b}$$

where α_1 is the thrust angle of attack , and it is usually small enough to justify the approximations indicated above.

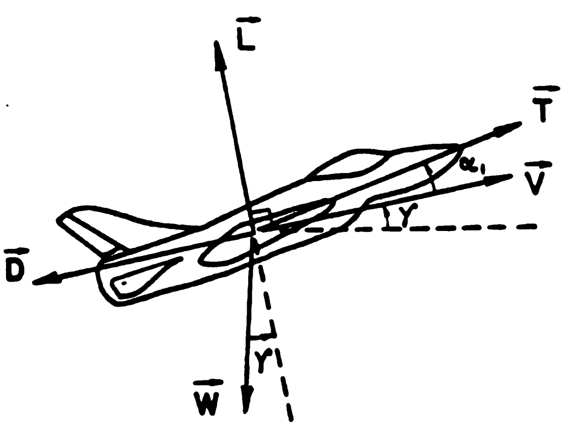

Fig.2.3 Aerodynamic and propulsive forces

For power flight, the mass of the vehicle is varying, and we have the equation for the mass flow rate

$$\frac{dm}{dt} = - \frac{c}{g} T \tag{2.19}$$

where T is the thrust magnitude and c is the specific fuel consumption which is a characteristic of the engine.

The usual dynamic equations used in trajectory analysis of high performance aircraft are considered as a point mass, constant gravity, thrust aligned with velocity and flight over a flat earth (the model we will use in next section). A flat earth model implies that the gravitational field is uniform, that is, the vector g is constant in both magnitude and direction (in spherical earth, g is function of r), therefore, both the longitude θ and the latitude ϕ are small. We can use the same procedure as in the case of a spherical earth to derive the equations of motion when a simple flat earth model is used. We recall the kinematic equations (2.16) and the force equations (2.17). They are the equations to be simplified. The equation for the mass flow rate (2.18) remains unchanged.

First, atmospheric flight operation is conducted in a relatively thin layer of the atmosphere as compared to the radius of the earth. Let h be the altitude of flight, and r_0 be the radius of the earth. Then

$$r = r_0 + h \tag{2.20}$$

and

$$\frac{r_0}{r} = \frac{r_0}{r_0 + h} = 1 - (\frac{h}{r_0}) + (\frac{h}{r_0})^2 - + \ldots\ldots \qquad (2.21)$$

The acceleration of the gravity $g(r)$ in spherical earth is inversely propotional to the square of the distance r, that is

$$g(r) = \frac{g_0 r_0^2}{r^2} \qquad (2.22)$$

where subscript zero denotes the reference level, usually taken as the sea level

Upon substituting (2.21) into (2.22), we have the acceleration of the gravity

$$g = g_0 \; [1 - 2(\frac{r}{r_0}) + 3(\frac{r}{r_0})^2 - + \ldots\ldots\ldots \qquad (2.23)$$

Taking earth radius as $r_0 = 6.37839 \times 10^7$ and $h=9.49742 \times 10^4$ meters, we have the ratio $h/r_0 = 1.489 \times 10^{-3}$. Therefore, it is appropriate to consider g as a constant. Next, in circular motion, the centrifugal equals the gravitational acceleration and we have

$$\frac{V_c^2}{r} = g \qquad (2.24)$$

where V_c is the circular speed along a circular orbit in the vacuum at a distance r.

We consider the ratio

$$\frac{V^2}{V_c^2} = \frac{V^2}{gr} \tag{2.25}$$

When the flight speed is small compared to the orbital speed, we have

$$\frac{V^2}{gr} << 1 \tag{2.26}$$

With this simplification, equation (2.17) becomes

$$\frac{dV}{dt} = \frac{1}{m} F_T - gSIN\gamma \tag{2.27a}$$

$$V \frac{d\gamma}{dt} = \frac{1}{m} F_N COS\beta - gCOS\gamma \tag{2.27b}$$

$$V \frac{d\psi}{dt} = \frac{F_N SIN\gamma}{mCOS\gamma} \tag{2.27c}$$

As we mentioned before, since the gravitartional field is uniform, both the longitude θ and the latitude ϕ are small. Hence, taking $COS\phi = 1$, we can write the last two equations of kinematic equations (2.16) as

$$r_0 \frac{d\theta}{dt} = VCOS\gamma COS\psi(1 - \frac{h}{r_0} + - \ldots\ldots\ldots\ldots\ldots) \tag{2.28a}$$

$$r_0 \frac{d\phi}{dt} = VCOS\gamma SIN\psi(1 - \frac{h}{r_0} + - \ldots\ldots\ldots\ldots\ldots) \tag{2.28b}$$

Neglecting the small term h/r_0 and considering that

$$X = r_0\theta \tag{2.29a}$$

$$Y = r_0\phi \tag{2.29b}$$

$$h = r - r_0 \tag{2.29c}$$

we can write (2.16) as

$$\frac{dX}{dt} = V\cos\gamma\cos\psi \tag{2.30a}$$

$$\frac{dY}{dt} = V\cos\gamma\sin\psi \tag{2.30b}$$

$$\frac{dh}{dt} = V\sin\gamma \tag{2.30c}$$

(2.27) and (2.30) together with (2.19) are the equations for flight over a flat earth.

II.3 SINGULARLY PERTURBED MODEL

In this section, we present a normalization scheme for determining mutiple time-scale properties of the flight mechanics model which was derived in the previous section.

II.3.1 NORMALIZATION SCHEME AND COMPARISION WITH ARDEMA'S RESULTS AND KELLEY'S ASSUMPTIONS

For convenience, we rewrite the equations of motion for flight over a flat earth derived in previous section. They are

$$\frac{dX}{dt} = VCOS\gamma COS\psi \tag{2.31a}$$

$$\frac{dY}{dt} = VCOS\gamma SIN\psi \tag{2.31b}$$

$$\frac{dh}{dt} = VSIN\gamma \tag{2.31c}$$

$$\frac{dV}{dt} = \frac{(T - D)}{m} - gSIN\gamma \tag{2.31d}$$

$$\frac{d\gamma}{dt} = \frac{g}{V} \left(\frac{LCOS\beta}{W} - COS\gamma\right) \tag{2.31e}$$

$$\frac{d\psi}{dt} = \frac{g}{W} \frac{LSIN\beta}{VCOS\gamma} \tag{2.31f}$$

$$\frac{dm}{dt} = - c \frac{T}{g} \tag{2.31g}$$

The new variable, the specific energy E, defined by

$$E = gh + \frac{V^2}{2} \tag{2.32}$$

is often introduced; it can be used in place of either h or V as a state variable in order to get better time-scale separation [15-16]. This fact will be shown later on. From (2.31) and (2.32), the state equation for E is

$$\frac{dE}{dt} = \frac{V}{m} (T(V, h) - D(\alpha, V, h)) \tag{2.33}$$

where T is thrust, $D = 1/2(C_{D_0} + \eta C_{L\alpha}\alpha^2)\rho_0 V^2 se^{-Kh}$ is drag (η is induced drag parameter see [13]) and α is angle of attack.

We introduce the following dimensionless variables

$$\tilde{X} = \frac{X}{R_N}, \quad \tilde{Y} = \frac{Y}{R_N}, \quad \tilde{h} = \frac{h}{h_N}$$

$$\tilde{V} = \frac{V}{V_N}, \quad \tilde{E} = \frac{E}{E_N}, \quad \tilde{m} = \frac{m}{m_0} \tag{2.34}$$

$$\tilde{\zeta} = \frac{\zeta}{\zeta_N}, \quad \tilde{t} = \frac{t}{t_N}, \quad \tilde{T} = \frac{T}{T_N}$$

$$\tilde{L} = \frac{L}{L_N} = \frac{L}{W_0 n_N}$$

where the subscript "N" stands for normalizing reference data; range R is defined as $R = (\Delta X^2 + \Delta Y^2)^{1/2}$, ζ is defined as $\zeta = (T - D)/W_0$; W_0 is initial weight and $n = L/W$ is load factor. It is important to point out that T - D is a small quantity which can be represented as $\epsilon\Delta$. We treat it as a whole when we normalize it; this is a crucial point in our scheme. Upon substituting (2.32) and (2.34) into (2.31), we obtain the dimensionless equations of motion as

$$\frac{d\tilde{X}}{d\tilde{t}} = \frac{t_N V_N}{R_N} \tilde{V} \mathrm{COS}\gamma \mathrm{COS}\psi \tag{2.35a}$$

$$\frac{d\tilde{Y}}{d\tilde{t}} = \frac{t_N V_N}{R_N} \tilde{V} \mathrm{COS}\gamma \mathrm{SIN}\psi \tag{2.35b}$$

$$\frac{d\tilde{h}}{d\tilde{t}} = \frac{t_N V_N}{h_N} \tilde{V} \mathrm{SIN}\gamma \tag{2.35c}$$

$$\frac{d\tilde{E}}{d\tilde{t}} = \frac{t_N V_N}{E_N} g\zeta_N \frac{\tilde{V}}{\tilde{m}} \tilde{\zeta} \tag{2.35d}$$

$$\frac{d\tilde{V}}{d\tilde{t}} = \frac{g t_N}{V_N} \left(\frac{\zeta_N \tilde{\zeta}}{\tilde{m}} - \mathrm{SIN}\gamma \right) \tag{2.35e}$$

$$\frac{d\gamma}{d\tilde{t}} = \frac{g t_N n_N}{V_N} \left(\frac{\tilde{L}\mathrm{COS}\beta}{\tilde{m}\tilde{V}} - \frac{\mathrm{COS}\gamma}{\tilde{V} n_N} \right) \tag{2.35f}$$

$$\frac{d\psi}{d\tilde{t}} = \frac{g t_N n_N}{V_N} \frac{\tilde{L}\mathrm{SIN}\beta}{\tilde{m}\tilde{V}\mathrm{COS}\gamma} \tag{2.35g}$$

$$\frac{d\tilde{m}}{d\tilde{t}} = - c \frac{T_N t_N}{W_o} \tilde{T} \tag{2.35h}$$

For easiness of comparison of time-scale properties, we introduce a measure of relative speed. The speed of each variable is measured with respect to the speed of one variable. For example , when the speeds are measured relative to the speed of V, we obtain the following expressions

$$\frac{\text{speed of } \tilde{X} \text{ or } \tilde{Y}}{\text{speed of } \tilde{V}} = \frac{V_N^2}{g R_N} = 2\mu \left(\frac{h_N}{R_N} \right) \tag{2.36a}$$

$$\frac{\text{speed of } \tilde{m}}{\text{speed of } \tilde{V}} = \frac{c T_N V_N}{g W_o} = 2\mu \left(\frac{c T_N h_N}{W_o V_N} \right) \tag{2.36b}$$

$$\frac{\text{speed of } \tilde{E}}{\text{speed of } \tilde{V}} = \frac{V_N^2 \zeta_N}{E_N} = \frac{2\mu}{1 + \mu} (\zeta_N) \tag{2.36c}$$

$$\frac{\text{speed of } \tilde{h}}{\text{speed of } \tilde{V}} = \frac{V_N^2}{g h_N} = 2\mu \tag{2.36d}$$

$$\frac{\text{speed of } \gamma \text{ or } \psi}{\text{speed of } \tilde{V}} = n_N \tag{2.36e}$$

where $\mu = V_N^2/2gh_N$; hence $E_N = gh_N + (V_N^2/2) = (1 + \mu)h_N g$.

Equations (2.36) give measures of state variable speeds for the seventh-order model (2.31) according to the normalization scheme. It will be shown later on that the time-scale separation properties are highly dependent upon the aircraft mission (i.e., flight conditions). In other words, changing flight conditions may cause state variables to be in different time scales.

Comparison with Ardema's results and Kelley's assumptions: Now, let us take the F-4C aircraft data as defined in Ardema and Rajan [11]

$$W_0 = 16967\text{Kg}, \quad s = 49.2\text{m}^2, \quad c = 1.08\text{hr}^{-1}, \quad g = 9.8\text{m/sec}^2 \tag{2.37}$$

There are two options for choosing the normalizing reference data; either the true maximum reference data or the typical reference data (the region of interest). Both normalizing reference data are given below

The maximum reference data are given by [11]

$$R_N = R_{max} = (\Delta X_{max}^2 + \Delta Y_{max}^2)^{1/2} = 12.2 \times 10^6 \text{m}$$

$$V_N = 590\text{m/sec}, \quad h_N = h_{max} = 25000\text{m}$$

$$E_N = E_{max} = h_{max} + \frac{V_{max}^2}{2g} = 42760\text{m} \tag{2.38}$$

$$\zeta_{max} = \frac{T_{max} - D_0}{W_0} = .52, \quad n_{max} = 6, \quad \frac{T_{max}}{W_0} = .6$$

The typical reference data are given by [11]

$$R_N = R_{typ} = 6 \times 10^5\text{m}, \quad V_N = V_{typ} = 340\text{m/sec} = \text{speed of sound}$$

$$h_N = h_{typ} = 6000\text{m}, \quad E_N = E_{typ} = h_{typ} + \frac{V_{typ}^2}{2g} = 11890\text{m} \tag{2.39}$$

$$\zeta_N = \zeta_{typ} = \frac{T_{typ} - D_0}{W_0} = .48, \quad n_N = 4.5, \quad \frac{T_{typ}}{W_0} = .5$$

Substitution of these two normalizing reference data into (2.36), yields the state variable relative speeds shown in Table 2.1

Variable	Speed	
	By maximum reference data	By typical reference data
m	.0108	.0052
X,Y	.0291	.0197
E	.4320	.4759
V	1.0000	1.0000
h	1.4208	1.9660
γ,ψ	6.0000	4.5000

Table 2.1 Estimate of state variables' speeds for F-4C aircraft by using the proposed normalization scheme

From Table 2.1 we see that both choices of reference data give the same general ordering of speeds from slow to fast. Inspection of the numerical values of the relative speeds shows a clear clustering of variables into time scales, with m, X and Y as slow variables and E, V, h, γ and ψ as fast variables. The variables in the slow group are slower than those in the fast group by more than one order of magnitude. This indicates that, for flight optimization problems, application of singular perturbation methods can decompose the problem into two lower-order problems. In particular, when h, V and γ are the variables of interest, one can approach the problem using a fourth-order model that comprises h, V, γ and ψ, with the option of using E in place of h or V. In this fourth-order model, the slow variable m is treated as a fixed parameter, which agree with practice. The slowness of m relative to V justifies neglecting the rate of change of mass relative to the rate of velocity in writing Newton's second law, which is a typical assumption in the literature as we explained in the previous section. Within the group of fast variables (E, V, h, γ, ψ), Table 2.1 shows other possibilities of time scale separation. The energy E is slower than V and h,which confirms that using energy in place of velocity or altitude results in better time scale separation with E treated as a slow variable relative to the rest of the group. This agrees with past experience. Finally, Table 2.1 shows γ and ψ as the fastest variables. Actually, the speed of ψ depends on the order of magnitude of the bank angle β because of the SINβ term on the right hand side of (2.35g). The relative speed of ψ defined above assumes that SINβ will be of order one. The case of small β will be considered later in this section. Let us first compare with Ardema's results.

Ardema's results [11] are shown in Table 2.2. His Method 1 predicts an ordering of the speeds of state variables that generally agrees with ours; the only exception is the heading angle ψ. Method 1 shows it to be the fastest variable of all (the speed is infinity), which is a contradiction to past experience. His Method 2 indicates that E, h, and V are very nearly of the same speed, which is another disagreement with past experience.

Variable	Speed			
	Method 1		Method 2	
	*	Δ	*	Δ
X , Y	.00049	.0140	.00013	.0394
E	.00550	.1571	.00270	.8182
h	.02300	.6571	.00290	.8788
V	.03500	1.0000	.00330	1.0000
γ	.09000	2.5714	.04400	13.3333
ψ	∞	∞	.05900	17.8788

Note: * is the original data from Ardema's paper

Δ for easiness of comparison with the results of our scheme, the speed of each variable is measured with respect to V in both Method 1 and Method 2

Table 2.2 Estimates of state variables' speeds for F-4C aircraft by Ardema's two methods

Let us now consider the case of vehicles flying in steady flight with small bank angle β, the heading angle ψ in equation (2.35g) can then be written as

$$\frac{d\psi}{d\tilde{t}} = \frac{g t_N n_N SIN\beta_N}{V_N} \frac{\tilde{L}}{\tilde{V}\tilde{m}COS\gamma} \left(\frac{SIN\beta}{SIN\beta_N}\right) \qquad (2.40)$$

where $SIN\beta$ is normalized as $SIN\beta/SIN\beta_N$. The relative speed in equation (2.36e) will become

$$\frac{\text{speed of } \psi}{\text{speed of } \tilde{V}} = n_N SIN\beta_N \qquad (2.41)$$

Taking the same normalizing reference data as given in (2.38) and (2.39), choosing the small bank angle as $\beta_N = 5^o = .087$radian for both normalizing reference data and substituting into (2.36), (2.41) respectively, the results are shown in the Table 2.3

Variable	Speed	
	By maximum reference data	By typical reference data
m	.0108	.0052
X , Y	.0291	.0197
E	.4320	.4759
ψ	.5229	.3922
V	1.0000	1.0000
h	1.4208	1.9660
γ	6.0000	4.5000

Table 2.3 Estimates of state variables' speeds for F-4C aircraft by using the proposed normalization scheme with small bank angle

Both of the normalizing reference data show that the heading angle ψ becomes slower when β is small, which is in agreement with Kelley's assumption [1].

II.3.2 ENERGY STATE MODELING

The use of energy as a state variable in place of altitude or velocity has been behind many applications of singular perturbation techniques to guidance and control (Kelley [17], Ardema [4]). The fact that energy is a slower variable compared with altitude or velocity can be explained using singular perturbation arguments. This was done in Kokotovic, Khalil and O'Reilly [19] and will be recalled here.

Consider the case when β is so small (i.e. for flight in a vertical plane) that m, X, Y and ψ are much slower than the other variables. Then the dynamics of h, V and γ can be described by the third-order model

$$\frac{dh}{d\tau} = V\mathrm{SIN}\gamma \tag{2.42a}$$

$$\frac{dV}{d\tau} = g(\epsilon\Delta - \mathrm{SIN}\gamma) \tag{2.42b}$$

$$\frac{d\gamma}{d\tau} = \frac{g}{V}\left(\frac{L}{W} - \mathrm{COS}\gamma\right) \tag{2.42c}$$

where $\epsilon\Delta$ is the difference of thrust minus drag per unit weight; both L and Δ are function of h, V and α. The system (2.42) has an equilibrium manifold at $\epsilon = 0$, defined by $\gamma = 0$ and $L = W$. The manifold is 1-dimensional. This indicates that the system has a slow variable which is constant at $\epsilon = 0$ in the τ-scale. A constant quantity at $\epsilon = 0$ in τ-scale is provided by the fact that without thrust and drag the energy is conserved. Thus, multiplying (2.42a) by g and (2.42b) by V and adding them together, we get at $\epsilon = 0$, for all $\tau \geq 0$ and all h, V and γ

$$g \frac{dh}{dt} + V \frac{dV}{dt} = 0, \qquad gh + \frac{1}{2} V^2 = \text{constant} \tag{2.43}$$

Hence as our slow variable, we take $E = gh + \frac{1}{2} V^2$ and obtain in t-scale, where $t = \epsilon\tau$

$$\frac{dE}{dt} = g\Delta V \tag{2.44a}$$

$$\epsilon \frac{dV}{dt} = g(\epsilon\Delta - \mathrm{SIN}\gamma) \tag{2.44b}$$

$$\epsilon \frac{d\gamma}{dt} = \frac{g}{V} \left(\frac{L}{W} - \mathrm{COS}\gamma\right) \tag{2.44c}$$

Rewrite (2.44) as

$$\frac{dE}{dt} = \frac{V}{m} (T - D) \tag{2.45a}$$

$$\epsilon \frac{dV}{dt} = \frac{\epsilon(T - D)}{m} - g\mathrm{SIN}\gamma \tag{2.45b}$$

$$\epsilon \frac{d\gamma}{dt} = \frac{L - W\mathrm{COS}\gamma}{mV} \tag{2.45c}$$

This energy modeling confirms that using energy in place of either h (or V) as a state variable yields a standard singularly perturbed model. Equation (2.45) will be used in Chapter III.

II.3.3 A SEVENTH-ORDER SINGULARLY PERTURBED MODEL

We have seen that the normalization scheme of Section II.3.1 produces measures of speeds of variables that are in agreement with past experience and practice. In particular, we have seen that the slowness of X and Y relative to V can be attributed to the smallness of (h_N/R_N) which is typical. The slowness of m relative to V is due to the smallness of ζ_N and $n_N SIN\beta_N$, respectively. These findings will now be used to write the equations of motion in the singularly perturbed form. The seventh-order model will comprise the state variables of the original model (2.31) except for h which is replaced by E. The singular perturbation parameters are taken as

$$\epsilon_1 = \frac{cT_N h_N}{W_0 V_N} \tag{2.46a}$$

$$\epsilon_2 = \frac{h_N}{R_N} \tag{2.46b}$$

$$\epsilon_3 = n_N SIN\beta_N \tag{2.46c}$$

$$\epsilon_4 = \zeta_N \tag{2.46d}$$

In view of our discussion above, and the numerical results of Section II.3.1, it is clear that

$$\epsilon_1,\ \epsilon_2 << \epsilon_3,\ \epsilon_4$$

Morever, depending on the smallness of β_N, ϵ_3 may be much smaller than ϵ_4. In some situations, ϵ_1 may be much small than ϵ_2. The seventh-order model takes the singularly perturbed form of equation (2.47) below.

$$\frac{d\tilde{m}}{d\tilde{t}} = -\epsilon_1(2\mu c_1)\tilde{T} \tag{2.47a}$$

$$\frac{d\tilde{X}}{d\tilde{t}} = \epsilon_2(2\mu c_1)\tilde{V}\text{COS}\gamma\text{COS}\psi \tag{2.47b}$$

$$\frac{d\tilde{Y}}{d\tilde{t}} = \epsilon_2(2\mu c_1)\tilde{V}\text{COS}\gamma\text{SIN}\psi \tag{2.47c}$$

$$\frac{d\psi}{d\tilde{t}} = \epsilon_3 c_1 \frac{\tilde{L}}{\tilde{m}\tilde{V}\text{COS}\gamma}\left(\frac{\text{SIN}\beta}{\text{SIN}\beta_N}\right) \tag{2.47d}$$

$$\frac{d\tilde{E}}{d\tilde{t}} = \epsilon_4\left(\frac{2\mu}{1+\mu}c_1\right)\frac{\tilde{V}}{\tilde{m}}\tilde{\zeta} \tag{2.47e}$$

$$\frac{d\tilde{V}}{d\tilde{t}} = c_1\left(\frac{\epsilon_4\tilde{\zeta}}{\tilde{m}} - \text{SIN}\gamma\right) \tag{2.47f}$$

$$\frac{d\gamma}{d\tilde{t}} = n_N c_1\left(\frac{\tilde{L}\text{COS}\beta}{\tilde{m}\tilde{V}} - \frac{\text{COS}\gamma}{\tilde{V}n_N}\right) \tag{2.47g}$$

where $c_1 = gt_N/V_N$ and $\mu = V_N^2/2gh_N$

Notice that this singularly perturbed form is expressed in the fastest time scale and not the slowest time scale as it is customary in the literature.

The fact that a model takes the singularly perturbed form

$$\dot{x} = f(x, z, u), \qquad x \in R^n,\ u \in R^n \tag{2.48a}$$

$$\epsilon \dot{z} = g(x, z, u), \qquad z \in R^m \tag{2.48b}$$

or

$$\frac{dx}{d\tau} = \epsilon f(x, z, u), \quad x \in R^n,\ u \in R^n \tag{2.49a}$$

$$\frac{dz}{d\tau} = g(x, z, u), \quad z \in R^m \tag{2.49b}$$

does not automatically mean that the system has a two-time scale property. Additional assumptions are needed to ensure the two-time scale property. Let us discuss these assumptions for the linear system

$$\dot{x} = A_{11}x + A_{12}z + B_1u \tag{2.50a}$$

$$\epsilon \dot{z} = A_{21}x + A_{22}z + B_2u \tag{2.50b}$$

Upon setting $\epsilon = 0$, (2.50) reduces to

$$\dot{x} = A_{11}x + A_{12}z + B_1u \tag{2.51a}$$

$$0 = A_{21}x + A_{22}z + B_2u \tag{2.51b}$$

A typical assumption in the singular perturbation literature, e.g. Kokotovic, Khalil and O'Reilly [19], is to require A_{22} to be nonsingular. This assumption guarantees that (2.51) represents a well-defined nth-order reduced model. It also guarantees that the system

(2.50) has a two-time scale property in the sense that its n+m eigenvalues cluster into n eigenvalues of order 0(1) and m eigenvalues of order $0(1/\epsilon)$. If A_{22} is singular but $[A_{22}\ B_2]$ has rank m, the equation (2.51) will still yield a well-defined nth-order reduced model by interchanging the roles of some components of z and u. This point will be illustrated in Chapter IV. The eigenvalues of (2.50) will not have m eigenvalues of order $0(1/\epsilon)$ in this case, but the use of feedback from z with coefficients of order 0(1) can locate m eigenvalues at locations of order $0(1/\epsilon)$, see Khalil [35]. In summary, we can say that the linear model (2.50) represents a standard singularly perturbed model if A_{22} is nonsingular or if $[A_{22}\ B_2]$ has rank m and z can be measured for feedback. The nonlinear model (2.48) will represent a standard singularly perturbed model if its linearization about every point, along a certain trajectory or in a certain set, satisfies the assumption A_{22} nonsingular or rank $[A_{22}\ B_2] = m$.

The singularly perturbed nature of the model (2.47) will be studied by linearization. Let us recall that $T = T(E, V)$, $D = \frac{1}{2}C_D\rho_0 V^2 se^{-Kh}$ and $L = \frac{1}{2}C_{L\alpha}\alpha\rho_0 V^2 se^{-Kh}$. Hence, $\bar{T} = \bar{T}(\bar{E}, \bar{V})$, $\bar{\zeta} = \bar{\zeta}(\bar{E}, \bar{V}, \alpha)$ and $\bar{L} = \bar{L}(\bar{E}, \bar{V}, \alpha)$. The lineraization of (2.47) with α and β treated as control variables is

$$\frac{d}{dt}\begin{bmatrix}\tilde{m}\\ \tilde{X}\\ \tilde{Y}\\ \psi\\ \tilde{E}\\ \tilde{V}\\ \gamma\end{bmatrix} = \begin{bmatrix} 0 & 0 & 0 & 0 & \epsilon_1 a_{15} & \epsilon_1 a_{16} & 0\\ 0 & 0 & 0 & \epsilon_2 a_{24} & 0 & \epsilon_2 a_{26} & \epsilon_2 a_{27}\\ 0 & 0 & 0 & \epsilon_2 a_{34} & 0 & \epsilon_2 a_{36} & \epsilon_2 a_{37}\\ \epsilon_3 a_{41} & 0 & 0 & 0 & \epsilon_3 a_{45} & \epsilon_3 a_{46} & \epsilon_3 a_{47}\\ \epsilon_4 a_{51} & 0 & 0 & 0 & \epsilon_4 a_{55} & \epsilon_4 a_{56} & 0\\ \epsilon_4 a_{61} & 0 & 0 & 0 & \epsilon_4 a_{65} & \epsilon_4 a_{66} & a_{67}\\ a_{71} & 0 & 0 & 0 & a_{75} & a_{76} & a_{77}\end{bmatrix}\begin{bmatrix}\tilde{m}\\ \tilde{X}\\ \tilde{Y}\\ \psi\\ \tilde{E}\\ \tilde{V}\\ \gamma\end{bmatrix}$$

$$+\begin{bmatrix}\epsilon_1 b_{11} & 0\\ 0 & 0\\ 0 & 0\\ \epsilon_3 b_{41} & \epsilon_3 b_{42}\\ \epsilon_4 b_{51} & 0\\ \epsilon_4 b_{61} & 0\\ b_{71} & b_{72}\end{bmatrix}\begin{bmatrix}\alpha\\ \beta\end{bmatrix} \qquad (2.52)$$

where

$$a_{15} = -2\mu c_1 \frac{\partial \tilde{T}}{\partial \tilde{E}}, \qquad a_{16} = -2\mu c_1 \frac{\partial \tilde{T}}{\partial \tilde{V}}$$

$$a_{24} = -2\mu c_1 \tilde{V} \mathrm{COS}\gamma \mathrm{SIN}\psi, \qquad a_{26} = 2\mu c_1 \mathrm{COS}\gamma \mathrm{COS}\psi, \qquad a_{27} = -2\mu c_1 \tilde{V} \mathrm{SIN}\gamma \mathrm{COS}\psi$$

$$a_{34} = 2\mu c_1 \tilde{V} \mathrm{COS}\gamma \mathrm{COS}\psi, \qquad a_{36} = 2\mu c_1 \mathrm{COS}\gamma \mathrm{SIN}\psi, \qquad a_{37} = -2\mu c_1 \tilde{V} \mathrm{SIN}\gamma \mathrm{SIN}\psi$$

$$a_{41} = -c_1 \frac{\tilde{L}\mathrm{SIN}\beta}{\tilde{m}^2\, \tilde{V}\mathrm{COS}\gamma \mathrm{SIN}\beta_N}, \qquad a_{45} = c_1 \frac{\partial \tilde{L}}{\partial \tilde{E}} \frac{1}{\tilde{m}\tilde{V}\mathrm{COS}\gamma} \cdot \frac{\mathrm{SIN}\beta}{\mathrm{SIN}\beta_N}$$

$$a_{46} = c_1 \left[\frac{\partial \tilde{L}}{\partial \tilde{V}} \frac{1}{\tilde{m}\tilde{V}\mathrm{COS}\gamma} \cdot \frac{\mathrm{SIN}\beta}{\mathrm{SIN}\beta_N} - \frac{\tilde{L}\mathrm{SIN}\beta}{\tilde{m}^2\tilde{V}\, \mathrm{COS}\gamma \mathrm{SIN}\beta_N} \right]$$

$$a_{47} = c_1 \frac{\tilde{L}\mathrm{SIN}\beta \mathrm{SIN}\gamma}{\tilde{m}\tilde{V}\mathrm{COS}^2\gamma \mathrm{SIN}\beta_N}, \qquad a_{51} = -\left(\frac{2\mu}{1+\mu} c_1\right) \frac{\tilde{V}\tilde{\zeta}}{\tilde{m}^2} \tag{2.53}$$

$$a_{55} = \left(\frac{2\mu}{1+\mu} c_1\right) \frac{\tilde{V}}{\tilde{m}} \frac{\partial \tilde{\zeta}}{\partial \tilde{E}}, \qquad a_{56} = \left(\frac{2\mu}{1+\mu} c_1\right) \frac{1}{\tilde{m}} \frac{\partial (\tilde{V}\tilde{\zeta})}{\partial \tilde{V}}$$

$$a_{61} = -c_1 \frac{\tilde{\zeta}}{\tilde{m}^2}, \qquad a_{65} = c_1 \frac{1}{\tilde{m}} \frac{\partial \tilde{\zeta}}{\partial \tilde{E}}$$

$$a_{66} = \frac{c_1}{\tilde{m}} \frac{\partial \tilde{\zeta}}{\partial \tilde{V}}, \quad a_{67} = -c_1 \mathrm{COS}\gamma$$

$$a_{71} = -n_N c_1 \frac{\tilde{L}\mathrm{COS}\beta}{\tilde{m}\,\tilde{V}^2}, \quad a_{75} = n_N c_1 \frac{\partial \tilde{L}}{\partial \tilde{E}} \frac{\mathrm{COS}\beta}{\tilde{m}\tilde{V}}$$

$$a_{76} = n_N c_1 \left[\frac{\mathrm{COS}\beta}{\tilde{m}} \frac{\partial}{\partial \tilde{V}}\left(\frac{\tilde{L}}{\tilde{V}}\right) - \frac{\mathrm{COS}\gamma}{n_N} \frac{\partial}{\partial \tilde{V}}\left(\frac{1}{\tilde{V}}\right)\right], \quad a_{77} = \frac{\mathrm{SIN}\gamma}{\tilde{V} n_N} n_N c_1$$

$$b_{11} = -2\mu c_1 \frac{\partial \tilde{T}}{\partial \alpha}, \quad b_{41} = c_1 \frac{\partial \tilde{L}}{\partial \alpha} \frac{\mathrm{SIN}\beta}{\tilde{m}\tilde{V}\mathrm{COS}\gamma\mathrm{SIN}\beta_N} \tag{2.54}$$

$$b_{42} = c_1 \frac{\tilde{L}\mathrm{COS}\beta}{\tilde{m}\tilde{V}\mathrm{COS}\gamma\mathrm{SIN}\beta_N}, \quad b_{51} = \frac{2\mu}{1+\mu} c_1 \frac{\tilde{V}}{\tilde{m}} \frac{\partial \tilde{\zeta}}{\partial \alpha}$$

$$b_{61} = c_1 \frac{1}{\tilde{m}} \frac{\partial \tilde{\zeta}}{\partial \alpha}, \quad b_{71} = n_N c_1 \frac{\partial \tilde{L}}{\partial \alpha} \frac{\mathrm{COS}\beta}{\tilde{m}\tilde{V}}, \quad b_{72} = -n_N c_1 \frac{\tilde{L}\mathrm{SIN}\beta}{\tilde{m}\tilde{V}}$$

When the parameters ϵ_1 to ϵ_4 are small, equation (2.52) takes the singularly perturbed form (2.50) with ($\tilde{m}$, $\tilde{X}$, $\tilde{Y}$, ψ, $\tilde{E}$) as slow variables and ($\tilde{V}$, γ) as fast variables. We rewrite (2.52) in partitioned form as

$$\frac{d}{dt}\begin{bmatrix}\tilde{m}\\ \tilde{X}\\ \tilde{Y}\\ \psi\\ \tilde{E}\\ \tilde{V}\\ \gamma\end{bmatrix} = \left[\begin{array}{c|cc} X & X & \\ \hline X & \epsilon_4 a_{66} & a_{67} \\ & a_{76} & a_{77}\end{array}\right]\begin{bmatrix}\tilde{m}\\ \tilde{X}\\ \tilde{Y}\\ \psi\\ \tilde{E}\\ \tilde{V}\\ \gamma\end{bmatrix} + \left[\begin{array}{c} X \\ \hline X\end{array}\right]\begin{bmatrix}\alpha\\ \beta\end{bmatrix} \tag{2.55}$$

Consider the determinant

$$\det\begin{bmatrix}\epsilon_4 a_{66} & a_{67}\\ a_{76} & a_{77}\end{bmatrix} = \epsilon_4 a_{66}a_{77} - a_{67}a_{76} \tag{2.56}$$

where $a_{67} = -c_1 \mathrm{COS}\gamma$ and

$$a_{76} = n_N c_1 \frac{\mathrm{COS}\beta}{\tilde{m}} \frac{V_N^2}{L_N} \frac{1}{2}\alpha\rho_0 s(C_{L\alpha} e^{-K(E - V^2/2g)} + Ve^{-K(E - V^2/2g)}\frac{\partial C_{L\alpha}}{\partial V}$$

$$+ C_{L\alpha} Ve^{-K(E - V^2/2g)}\frac{KV}{g}) + n_N c_1 \frac{\mathrm{COS}\gamma}{n_N} \frac{V_N^2}{V^2} > 0$$

Thus, for $|\gamma| < 90^{\circ}$ and small ϵ_4 , the determinant (2.56) is positive and the matrix is nonsingular. In other words, (2.52) is in a standard singularly perturbed form, where $\tilde{m}$, $\tilde{X}$, $\tilde{Y}$, $\tilde{E}$, ψ are slow variables and $\tilde{V}$, γ are fast variables. Neglecting the transinents of $\tilde{V}$ and γ, equation (2.52) can be reduced to the fifth order model

$$\frac{d}{dt}\begin{bmatrix} \tilde{m} \\ \tilde{X} \\ \tilde{Y} \\ \psi \\ \tilde{E} \end{bmatrix} = \begin{bmatrix} \epsilon_1 l_1 & 0 & 0 & 0 & \epsilon_1 l_2 \\ \epsilon_2 l_3 & 0 & 0 & \epsilon_2 a_{24} & \epsilon_2 l_4 \\ \epsilon_2 l_5 & 0 & 0 & \epsilon_2 a_{34} & \epsilon_2 l_6 \\ \epsilon_3 l_7 & 0 & 0 & 0 & \epsilon_3 l_8 \\ \epsilon_4 l_9 & 0 & 0 & 0 & \epsilon_4 l_{10} \end{bmatrix} \begin{bmatrix} \tilde{m} \\ \tilde{X} \\ \tilde{Y} \\ \psi \\ \tilde{E} \end{bmatrix} + \begin{bmatrix} \epsilon_1 d_1 & \epsilon_1 d_2 \\ \epsilon_2 d_3 & \epsilon_2 d_4 \\ \epsilon_2 d_5 & \epsilon_2 d_6 \\ \epsilon_3 d_7 & \epsilon_3 d_8 \\ \epsilon_4 d_9 & \epsilon_4 d_{10} \end{bmatrix} \begin{bmatrix} \alpha \\ \beta \end{bmatrix} \tag{2.57}$$

Now, if ϵ_3 and ϵ_4 are of the same order (in general it is) and much larger than ϵ_1, ϵ_2, (2.57) can then be partitioned as

$$\frac{d}{dt}\begin{bmatrix}\tilde{m}\\ \tilde{X}\\ \tilde{Y}\\ \psi\\ \tilde{E}\end{bmatrix} = \left[\begin{array}{c|c} X & X \\ \hline X & \underbrace{\begin{matrix}0 & \epsilon_3 l_8\\ 0 & \epsilon_4 l_{10}\end{matrix}}_{A_{22}}\end{array}\right]\begin{bmatrix}\tilde{m}\\ \tilde{X}\\ \tilde{Y}\\ \psi\\ \tilde{E}\end{bmatrix} + \underbrace{\left[\begin{array}{cc} \multicolumn{2}{c}{X} \\ \hline \epsilon_3 d_7 & \epsilon_3 d_8\\ \epsilon_4 d_9 & \epsilon_4 d_{10}\end{array}\right]}_{B_2}\begin{bmatrix}\alpha\\ \beta\end{bmatrix} \tag{2.58}$$

The matrix A_{22} is not nonsingular, but $[A_{22} \;\; B_2]$ has rank 2; hence equation (2.58) still yields a well-defined third-order reduced model. If ϵ_3 is much smaller than ϵ_4, we should partition (2.58) with $(\tilde{m}, \tilde{X}, \tilde{Y}, \psi)$ as slow variables and $\tilde{E}$ as a fast variable.

Finally, if ϵ_1 and ϵ_2 are of the same order, then $\tilde{m}$, $\tilde{X}$, $\tilde{Y}$ are grouped in the same time-scale. If ϵ_1 is smaller than ϵ_2, again we can partition the third-order model of $(\tilde{m}, \tilde{X}, \tilde{Y})$ so that $\tilde{m}$ is slower than $(\tilde{X}, \tilde{Y})$.

The above linearization analysis confirms that the model (2.47) is a well-defined singularly perturbed model with $(\tilde{V}, \gamma)$ as the fastest variables, followed by $(\psi, \tilde{E})$ and then by $(\tilde{m}, \tilde{X}, \tilde{Y})$ as the slowest variables. This generally agrees with our previous analysis.

II.3.4 A FOURTH-ORDER SINGULARLY PERTURBED MODEL FOR STEADY LEVEL TURNING PROBLEM AND COMPARISION WITH CALISE'S RESULTS

In this section, we consider a steady-level turning problem for two-dimensional flight in the horizontal plane. In order to maintain the flight in the horizontal plane, the bank angle β should satisfy (see Fig.2.4)

$$L\cos\beta = W \tag{2.59}$$

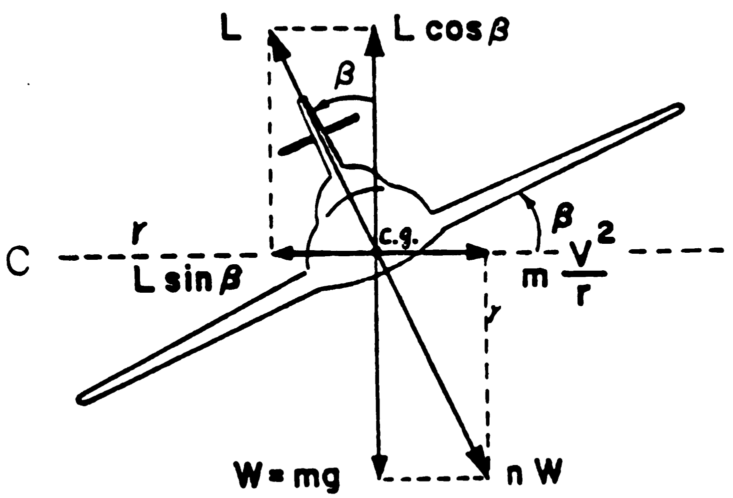

Fig.2.4 Equilibrium of force in a coordinate turn

The motion can be adequately described by a fourth-order model derived from the seventh-order model (2.31) by assuming constant mass, constant altitude and small flight path angle ($\gamma \cong 0$). Hence equation (2.31c), (2.31e) and (2.31g) can be dropped yielding the fourth-order model

$$\frac{dX}{dt} = V\cos\psi \tag{2.60a}$$

$$\frac{dY}{dt} = V\sin\psi \tag{2.60b}$$

$$\frac{dV}{dt} = \frac{(T - D)}{m} \tag{2.60c}$$

$$\frac{d\psi}{dt} = \frac{L\sin\beta}{mV} \tag{2.60d}$$

In Calise's paper [6], he takes D as

$$D = qsC_{D_o} + kL^2/qs \tag{2.61a}$$

$$q = \frac{1}{2}\rho V^2 \tag{2.61b}$$

$$L^2 = L_n^2 + W^2 \tag{2.61c}$$

where L_n is the component of total lift (L) in the horizontal plane, i.e., $L_n = L\sin\beta$, C_{D_o} is the zero lift drag coefficient and k is the lift induced drag coefficient.

Upon substituting the normalization (2.34) into (2.60), the dimensionless equations of motion are

$$\frac{d\tilde{X}}{d\tilde{t}} = \frac{t_N V_N}{R_N} \tilde{V}\cos\psi \tag{2.62a}$$

$$\frac{d\tilde{Y}}{d\tilde{t}} = \frac{t_N V_N}{R_N} \tilde{V}\sin\psi \tag{2.62b}$$

$$\frac{d\tilde{V}}{d\tilde{t}} = \frac{t_N g\zeta_N}{V_N} \frac{\tilde{\zeta}}{\tilde{m}} \tag{2.62c}$$

$$\frac{d\psi}{d\tilde{t}} = \frac{g t_N n_N \sin\beta_N}{V_N} \cdot \frac{\tilde{L}\sin\beta}{\tilde{m}\tilde{V}\cos\gamma\sin\beta_N} \tag{2.62d}$$

The speeds relative to the speed of V are

$$\frac{\text{speed of } \tilde{X} \text{ or } \tilde{Y}}{\text{speed of } \tilde{V}} = \frac{V_N^2}{gR_N\zeta_N} \tag{2.63a}$$

$$\frac{\text{speed of } \psi}{\text{speed of } \tilde{V}} = \frac{n_N \sin\beta_N}{\zeta_N} \tag{2.63b}$$

Comparison with Calise's results: Let us choose the air-launched Missile II as defined in Calise [6] which is a steady level turning problem under the assumptions of constant altitude, constant mass and small flight path angle γ. The normalizing reference data given by Calise are

$$R_N = 12.2 \times 10^6 \text{m}, \qquad V_N = 304.8\text{m/sec}$$

$$D = \frac{1}{2}\rho V_N^2 sC_{D_o} + \frac{2kL_N^2}{\rho V_N^2 s} = 939.99\text{kg}, \qquad n_N = 25$$

$$T_N = 2273\text{kg}, \qquad \zeta_N = \frac{T_N - D}{W_o} = 14.67, \quad L_N = W_o n_N = 2272.5\text{Kg} \tag{2.64}$$

$$r_N = \frac{V_N^2}{gn_N} = 379.2\text{m}, \qquad \beta_N = 80^o$$

other values needed are

$$W_o = 90.9\text{kg}, \qquad s = .016\text{m}^2, \qquad \rho = .8761\text{kg/m}^3$$

$$C_{D_o} = 1.2, \qquad k = .02, \qquad g = 9.8\text{m/sec}^2 \tag{2.65}$$

These data are substituted in (2.62) and the results, given in Table 2.4, show that (X,Y) are slow variables, while (ψ, V) are much faster than (X, Y).

Variable	Speed by normalizing reference data
X , Y	.00053
V	1.00000
ψ	1.67827

Table 2.4 Estimates of state variables' speeds for Missile II in steady level turning flight by using the proposed normalization scheme

Calise [6] classifies the speeds of variables as follow: (X, Y) are in the same time scale and are the slowest variables, the heading angle ψ is faster and the velocity V is even much faster than ψ. The nondimensional variable equations he obtained are shown below

$$\frac{dX}{dt} = V\cos\psi \tag{2.66a}$$

$$\frac{dY}{dt} = V\sin\psi \tag{2.66b}$$

$$\frac{r_{min}}{R_N}\frac{d\psi}{dt} = \frac{L}{V} \tag{2.66c}$$

$$\frac{1}{\xi_{max}}\left(\frac{r_{min}}{R_N}\right)\frac{dV}{dt} = \frac{T}{n_{max}} - \frac{D}{\xi_{max}} \tag{2.66d}$$

where $r_N = r_{min} = \frac{V^2}{gn}$, $\xi_{max} = T_{max}/N$ and r_{min} is the radius of curvature (see Fig.2.4) which is defined as a horizontal arc (centre C, radius r).

Substituting the normalizing reference data given by (2.64) into Calise's nondimensional equation (2.66) yields

$$\frac{dX}{dt} = V\cos\psi \tag{2.67a}$$

$$\frac{dY}{dt} = V\sin\psi \tag{2.67b}$$

$$.0003\ \frac{d\psi}{dt} = \frac{L}{\psi} \tag{2.67c}$$

$$.0003 \frac{dV}{dt} = T - D \tag{2.67d}$$

Equation (2.67) shows that even in Calise's normalization, (ψ, V) are in the same time scale and they are much faster than (X, Y) which agrees with the conclusion of our normalization. It also shows that Calise's assumption that V is much faster than ψ is not justified.

II.4 CONCLUDING REMARKS

A normalization scheme approach for time scale separation analysis of nonlinear dynamic systems has been proposed. The main point of this approach is the decomposition of a high order, nonlinear complex dynamic flight vehicles systems into several (multiple) lower order systems in an easy and globally valid way. The dynamic state equations and the normalizing reference data are the only information required.

This approach was applied to a typical class of flight vehicles dynamic equations. The numerical examples showed that the time scale separation as computed by this approach generally agree with previous practice and assumptions.

III. SINGULAR PERTURBATIONS IN FLIGHT MECHANICS

In this chapter, the application of singular perturbation techniques (SPT) to trajectory optimization problems in flight mechanics is discussed. It is emphasized that auto-pilot implementation of the open loop control, derived using singular perturbation approximation, may cause boundary-layer instability when unsatble modes are present in the uncontrolled system. In other words, real-time implementations generally require the optimal solution to be expressed in a feedback form. The purpose of this chapter is to propose feedback stabilization schemes. Linear and nonlinear feedback stabilization controls are used to circumvent this instability problem.

III.1 USE OF SINGULAR PERTURBATIONS TO APPROXIMATE OPTIMAL TRAJECTORIES

In this section, we review the use of singular perturbation techniques to approximate optimal trajectories in flight mechanics problems. As an illustration, we obtain an approximate solution to the aircraft minimum time-to-climb problem. Outer (reduced), boundary-layer (inner) and composite solutions are shown.

Originally, the method of singular perturbations was applied in initial value problems like Cole [20], Tihonov [21] and Wasow [22]. It was first introduced into optimal control theory by Kokotovic and Sannuti [35]. The two-point boundary value problems (TPBVP'S) arising in optimal control were investigated by Chow [23], Freedman and Granoff [24], Vasile'va [25], Wilde and Kokotovic [26]. The singular perturbation method was also applied widely to aircraft and missile performance optimization problems as in Kelley [2, 3, 17], Ardema [4, 27], Calise [5, 6, 18, 28], Shinar et al. [29, 30], Washburn, et al. [7] and Chakvarty [46].

Two point boundary value problems, which arise in the application of optimal control theory to nonlinear control problems in flight mechanics, are known to be of a computational complexity prohibitive practical applications, especally for on-board real-time implementation. For this reason model order reduction concepts, i.e. neglecting fast dynamics which are thought to have small effect on the solution behavior, have received much attention in the past. One of the pioneering methods is "energy state approximation" by Rutowski [15], which has been applied in performance optimization of supersonic aircraft by Bryson ,et al. [16]. The method, however, exhibits undesirable features and may have considerable errors.

Considerable effort has been extended in searching for simplification techniques to produce results which are meaningful and attainable at reasonable cost. From the research of the past decade, singular perturbation theory has emerged as the most promising approach to meet the simplification goal. Application of singular perturbations to various performance optimization problems in flight mechanics has been reported by Kelley, Ardema, Calise, etc., in the papers cited above.

III.1.1 SINGULARLY PERTURBED TRAJECTORY OPTIMIZATION

Consider the singularly perturbed system

$$\dot{x} = f(x, z, t, \epsilon, u) \tag{3.1a}$$

$$\epsilon \dot{z} = g(x, z, t, \epsilon, u) \tag{3.1b}$$

where x and z are n and m dimensional state vectors, and u is an r-dimensional control vector. The small positive parameter ϵ is identified as a time scaling parameter whose presence increases the system order. For $\epsilon = 0$, z ceases to be a state vector and the order of system (3.1) reduces to n. The objective of the design is to find an optimal control u(t) which takes the initial states $x(t_0) = x_0$, $z(t_0) = z_0$ to the final states $x(t_f) = x_f$, $z(t_f) = z_f$ while minimizing the cost functioanl

$$J = \int_{t_0}^{t_f} V[x(t), z(t), u(t), \epsilon, t]dt \tag{3.2}$$

The functions f, g, and V are assumed to be sufficiently differentiable in all their arguments in an appropriately defined domain.

To obtain the necessary conditions for optimal control, we introduce the Hamiltonian

$$H(x, z, \lambda_x, \lambda_z, u, \epsilon, t) = - V + \lambda_x^T f + \lambda_z^T g \tag{3.3}$$

where λ_x and λ_z are costate variables corresponding to x and z respectively. The maximum principle implies that the costate variables λ_x and λ_z satisfy the equations

$$\dot{\lambda}_x = - \nabla_x H \tag{3.4a}$$

$$\epsilon \dot{\lambda}_z = - \nabla_z H \tag{3.4b}$$

while $\lambda_x(t_f)$ and $\lambda_z(t_f)$ can not be a priori determined because the terminal states are not free. The maximum principle also implies that along an optimal trajectory

$$\nabla_u H = 0 \tag{3.5}$$

Assuming that (3.5) uniquely defines u in terms of x, z, λ_x, and λ_z, substitution of u from (3.5) in the state and costate equations (3.1) and (3.4), yields the form

$$\dot{x} = f(x, \lambda_x, z, \lambda_z, \epsilon, t) \tag{3.6a}$$

$$\dot{\lambda}_x = F(x, \lambda_x, z, \lambda_z, \epsilon, t) \tag{3.6b}$$

$$\epsilon \dot{z} = g(x, \lambda_x, z, \lambda_z, \epsilon, t) \tag{3.6c}$$

$$\epsilon \dot{\lambda}_z = G(x, \lambda_x, z, \lambda_z, \epsilon, t) \tag{3.6d}$$

Equations (3.6) define a TPBVP of differential order of 2(n+m). We call the solution of (3.6) the "exact solution", and the solution of the system with ϵ set to zero the "reduced" solution. It is obvious that in general the reduced solution will not satisfy both initial and terminal conditions. At least locally, the behavior of the reduced solution will be radically different from that of the exact solution. In fact, the best that can be hoped for is that the reduced solution gives a good approximation for fast variable z everywhere except near $z(t_0) = z_0$ and $z(t_f) = z_f$. The phenomenon of boundary-layers occurs in all singular perturbation problems. In such problems, the solution is sought in two (or in some cases, several) separate regions. In an outer region the variables are relatively slowly varying and can be approximated by the reduced solution, which does not generally satisfy all boundary conditions. In an inner (boundary-layer) region, the variables are relatively rapidly varying. They satisfy appropriate boundary condition and converge asymptotically to the reduced solution.

Reduced (zeroth-order outer) solution: The solution of the nonlinear two-point boundary values problem (3.6) may be approximated by setting $\epsilon = 0$ in (3.6). This leads to a reduced problem (variable are denote by the superscript ^{0})

$$\dot{x}^0 = f(x^0, \lambda_x^0, z^0, \lambda_z^0, 0, t) \tag{3.7a}$$

$$\dot{\lambda}_x^0 = F(x^0, \lambda_x^0, z^0, \lambda_z^0, 0, t) \tag{3.7b}$$

$$0 = g(x^0, \lambda_x^0, z^0, \lambda_z^0, 0, t) \tag{3.7c}$$

$$0 = G(x^0, \lambda_x^0, z^0, \lambda_z^0, 0, t) \tag{3.7d}$$

with boundary conditions $x^0(t_0) = x_0$ and $x^0(t_f) = x_f$

The solution of this reduced problem can be an $O(\epsilon)$ approximation for original problem away from the boundary points, but it cannot satisfy the initial and terminal conditions for z.

Boundary-layer (zeroth-order inner) solution: The zeroth-order initial (left) boundary-layer solution is carried out using a stretched time scale

$$\tau = \frac{t - t_0}{\epsilon} \tag{3.8}$$

Substituting (3.8) into (3.6) and again setting $\epsilon = 0$ leads to the following zeroth-order equations (variables in this initial boundary-layer problem are denoted by superscript il)

$$\frac{dx^{il}}{d\tau} = 0 \quad , \qquad x^{il}(\tau) = \text{constant} = x_0 \tag{3.9a}$$

$$\frac{d\lambda_x^{il}}{d\tau} = 0 \quad , \qquad \lambda_x^{il}(\tau) = \text{constant} \tag{3.9b}$$

$$\frac{dz^{il}}{d\tau} = g^{il}(X_0, \lambda_x^{il}, z^{il}, \lambda_z^{il}, 0, t_0) \quad , \qquad z^{il}(t_0) = z_0 \tag{3.9c}$$

$$\frac{d\lambda_z^{il}}{d\tau} = - \frac{\partial H^{il}}{\partial \tau} = G^{il}(x_0, \lambda_x^{il}, z^{il}, \lambda_z^{il}, 0, t_0) \tag{3.9d}$$

Similarly, the zeroth-order terminal (right) boundary-layer equations are formed by introducing the stretching transformation

$$\sigma = \frac{t_f - t}{\epsilon} \tag{3.10}$$

into equation (3.6) and setting $\epsilon = 0$, resulting in equations which are similar to the initial boundary-layer equations (3.9) but in the reverse direction (i.e. opposite sign), and with slow variables frozen at their terminal values instead of initial values.

The reduced and boundary-layer solutions are combined according to the formula

$$z_{app} = z^{o}(t) + [z^{il}(\frac{t - t_0}{\epsilon}) - z^{o}(t_0)] + [z^{il}(\frac{t_f - t}{\epsilon}) - z^{o}(t_f)] \tag{3.11}$$

with similar expressions for λ_z and u. The right-hand side of (3.11) shows that near the initial point $t = t_0$, the solution is approximated by the initial boundary-layer. Away from the boundaries, it is approximated by the reduced solution. Near the terminal point $t = t_f$, it is approximated by the terminal boundary-layer. For x and λ_x, the formula (3.11) reduces to the reduced solutions x^{o} and λ_x^{o}, respectively.

The accuracy of this approximation certainly depends on the value of ϵ. This zeroth-order approximation can be improved by the first-order solution obtained by the method of " Matched Asymptotic Expansions " (see [4]).

III.1.2 ILLUSTRATIVE EXAMPLE (A MINIMUM TIME-TO-CLIMB PROBLEM)

Let us consider the minimum time-to-climb (MTC) problem which is defined as follows. Find a control $\alpha(t)$ that steers the nonlinear singularly perturbed system (see Section II.3.2)

$$\dot{E} = \frac{V}{m}(T - D) \tag{3.12a}$$

$$\epsilon\dot{V} = \frac{\epsilon(T - D)}{m} - gSIN\gamma \tag{3.12b}$$

$$\epsilon\dot{\gamma} = \frac{L - WCOS\gamma}{mV} \tag{3.12c}$$

from the initial state $E(t_0) = E_0$, $V(t_0) = V_0$ and $\gamma(t_0) = \gamma_0$ to the final state $E(t_f) = E_f$, $V(t_f) = V_f$ and $\gamma(t_f) =$ free, while minimizing t_f.

The aerodynamics are recalled here as (see Section II.3.1 and II.3.3)

$$\begin{aligned} D(\alpha, V, h) &= \frac{1}{2}(C_{D_o} + \eta C_{L\alpha}\alpha^2)\rho_0 s e^{-Kh} V^2 \\ L(\alpha, V, h) &= \frac{1}{2} C_{L\alpha}\alpha\rho_0 V^2 s e^{-Kh} \end{aligned} \tag{3.13}$$

where α is the control variable, and $T = T(V, h)$.

Application of the maximum principle to the singularly perturbed system (3.12), gives the necessary conditions

$$\dot{E} = gV\zeta \tag{3.14a}$$

$$\epsilon\dot{V} = \epsilon g\zeta - gSIN\gamma \tag{3.14b}$$

$$\epsilon\dot{\gamma} = \frac{L - WCOS\gamma}{mV} \tag{3.14c}$$

$$\dot{\lambda}_E = -\frac{\partial H}{\partial E} = -\lambda_E Vg\frac{\partial\zeta}{\partial E} - \epsilon\lambda_V g\frac{\partial\zeta}{\partial E} - \frac{\lambda_\gamma}{m}\frac{\partial}{\partial E}(\frac{L}{mV}) \tag{3.15a}$$

$$\epsilon\dot{\lambda}_V = -\frac{\partial H}{\partial V} = -g\lambda_E\frac{\partial}{\partial V}(V\zeta) - \epsilon g\lambda_V\frac{\partial\zeta}{\partial V}$$

$$- \frac{\lambda_\gamma}{m}\frac{\partial}{\partial V}(\frac{L - WCOS\gamma}{V}) \tag{3.15b}$$

$$\epsilon\dot{\lambda}_\gamma = -\frac{\partial H}{\partial\gamma} = \lambda_V gCOS\gamma - \lambda_\gamma\frac{gSIN\gamma}{V} \tag{3.15c}$$

$$\frac{\partial H}{\partial\alpha} = 0\text{, yields}\quad \alpha = \frac{\lambda_\gamma}{2\eta V(\lambda_E V + \epsilon\lambda_V)} \tag{3.16}$$

where $\zeta = (T - D)/W$ (see II.3.1), and the Hamiltonian H is given by

$$H = 1 + \lambda_E(Vg\zeta) + \lambda_V(\epsilon g\zeta - gSIN\gamma) + \lambda_\gamma(\frac{L - WCOS\gamma}{mV}) \tag{3.17}$$

The reduced problem is given by

$$\gamma^o = 0\ ,\quad L^o = W\ ,\quad \lambda_V^o = 0\ ,\quad g\lambda_E^o(\frac{\partial}{\partial V}(V\zeta))^o - \frac{\lambda_\gamma^o}{mV^o}(\frac{\partial L}{\partial V})^o = 0 \tag{3.18a}$$

$$\dot{E}^o = V^o\zeta^o g \tag{3.18b}$$

$$\dot{\lambda}_E^{o} = -\lambda_E^{o} V^{o} g \left(\frac{\partial \zeta}{\partial E}\right)^{o} - \frac{\lambda_\gamma^{o}}{m} \left(\frac{\partial}{\partial E}\left(\frac{L}{mV}\right)\right)^{o} \tag{3.18c}$$

with the boundary conditions $E(t_0) = E_0$ and $E(t_f) = E_f$.

Since this system is autonomous, $H = 0$ is a constant of the motion, the relations of (3.18a) and (3.17) lead to

$$1 + \lambda_E^{o} \zeta^{o} V^{o} g = 0 \text{ , yields } \lambda_E^{o} = -\frac{1}{V^{o} \zeta^{o} g} \tag{3.18d}$$

and the control law is given by

$$\alpha^{o} = \frac{\dot{\lambda}_\gamma^{o}}{2(\lambda_E^{o} \eta V^{o^2})} \tag{3.19}$$

The reduced control (3.19) is the same as the control calculated using the energy state approximation by Bryson et al. [16]. This follows from the well-posedness of the singularly perturbed control problem, as shown in Section 6.3 of [19].

The left boundary-layer problem is given by

$$\frac{dE^{il}}{d\tau} = 0 \tag{3.20a}$$

$$\frac{dV^{il}}{d\tau} = -gSIN\gamma^{il} \tag{3.20b}$$

$$\frac{d\gamma^{il}}{d\tau} = \frac{L^{il} - WCOS\gamma^{il}}{mV^{il}} \tag{3.20c}$$

$$\frac{d\lambda_E^{il}}{d\tau} = 0 \tag{3.21a}$$

$$\frac{d\lambda_V^{il}}{d\tau} = -g\lambda_E^{il} \frac{\partial}{\partial V^{il}}(V^{il}\varsigma^{il}) - \frac{\lambda_\gamma^{il}}{m} \frac{\partial}{\partial V^{il}}\left(\frac{L^{il} - W\cos\gamma^{il}}{V^{il}}\right) \tag{3.21b}$$

$$\frac{d\lambda_\gamma^{il}}{d\tau} = \lambda_V^{il} g\cos\gamma^{il} - \lambda_\gamma^{il} \frac{g\cos\gamma^{il}}{V^{il}} \tag{3.21c}$$

with initial conditions $E^{il}(\tau_0) = E_0$, $V^{il}(\tau_0) = V_0$ and $\gamma^{il}(\tau_0) = \gamma_0$ and the control law is

$$\alpha^{il} = \frac{\lambda_\gamma^{il}}{2(\lambda_E^{il}\eta V^{il^2})} \tag{3.22}$$

The right boundary-layer problem is similar to (3.20) and (3.21) but in the reverse direction. The control law is

$$\alpha^{ir} = \frac{\lambda_\gamma^{ir}}{2(\lambda_E^{ir}\eta V^{ir^2})} \tag{3.23}$$

To illustrate the solution, a numerical example is now considered. The aircraft is "airplane 2" of [16]. The boundary conditions are selected as

$E_0 = 1500000$; $V_0 = .5$ Mach ; $\gamma_0 = 0^0$

$E_f = 5000000$; $V_f = 2.0$ Mach ; $\gamma_f =$ free

Combining the reduced solution, left boundary-layer and right boundary-layer solutions together, gives the results of energy E, velocity V and flight path angle γ shown in Figs.3.1-3.3 respectively, the flight trajectory (path) of the various solutions in the (h, V) plane is also shown in Fig.3.4. The minimum time estimate by this SPT approximation is 170 sec which is the time estimate on the slow manifold (reduced solution) 60 sec plus time to dive (left boundary-layer) 60 sec and to zoom (right boundary-layer) 50 sec (see Fig.3.4). It is important to mention here that for this minimum time-to-climb problem, t_f is unknown (to be determined). In order to estimate t_f, we solve (i.e. integrate) the right boundary-layer in reverse direction until it matches the slow manifold, then t_f can be determined. The minimum t_f we obtained by this approximation is at about 5% error compared with the exact solution obtained by using steepest descent (162 sec, see [4, 16]), but singular perturbation approximation requires substantially less computational cost. The approximate control which is formed as

$$\alpha_{app}(t) = \alpha^{o}(t) + [\alpha^{il}(\frac{t - t_0}{\epsilon}) - \alpha^{o}(t_0)] + [\alpha^{ir}(\frac{t_f - t}{\epsilon}) - \alpha^{o}(t_f)]$$

is shown in Fig.3.5.

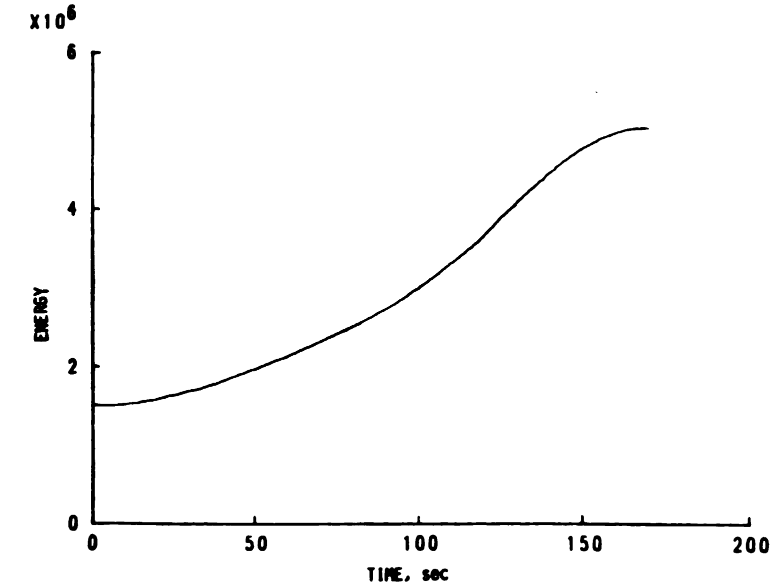

Fig.3.1 Energy time histories for airplane 2

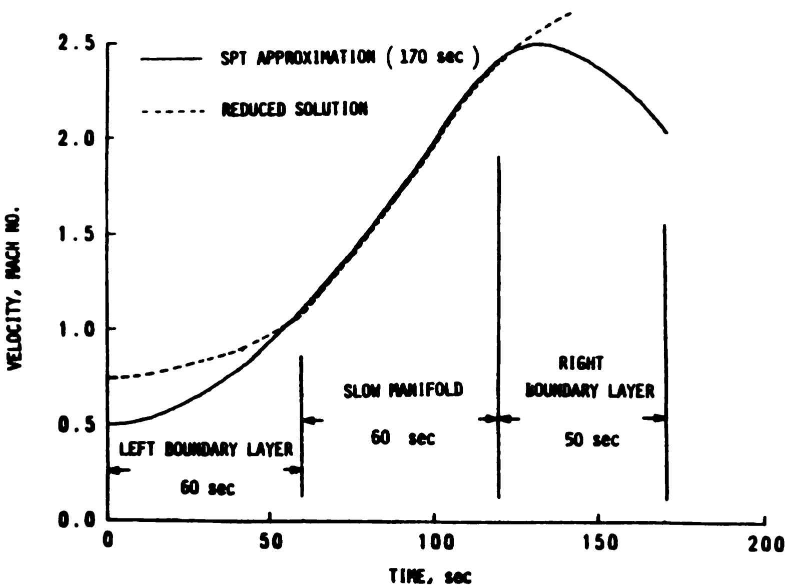

Fig.3.2 Velocity time histories for airplane 2

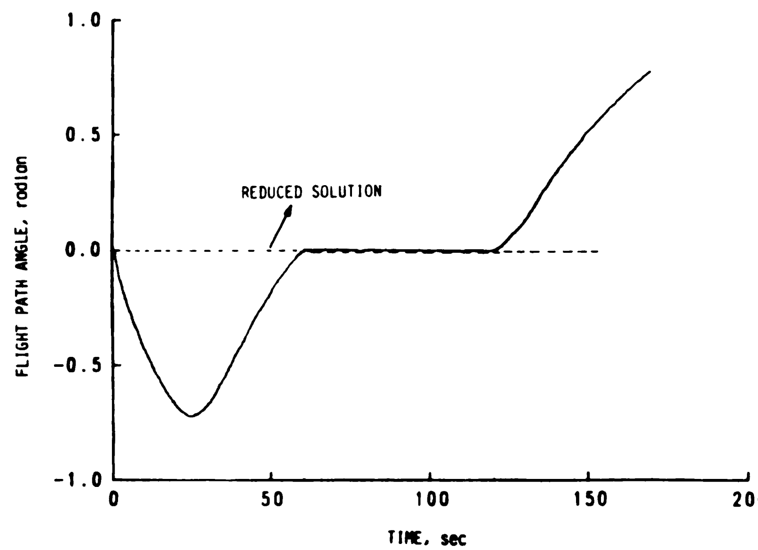

Fig.3.3 Flight path angle time histories for airplane 2

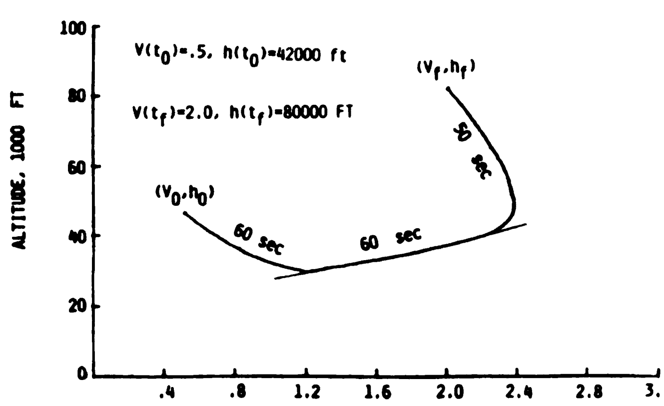

Fig.3.4 Flight trajectory for airplane 2

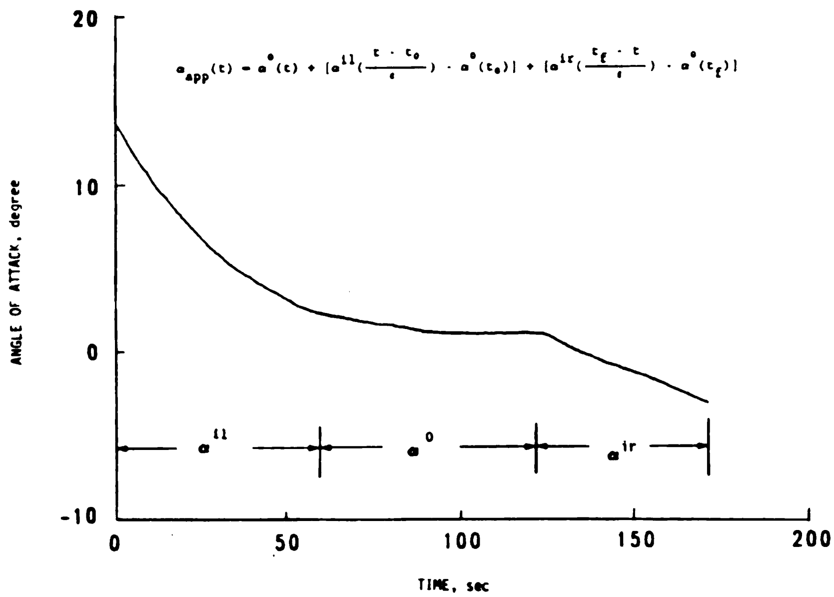

Fig.3.5 Approximate control (α_{app}) for airplane 2

III.2 AUTO-PILOT IMPLEMENTATION

Optimal flight controls are dependent on many factors such as aerodynamics, motor performance, system weight, operational constraints, mission requirements, atmospheric conditions, and the index of performance to be optimized. To establish best possible vehicle performance it is necessary to determine or approximate the optimal control solution. A separate but equally important issue is the real time auto-pilot (on-board) implementation.

Recently, a number of flight mechanics optimization problems have been solved using singular perturbation techniques and resulting in state-feedback control laws, suitable for on-board implementation [18, 31, 32]. In the cited work feedback is introduced to reduce on-line computations while improving accuracy. Calise [18] presents a partial evaluation of the use of singular perturbation methods for developing a computer algorithm for on-line optimal control. He expresses the singular perturbation approximation of optimal control in feedback form (near-optimal feedback control). Emphasis is placed on deriving a solution in a form that minimizes on-board computational requirements and improves accuracy. Visser and Shinar [31] introduce a first order correction feedback control law to improve the accuracy of the singular perturbation approximation for real time implementation. Weston ,et al. [32] proposed a feedback control and discusses its auto-pilot implementation . They linearize the fast boundary-layer system about the reduced solution and obtain feedback control for boundary-layer, where feedback coefficients are function of the slow variables. No one investigated the use of feedback for boundary-layer stabilization.

We mentioned before that the use of open loop control via singular perturbation approximation for on-line, auto-pilot implementation may cause boundary-layer instability when unstable modes are present in the uncontrolled system. This fact was demonstrated on a second-order example in Wilde and Kokotovic [26]. This instability problem can be overcome by using feedback control to stabilize the boundary-layer system. In this section, we emphasize the role of feedback implementation in stabilizing the boundary-layer dynamics and introduce such feedback controls from boundary-layer stabilization viewpoint rather than from near-optimality viewpoint as in earlier work. We propose two feedback stabilization scheme to circumvent this instability problem.

III.2.1 BOUNDARY-LAYER INSTABILITY PROBLEM

In order to investigate the phenomenon of boundary-layer instability, let us illustrate it by considering the flight mechanics model (3.12), the left boundary-layer equations are

$$\frac{dV}{d\tau} = - gSIN\gamma = F_1 \tag{3.24a}$$

$$\frac{d\gamma}{d\tau} = \frac{L - WCOS\gamma}{mV} = F_2 \tag{3.24b}$$

The Jacobian matrix, evaluated along the reduced solution, is given by

$$J = \begin{bmatrix} \frac{\partial F_1}{\partial V} & \frac{\partial F_1}{\partial \gamma} \\ \\ \frac{\partial F_2}{\partial V} & \frac{\partial F_2}{\partial \gamma} \end{bmatrix} = \begin{bmatrix} 0 & -g \\ \\ a & 0 \end{bmatrix} \tag{3.25}$$

where

$$a = \frac{1}{2m}\alpha C_{L\alpha}\rho_0 se^{-Kh} + \frac{1}{2m}\alpha\rho_0 sV(e^{-Kh}\frac{\partial C_{L\alpha}}{\partial V} + C_{L\alpha}e^{-Kh}\ \frac{KV}{g}) > 0$$

The chacteristic equation of (3.25) is

$$S^2 + ga = 0 \tag{3.26}$$

The two roots are on the imaginary axis, so, this system does not satisfy the requirement $Re\lambda(J)<0$.

Application of the approximate control α_{app} of the previous section to the flight mechanics model (3.12), results in the trajectories shown in Fig.3.6. This shows that the trajectory of the left boundary-layer moves away from the slow manifold for real time on-line implementation. But, for off-line calculation, the left boundary-layer is matched to the slow manifold (see previous section) which illustrates the nature of instability properties for on-line implementation.

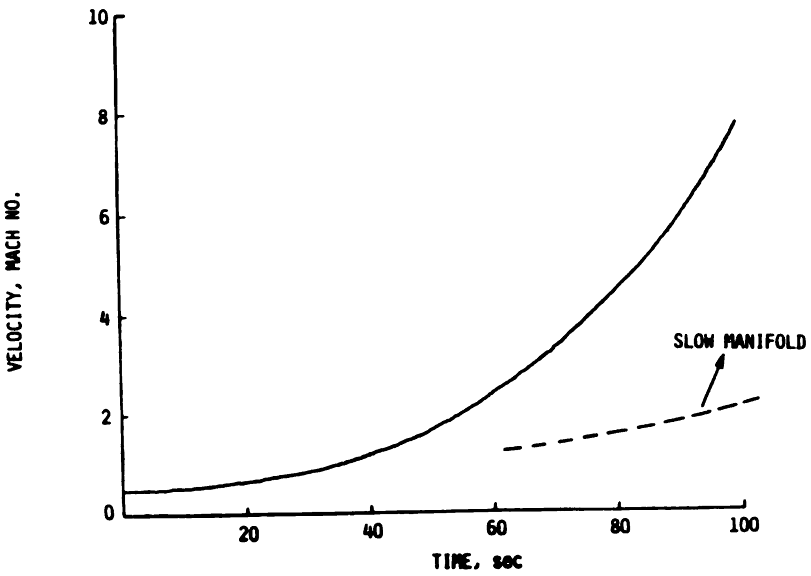

Fig.3.6 Boundary-layer instability for airplane 2

III.2.2 FEEDBACK STABILIZATION

In order to stabilize the boundary-layer, two feedback stabilization control laws are proposed: (a) a linear feedback control; and (b) a nonlinear feedback control.

(a). <u>Linear feedback control</u>: Let us consider the flight mechanics problem and introduce the linear feedback stabilization control as

$$\alpha_L = \alpha^0 - K_1(V - V^0) - K_2(\gamma - \gamma^0) \tag{3.27}$$

with feedback from fast variables V and γ. The feedback terms are effective only on the boundary-layer because $V - V^0$ and $\gamma - \gamma^0$ are $O(\epsilon)$ on the slow manifold.

Substituting (3.27) into boundary-layer system (3.24) yields the Jacobian matrix

$$J = \begin{bmatrix} \dfrac{\partial F_1}{\partial V} & \dfrac{\partial F_1}{\partial \gamma} \\ \\ \dfrac{\partial F_2}{\partial V} & \dfrac{\partial F_2}{\partial \gamma} \end{bmatrix} = \begin{bmatrix} 0 & -g \\ \\ a - k_1 b & -k_2 b \end{bmatrix} \tag{3.28}$$

whose characteristic equation is

$$S^2 + Sk_2 b + g(a - k_1 b) = 0 \ , \qquad \text{where } b = \frac{1}{2m}\rho_0 s C_{L\alpha} e^{-Kh} V \tag{3.29}$$

For asymptotic stability, we should choose $k_1 < a/b$ and $K_2>0$. Taking $k_1 = -2$ and $K_2 = 5$ for this problem, the simulation result is shown in Fig.3.7. This shows that the linear feedback law indeed stabilizes the boubdary-layer and follows the slow manifold closely. With initial conditions sufficiently close to the slow manifold, the auto-pilot will be able to follow the nominal path over the entire range by using this linear feedback control law. But when the initial conditions are far away from the slow manifold, the trajectory will not follow the nominal path any more. The resulting trajectories, shown in Fig.3.8, illustrate the "local" nature of the linear feedback control.

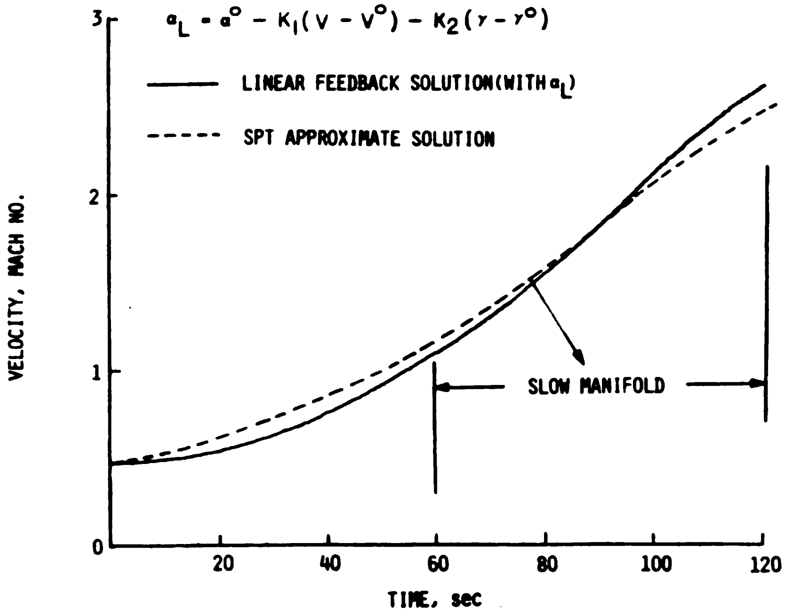

Fig.3.7 Boundary-layer stabilization (with linear feedback stabilization control) for airplane 2

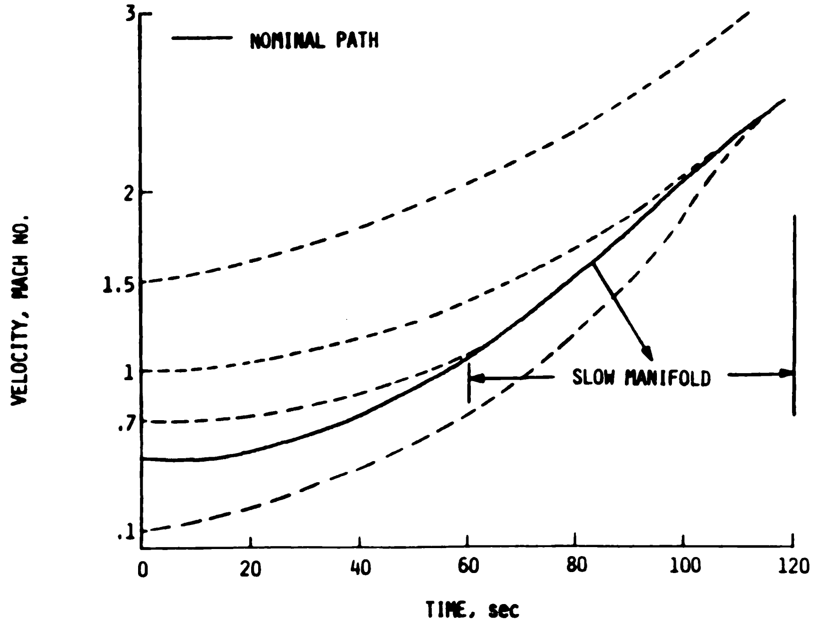

Fig.3.8 Boundary-layer stabilization (with linear feedback stabilization control) with initial disturbance for airplane 2

(b). Nonlinear feedback control: In order to obtain nonlocal boundary-layer stabilization, we use a nonlinear feedback control law. let us rewrite the flight mechanics model (3.12) as

$$\dot{E} = \frac{V}{m}[T(E, V) - \frac{1}{2}\rho V^2 s(C_{D_0}(V) + \eta C_{L\alpha}(V)\alpha^2)] \tag{3.30a}$$

$$\epsilon\dot{V} = \frac{\epsilon g}{W}[T(E, V) - \frac{1}{2}\rho V^2 s(C_{D_0}(V) + \eta C_{L\alpha}(V)\alpha^2] - gSIN\gamma \tag{3.30b}$$

$$\epsilon\dot{\gamma} = \frac{g}{2W}\rho V s C_{L\alpha}(V)\alpha - \frac{g}{V}COS\gamma \tag{3.30c}$$

The nonlinear feedback control law is chosen as

$$\alpha_N = \frac{2W}{\rho V_E^2 sC_{L\alpha}(V_E)} - \frac{2W}{\rho V^2 sC_{L\alpha}(V)} + \frac{2W\mathrm{COS}\gamma}{\rho V^2 sC_{L\alpha}(V)} - \frac{2Wb'\gamma}{\rho gsVC_{L\alpha}(V)} \tag{3.31}$$

where b' is a positive constant and V_E is the energy state approximation solution [see 16] which is the same as the reduced solution V^0 we obtained from previous section III.1.2. Again, this control is effective only on the boundary-layer because on the slow manifold, α_N is $O(\epsilon)$ close to α^0.

After substituting (3.31) into (3.30), the boundary-layer equations are given by

$$\frac{dV}{d\tau} = -g\mathrm{SIN}\gamma = F_1 \tag{3.32a}$$

$$\frac{d\gamma}{d\tau} = \frac{g}{VV_E^2 C_{L\alpha}(V_E)}[V^2 C_{L\alpha}(V) - V_E^2 C_{L\alpha}(V_E)] - b'\gamma = F_2 \tag{3.32b}$$

We assume that $V^2 C_{L\alpha}(V)$ is monotonically increasing (in general it is), which implies that the first term on the right-hand side of equation (3.32b) is a first-quadrant-third-quadrant function in $(V - V_E)$.

Consider a Lyapunov function candidate

$$\nu(V, \gamma) = \int_0^{V-V_E} \frac{1}{(V_E + x)V_E^2 C_{L\alpha}(V_E)}[(V_E + x)^2 C_{L\alpha}(V_E + x) - V_E^2 C_{L\alpha}(V_E)]dx$$
$$+ (1 - \mathrm{COS}\gamma) \tag{3.33}$$

Taking the derivative of ν, we have

$$\frac{d\nu}{d\tau} = -b'\gamma \mathrm{SIN}\gamma < 0 \quad , \qquad \text{for } -\pi < \gamma < \pi \tag{3.34}$$

where $d\nu/d\tau = 0$ implies $\gamma = 0$, $V = V_E$. So, by Lasalle's theorem [see 34], the equilibrium point ($V = V_E$, $\gamma = 0$) is asymptotically stable. Moreover, it was shown by Vasileva [25] and Tihonov [21] that if the domain of interest is bounded and closed, then the property of asymptotic stability for every fixed slow variable, implies the property of asymptotic stability uniformly in the slow variable. So, this system is asymptotically stable uniformly in slow solution V_E (i.e. V^0). Therefore, all the conditions of Tihonov theorem [21] are satisfied.

The Jacobian matrix of the boundary-layer equation (3.32) is

$$J = \begin{bmatrix} \dfrac{\partial F_1}{\partial V} & \dfrac{\partial F_1}{\partial \gamma} \\ & \\ \dfrac{\partial F_2}{\partial V} & \dfrac{\partial F_2}{\partial \gamma} \end{bmatrix} = \begin{bmatrix} 0 & -g \\ & \\ a' & -b' \end{bmatrix} \tag{3.35}$$

where b' is positive constant and

$$a' = \frac{2g}{V_E^2} + \frac{g}{V_E C_{L\alpha}(V_E)} \left(\frac{\partial C_{L\alpha}(V)}{\partial V}\right)_{V=V_E} > 0$$

and its characteristic equation is

$$S^2 + b'S + a'g = 0 \tag{3.36}$$

All roots of (3.36) are in the open left-half complex plane.

Fig.3.9 shows the simulation of the trajectory when the nonlinear feedback control (3.31) is applied to the full singularly perturbed system (3.30). The simulation shows that the nonlinear feedback control law for on-line, auto-pilot implementation will also stabilize the boundary-layer. Again, tests were performed with initial conditions up to Mach number 1.5. The resulting trajectories are shown in Fig.3.10. These show that the nonlinear feedback control law is able to control the aircraft so that it approaches the neighborhood of the nominal path for initial perturbations larger than those of the linear feedback control. Notice, in particular, the trajectory starting at Mach number 1.5 and compare Figures 3.8 and 3.10. This comparision emphasizes the nonlocal nature of the nonlinear feedback control vs the local nature of the linear one.

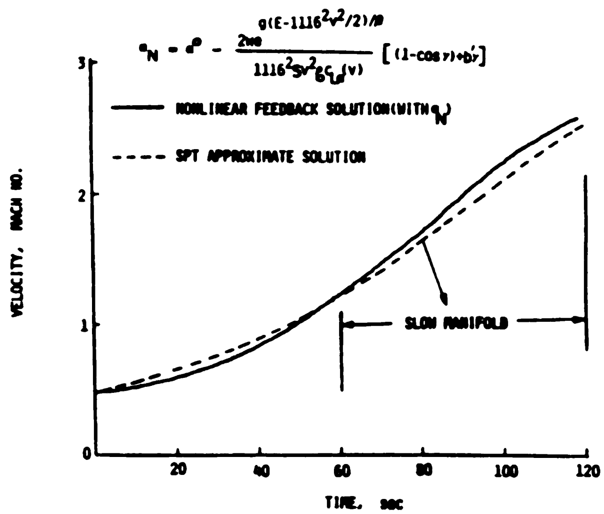

Fig.3.9 Boundary-layer stabilization (with nonlinear feedback stabilization control) for airplane 2

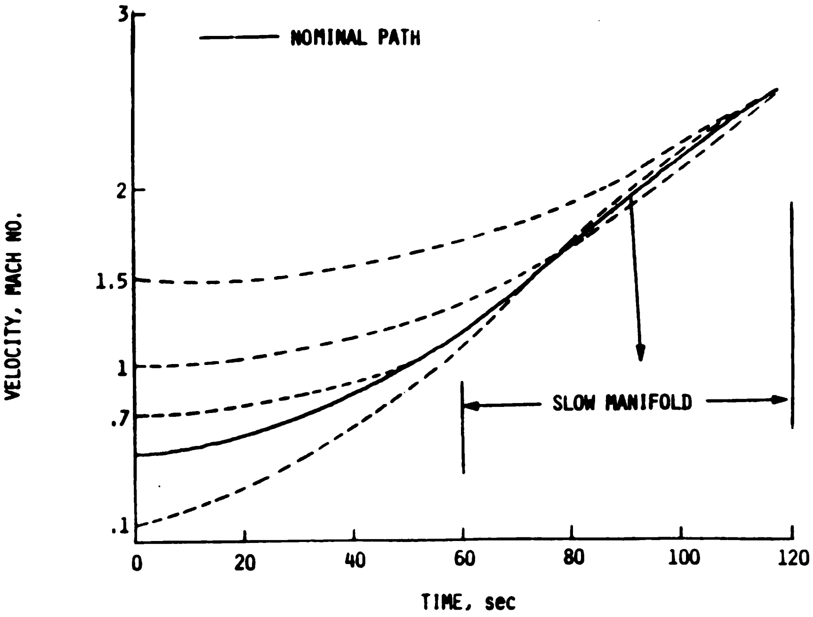

Fig.3.10 Boundary-layer stabilization (with nonlinear feedback stabilization control) with initial disturbance for airplane 2

IV. STEERING CONTROL OF SINGULARLY PERTURBED SYSTEMS: A COMPOSITE CONTROL APPROACH

In this chapter, we develop a composite control approach to the problem of steering the state of a singularly perturbed system from a given initial state to a given final state, while minimizing a cost functional. Asymptotic validity of the composite control is established by showing that its application to the singularly perturbed system results in a final state which is $O(\epsilon)$ close to the desired state. Moreover, the cost under the composite control is $O(\epsilon)$ close to the optimal cost of the reduced control problem. The performance of the composite control is illustrated by examples.

IV.1 PROBLEM STATEMENT AND COMPOSITE CONTROL APPROACH

Consider the singularly perturbed system

$$\dot{x} = f(x, z, u, \epsilon, t) \tag{4.1a}$$

$$\epsilon\dot{z} = a(x, \epsilon, t) + A(x, \epsilon, t)z + B(x, \epsilon, t)u + \epsilon g_1(x, z, u, \epsilon, t) \tag{4.1b}$$

where $x \epsilon R^n$, $z \epsilon R^m$, $u \epsilon R^r$ and ϵ is a small positive parameter. A control $u(t)$ is sought to steer the state x, z from an initial state $x(t_0) = x_0$, $z(t_0) = z_0$ to a terminal state $x(t_f) = x_f$ and $z(t_f) = z_f$, while minimizing the cost functional

$$J = \int_{t_0}^{t_f} [V_1(x, \epsilon, t) + z^T V_2(x, \epsilon, t)z + u^T R(x, \epsilon, t)u]dt \tag{4.2}$$

This problem will be studied under the following assumption

Assumption 4.1: The functions, f, a, A, B, g_1, V_1, V_2 and R are assumed to be sufficiently smooth in all their arguments, i.e. differentiable a sufficient number of times, in a domain of interest. Furthermore,

V_1 and V_2 are positive semidefinite and R is positive definite in the same domain. Other assumptions will be made later on.

This optimal control problem has been studied by many researchers; see, for example, O'Malley [36], Sannuti [37], Chow [23] and Kokotovic, Khalil and O'Reilly [19]. In these studies, asymptotic approximations of the optimal trajectories are obtained via analyzing the singularly perturbed two-point boundary value problem that results from applying the maximum principle. These asymptotic approximations have been extensively used in flight mechanics problems; see, for example, Kelley [3], Ardema [4], Calise [18] and Visser and Shinar [31].

We develop a composite control approach to the steering control problem. Composite control of singularly perturbed systems has been known in the context of stabilizing feedback control. It was first introduced by Chow and Kokotovic [38] for linear systems and later generalized to nonlinear systems by Chow and Kokotovic [39], Suzuki [40] and Saberi and Khalil [41]. According to this approach, a stabilizing feedback control is sought as the sum of two components. The first component is a reduced control that stabilizes the reduced system, obtained by setting $\epsilon = 0$ and eliminating fast variables (z in (4.1)). The second component stabilizes the boundary-layer system. In our steering control problem, the composite control will be sought as the sum of three components. The first one is the reduced control which solves the simplified problem obtained upon setting $\epsilon = 0$. The second component is a feedback component that stabilizes the boundary-layer system. The third component is a right boundary-layer component that steers the fast variable z from the reduced solution to the desired terminal state z_f. The three components are derived in the next section.

The proposed composite control is similar to that of Chow [23] in that it comprises three components, but with different procedures of calculating the boundary-layer components. In our method, the boundary-layer controls do not optimize cost functionals as in Chow. The left boundary-layer control is a feedback stabilizing control that ensures boundary-layer stability, while the right boundary-layer control is the well-known minimum energy control that steers the state of the linear boundary-layer system to its target state. Our analysis does not involve asymptotic analysis of the full optimal control. Therefore, our assumptions are weaker than those of Chow.

IV.2 DERIVATION OF THE COMPOSITE CONTROL

IV.2.1 THE REDUCED CONTROL

The reduced (or slow) problem is obtained by setting $\epsilon = 0$ in (4.1)-(4.2) and dropping the requirement $z(t_0) = z_0$, $z(t_f) = z_f$, that is the reduced problem is defined as

$$\dot{x}^o = f(x^o, z^o, u^o, 0, t), \qquad x^o(t_0) = x_0, \quad x^o(t_f) = x_f \tag{4.3a}$$

$$0 = a(x^o, 0, t) + A(x^o, 0, t)z^o + B(x^o, 0, t)u^o \tag{4.3b}$$

$$J^o = \int_{t_0}^{t_f} [V_1(x^o, 0, t) + (z^o)^T V_2(x^o, 0, t)z^o + (u^o)^T R(x^o, 0, t)u^o]dt \tag{4.4}$$

where the superscript "^{0}" stands for the solution of the reduced problem. For the reduced problem to be well-defined, we must be able to use the algebraic equation (4.3b) to reduced the (n+m)-dimensional state vector x^0, z^0 to an n-dimensional vector. A typical assumption in the singular perturbation literature, e.g., Kokotovic, Khalil and O'Reilly [19], is to require the matrix $A(x^0, 0, t)$ to be nonsingular. This assumption, however, is not needed in the asymptotic analysis of the two-point boundary-layer value problem associated with the full problem (4.1) - (4.2). It is also restrictive and eliminates the interesting problems that arise in flight mechanics. Therefore, we make the following weaker assumption.

<u>Assumption 4.2:</u> The mx(m+r) matrix $[A(x^0, 0, t) \;\; B(x^0, 0, t)]$ has m linearly independent columns in the domain of interest.

This assumption implies that rank$[A \;\; B]$=m for all x^0 and t, but not vice-versa. A weaker assumption would be to require rank$[A \;\; B]$=m, but this would complicate the analysis. Assumption 4.2 guarantees the existence of a permutation matrix P such that the first m columns of $[A \;\; B]P$ are linearly independent for all x^0 and t, e.g.

$$[A_2(x^0, t) \;\; B_2(x^0, t)] = [A(x^0, 0, t) \;\; B(x^0, 0, t)]P \tag{4.5}$$

where $A_2(x^0, t)$ is nonsingular. Defining $\bar{z}^0$ and $\bar{u}^0$ by

$$\begin{bmatrix} z^0 \\ u^0 \end{bmatrix} = P \begin{bmatrix} \bar{z}^0 \\ \bar{u}^0 \end{bmatrix} \triangleq \begin{bmatrix} P_{11} & P_{12} \\ P_{21} & P_{22} \end{bmatrix} \begin{bmatrix} \bar{z}^0 \\ \bar{u}^0 \end{bmatrix} \tag{4.6}$$

the algebraic equation (4.3b) can be rearranged as

$$0 = a + [A \quad B]PP^T \begin{bmatrix} z^0 \\ u^0 \end{bmatrix} = a + [A_2 \quad B_2] \begin{bmatrix} \bar{z}^0 \\ \bar{u}^0 \end{bmatrix} \tag{4.7}$$

Hence, the reduced problem (4.3) - (4.4) can be rewritten as

$$\dot{x}^0 = \bar{f}(x^0, \bar{z}^0, \bar{u}^0, t) \quad , \qquad x^0(t_0) = x^0 \ , \quad x^0(t_f) = x_f \tag{4.8a}$$

$$0 = a(x^0, 0, t) + A_2(x^0, t)\bar{z}^0 + B_2(x^0, t)\bar{u}^0 \tag{4.8b}$$

$$J^0 = \int_{t_0}^{t_f} \{V_1(x^0, 0, t) + [(\bar{z}^0)^T \quad (\bar{u}^0)^T]P^T \begin{bmatrix} V_2(x^0, 0, t) & 0 \\ 0 & R(x^0, 0. t) \end{bmatrix} \cdot P \begin{bmatrix} \bar{z}^0 \\ \bar{u}^0 \end{bmatrix} \}dt \tag{4.9}$$

where $\bar{f}(x^0, \bar{z}^0, \bar{u}^0, t) = f(x^0, P_{11}\bar{z}^0 + P_{12}\bar{u}^0, P_{21}\bar{z}^0 + P_{22}\bar{u}^0, 0, t)$, and $A_2(x^0, t)$ is nonsingular. Note that if $A(x^0, 0, t)$ is nonsingular to start with, the permutation matrix P is taken to be the identity matrix. Problem (4.8) - (4.9) satisfies the standard assumption of nonsingularity of $A_2(x^0, t)$. Substitution of

$$\bar{z}^0 = -A_2^{-1}(a + B_2\bar{u}^0) \tag{4.10}$$

into (4.8a) and (4.9) yields

$$\dot{x}^0 = \bar{f}^0(x^0, \bar{u}^0, t) \quad , \qquad x^0(t_0) = x_0 \ , \quad x^0(t_f) = x_f \tag{4.11}$$

$$J^0 = \int_{t_0}^{t_f} [Q_0(x^0, t) + 2D_0^T(x^0, t)\bar{u}^0 + (\bar{u}^0)^T R_0(x^0, t)\bar{u}^0]dt \tag{4.12}$$

where

$$\bar{f}^0(x^0, \bar{u}^0, t) = \bar{f}(x^0, -A_2^{-1}(a + B_2\bar{u}^0), \bar{u}^0, t) \tag{4.13}$$

$$Q_0 = V_1 + a^T A_2^{-T} M_{11} A_2^{-1} a \tag{4.14a}$$

$$D_0 = B_2^T A_2^{-T} M_{11} A_2^{-1} a - M_{12}^T A_2^{-1} a \tag{4.14b}$$

$$R_0 = B_2^T A_2^{-T} M_{11} A_2^{-1} B_2 - B_2^T A_2^{-T} M_{12} - M_{12}^T A_2^{-1} B_2 + M_{22} \tag{4.14c}$$

$$M_{11} = P_{11}^T V_2 P_{11} + P_{21}^T R P_{21} \tag{4.14d}$$

$$M_{12} = P_{11}^T V_2 P_{12} + P_{12}^T R P_{22} \tag{4.14e}$$

and

$$M_{22} = P_{12}^T V_2 P_{12} + P_{22}^T R P_{22} \tag{4.14f}$$

The reduced control problem (4.11), (4.12) is formally correct in the sense that its necessary conditions for optimality coincide with the necessary conditions of the full problem (4.1) - (4.2) upon setting $\epsilon = 0$. This fact is shown in section 6.3 of Kokotovic, Khalil and O'Reilly [19] for the reduced problem (4.8) - (4.9), which is the same as the reduced problem (4.11) - (4.12). We assume that

Assumption 4.3: The reduced control problem (4.11) - (4.12) has a unique optimal solution $\bar{u}^0(t)$, $x^0(t)$, which is continuously differentiable on $[t_0, t_f]$. Once $\bar{u}^0(t)$ and $x^0(t)$ are calculated, $\bar{z}^0(t)$ can be obtained from (4.10), and the reduced control $u^0(t)$ is given by

$$u^0 = P_{21}\bar{z}^0 + P_{22}\bar{u}^0 \tag{4.15}$$

IV.2.2 BOUNDARY-LAYER STABILIZING CONTROL

A characteristic phenomenon of singularly perturbed systems is the presence of boundary layers during which the fast variable z approaches it reduced, or quasi-steady state trajectory. For this phenomenon to take place, the boundary-layer system needs to be asymptotically stable, see Kokotovic, Khalil and O'Reilly [19]. For the system (4.1) this will be the case if the matrix $A(x, 0, t)$ is Hurwitz uniformly in x and t, i.e., $\mathrm{Re}\lambda[A(x, 0, t)] \le -c < 0$ for all x and t in the domain of interest.

If this condition holds, application of the reduced control (4.15) to the system (4.1) will result in trajectories of x, z and u which approach x^o, z^o and u^o after a boundary-layer. If A(x, 0, t) is not Hurwitz, feedback must be used to stabilize the boundary-layer system. It is important to notice that without feedback, the boundary-layer will be unstable even when open-loop boundary-layer corrections are added to u^o. This fact was demonstrated on a second-order example in Wilde and Kokotovic [26], and on a flight mechanics model in Chapter III. The boundary-layer system is obtained by expressing (4.1b) in the fast time-scale $\tau = (t - t_1)/\epsilon$, $t_1 \geq t_0$, and then setting $\epsilon = 0$. It is given by

$$\frac{dz}{d\tau} = a(x, 0, t) + A(x, 0, t)z + B(x, 0, t)u \tag{4.16}$$

where $u = u^o + u_F$ and x, u^o and t are frozen at their values at $t = t_1$. Notice that the boundary-layer stability should hold along the reduced trajectory and not only at the initial time t_0. If A(x, 0, t) is not Hurwitz or it is Hurwitz but its stability properties are not adequate, u_F can be used to stabilize the system. Let us first shift the equilibrium of (4.16) to the origin. The steady-state of (4.16), with $u_F = 0$, is

$$0 = a(x, 0, t) + A(x, 0, t)z^o + B(x, 0, t)u^o \tag{4.17}$$

Substracting (4.17) from (4.16) and setting $z_F = z - z^o$, we obtain

$$\frac{dz_F}{d\tau} = A(x,\ 0,\ t)z_F + B(x,\ 0,\ t)u_F \tag{4.18}$$

with x and t treated as fixed parameters. The system (4.18) is a linear system whose stabilizability is stated in the following assumption.

Assumption 4.4: The pair [A(x, 0, t)   B(x, 0, t)] is stabilizable uniformly in x and t in the domain of interest, e.g., there exists a sufficiently smooth matrix K(x, t) such that

$$\mathrm{Re}\lambda(A(x,\ 0,\ t) + B(x,\ 0,\ t)K(x,\ t)) < -c < 0 \tag{4.19}$$

Thus, the boundary-layer stabilizing control is given by

$$u_F = K(x,\ t)z_F = K(x,\ t)(z - \overset{o}{z}) \tag{4.20}$$

IV.2.3 RIGHT BOUNDARY-LAYER CONTROL

So far, we have derived the reduced control $\overset{o}{u}$ and the boundary-layer stabilizing control u_F. Application of $u = \overset{o}{u} + u_F$ to the system (4.1), (4.1) will result in a trajectory x(t), z(t) that approaches the reduced state $\overset{o}{x}(t)$, $\overset{o}{z}(t)$ after an $O(\epsilon \ln\frac{1}{\epsilon})$ boundary-layer and then moves along it. At the terminal time t_f, $x(t_f)$ and $z(t_f)$ will be in an $O(\epsilon)$ neighborhood of $\overset{o}{x}(t_f) = x_f$ and $\overset{o}{z}(t_f)$. Since $\overset{o}{z}(t_f) \neq z_f$, in general, a terminal boundary-layer control u_b should be added to $\overset{o}{u} + u_F$, whose function would be to steer z(t) from an $O(\epsilon)$ neighborhood of the desired state z_f. This motion will take place over a time interval $[t_f-\Delta,\ t_f]$, $\Delta>0$. To derive u_b, we consider the boundary-layer system (4.16) with $u = u^0 + u_F + u_b$ and with $t_1 = t_f$, that is with x, z^0, u^0 and t frozen at $x(t_f)$, $z^0(t_f)$, $u^0(t_f)$ and t_f, respectively. Anticipating that $x(t_f)$ will be within $O(\epsilon)$ of x_f, we freeze x at x_f instead of $x(t_f)$. Thus, the right boundary-layer model is given by

$$\frac{dz}{d\sigma} = a(x_f,\ 0,\ t_f) + A(x_f,\ 0,\ t)z + B(x_f,\ 0,\ t)[$$

$$u^0(t_f) + K(x_f,\ t_f)(z - z^0(t_f)) + u_b]$$

$$= a(x_f,\ 0,\ t_f) + H(x_f,\ t_f)z + B(x_f,\ 0,\ t_f)[u^0(t_f) -$$

$$K(x_f,\ t_f)z^0(t_f) + u_b] \qquad (4.21)$$

where $\sigma = (t - t_f)/\epsilon$ and $H = A + BK$. Equation (4.21) has equilibrium at $z = z^0(t_f)$. Defining $z_b = z - z^0(t_f)$, we obtain

$$\frac{dz_b}{d\sigma} = H(x_f,\ t_f)z_b + B(x_f,\ 0,\ t)u_b \qquad (4.22)$$

The right boundary-layer control problem is to move z_b from $z_b = 0$ at $\sigma = -\Delta/\epsilon$ to $z_b = z_f - z^0(t_f)$ at $\sigma = 0$. Since the system (4.22) is linear, the solutuion of this steering control problem is well-known, e.g., Chen [42]. It requires the following assumption

<u>Assumption 4.5:</u> The pair $[A(x_f,\ 0,\ t)\ \ B(x_f,\ 0,\ t)]$ is controllable. Since $H = A + BK$, controllability of (A, B) implies controllibility of (H, B) for any matrix K. The minimum energy control that moves z_b from $z_b(-\Delta/\epsilon) = 0$ to $z_b(0) = z_f - z^0(t_f)$ is given by (Chen [42])

$$u_b(\sigma) = B^T(e^{-\sigma H})^T W^{-1}(\Delta/\epsilon)(z_b(0) - e^{H\Delta/\epsilon} z_b(-\Delta/\epsilon)) \tag{4.23}$$

where the controllability Grammian $W(\Delta/\epsilon)$ is given by

$$W(\Delta/\epsilon) = \int_{-\Delta/\epsilon}^{0} e^{-\sigma H} B B^T (e^{-\sigma H})^T d\sigma = \int_{0}^{\Delta/\epsilon} e^{\lambda H} B B^T (e^{\lambda H})^T d\lambda \tag{4.24}$$

In (4.23) and (4.24) the arguments of $H(x_f, t_f)$ and $B(x_f, 0, t_f)$ are omitted for convenience. Due to the Hurwitz property of H, the matrix $W(\Delta/\epsilon)$ may be approximated by $W_\infty = W(\infty)$, i.e.,

$$\begin{aligned} W(\Delta/\epsilon) &= W(\infty) - \int_{\Delta/\epsilon}^{\infty} e^{\lambda H} B B^T (e^{\lambda H})^T d\lambda \\ &\triangleq W(\infty) - E(\Delta/\epsilon) \end{aligned} \tag{4.25}$$

where

$$\left\| E(\Delta/\epsilon) \right\| \le \int_{\Delta/\epsilon}^{\infty} K e^{-\alpha\lambda} d\lambda \le \frac{K}{\alpha} e^{-\alpha\Delta/\epsilon} = O(\epsilon) \tag{4.26}$$

Moreover, $e^{H\Delta/\epsilon}$ is $O(\epsilon)$. Thus, u_b can be approximated by

$$u_b(\sigma) = B^T(e^{-\sigma H})^T W^{-1}(\infty)(z_f - z^0(t_f)) \tag{4.27}$$

where $W(\infty)$ satisfies the algebraic Lyapunov equation

$$HW(\infty) + W(\infty)H^T + BB^T = 0 \tag{4.28}$$

In the t time scale, u_b is given by

$$u_b(t) = B^T(e^{(t_f - t)H/\epsilon})^T W^{-1}(\infty)(z_f - z^0(t_f)) \tag{4.29}$$

It is important to notice that $u_b(t)$ is indenpendent of the constant Δ. It depends only on the final time t_f. If t_f is known, the expression (4.29) can be calculated and inplemented from the initial time t_0. Due to the exponential term $\exp((t_f-t)H/\epsilon)$, the expression (4.29) will be effective only in an $O(\epsilon\ln(1/\epsilon))$ neighborhood of t_f. The final time t_f will be known if t_f is fixed to start with. When t_f is free, it should be estimated. Let $\overset{o}{t}_f$ be the final time determined from the solution of the reduced problem. Then t_f can be taken as $t_f = \overset{o}{t}_f + \delta(\epsilon)$ where $\delta(\epsilon)$ satisfies

$$\left\| B^T (e^{\delta(\epsilon)H/\epsilon})^T W^{-1}(\infty)(z_f - \overset{o}{z}(t_f)) \right\| = O(\epsilon) \tag{4.30}$$

It can be shown that $\delta(\epsilon) = O(\epsilon\ln(1/\epsilon))$, hence $\delta(\epsilon)\to 0$ as $\epsilon\to 0$.

The composite control is taken as

$$\begin{aligned} u_c &= \overset{o}{u} + u_F + u_b \\ &= \overset{o}{u} + K(x, t)[z - \overset{o}{z}(t)] + B^T(x_f, 0, t)[\exp((t_f - t)H(x_f, t_f)/\epsilon)]^T \\ &\quad W^{-1}(\infty)(z_f - \overset{o}{z}(t_f)) \end{aligned} \tag{4.31}$$

IV.3 ASYMPTOTIC VALIDITY OF THE COMPOSITE CONTROL

Asymptotic validity of the composite control is established by the following theorem

THEOREM 4.1: Suppose that Assumptions 4.1 - 4.5 hold and that the composite control (4.31) is applied to the singularly perturbed system

(4.1). Then, there exsits $\epsilon^{*}>0$ such that for all $\epsilon \in (0, \epsilon^{*}]$

$$\left\| x(t_f) - x_f \right\| = O(\epsilon) \tag{4.32}$$

$$\left\| z(t_f) - z_f \right\| = O(\epsilon) \tag{4.33}$$

$$\left\| J(u_c) - J^{0}(u^{0}) \right\| = O(\epsilon) \tag{4.34}$$

The theorem states that application of the composite control (4.31) to the singularly perturbed system (4.1) results in a final state which is $O(\epsilon)$ close to the desired final state and a cost which is $O(\epsilon)$ close to the optimal cost of the reduced control problem.

<u>Proof</u>: Consider the singularly perturbed system (4.1) under the composite control

$$\dot{x} = f(x,\ z,\ u^{0} + u_F + u_b,\ \epsilon,\ t) \tag{4.35a}$$

$$\epsilon\dot{z} = a\ (x,\ \epsilon,\ t) + A\ (x,\ \epsilon,\ t)z + B\ (x,\ \epsilon,\ t)(u^{0} + u_F + u_b)$$

$$+ \epsilon g_1(x,\ z,\ u,\ \epsilon,\ t) \tag{4.35b}$$

$$J = \int_{t_0}^{t_f} [V_1(x,\ \epsilon,\ t) + z^T V_2(x,\ \epsilon,\ t)z + u^T R(x,\ \epsilon,\ t)u]dt \tag{4.36}$$

where x, z, u are functions of t and $u = u_c = u^{0} + u_F + u_b$ is established by (4.31).During the proof we will need to use the property that over the time interval $[t_0, t_f]$ the full solution $(x(t), z(t), u(t))$ exists and is bounded. This follows from the existence of the reduced solution (Assumption 4.3) and the closeness of the full and reduced solution for sufficiently small ϵ. This closeness, however, is to be established in the midest of the proof. Therefore, we cannot start by assuming the boundness of the full solution. To circumvent this problem we take a large enough compact set S; defined by $S = \{x, z, u \mid \|x\| \le r, \|z\| \le r, \|u\| \le r\}$ and let $T = \min(t_f$, first exist time from S). All analysis will be done over the time interval $[t_0, T]$ for which the full solution is bounded. Then we will show that r can be chosen large enough such that, for sufficiently small ϵ, the first exist time from S will be greater than t_f. Since f and g_1 are continuous function of x, z, and u, this implies that f and g_1 are bounded by a constant which is function of r. Let us introduce the quantities

$$\delta a = a(x, \epsilon, t) - a(\overset{o}{x}, 0, t), \quad \delta_1 A = A(x, 0, t) - A(\overset{o}{x}, 0, t)$$

$$\delta A = A(x, \epsilon, t) - A(\overset{o}{x}, 0, t), \ \delta_1 B = B(x, 0, t) - B(\overset{o}{x}, 0, t) \quad (4.37)$$

$$\delta B = B(x, \epsilon, t) - B(\overset{o}{x}, 0, t)$$

and

$$\phi = z(t) - \overset{o}{z}(t) \quad (4.38)$$

Substition of (4.37) and (4.38) into (4.35b), yields

$$\epsilon\dot{z} = (\delta a + \delta Az + \delta Bu + \delta_1 Az^{o} + \delta_1 Bu^{o} + \epsilon g_1(x, z, u, \epsilon, t)) + a(x^{o}, 0, t)$$
$$+ A(x^{o}, 0, t)z^{o} + B(x^{o}, 0, t)u^{o} + [A(x, 0, t) +$$
$$B(x, 0, t)K(x, t)]\phi + B(x, 0, t)u_b \tag{4.39}$$

$$\epsilon(\dot{z} - \dot{z}^{o}) = \epsilon\dot{\phi} = H(x, t)\phi + B(x^{o}, 0, t)u_b + \epsilon\Delta_1 + \epsilon\Delta_2 \tag{4.40}$$

where $\Delta_1 = \Delta_1(t) = \delta a + \delta Az + \delta Bu + \delta_1 A\, z^{o} + \delta_1 Bu^{o}$, $\Delta_2 = \Delta_2(t) =$ $g_1(x, z, u, \epsilon, t) - \dot{z}^{o}$ and $H(x, t) = A(x, o, t) + K(x, t)B(x, 0, t)$

From Assumptions 4.1 - 4.5, we have

$$\mathrm{Re}\lambda(H(x\ , 0, t)) \leq -\delta < 0\ , \qquad \text{for all } t \in [t_0, T] \tag{4.41}$$

$$\left\| H(x\ , 0, t) \right\| \leq \gamma\ , \qquad \text{for all } t \in [t_0, T] \tag{4.42}$$

$$\left\| \frac{d}{dt} H(x\ , 0, t) \right\| \leq \beta\ , \qquad \text{for all } t \in [t_0, T] \tag{4.43}$$

Under (4.41) - (4.43), there exist positive constant α_1 and K_1 such that the transition matrix of equation (4.40) satisfies (see [19])

$$\left\| \Phi(t, t_0) \right\| \leq K_1 e^{-\alpha_1(t - t_0)/\epsilon}\ , \qquad \text{for all } t \in [t_0, T] \tag{4.44}$$

Now, applying the variation of constants formula to equation (4.40) yields

$$\phi(t) = \Phi(t, t_0)\phi(t_0) + \frac{1}{\epsilon}\int_{t_0}^{t} \Phi(t, \tau)B_2(x(\tau), 0, \tau)u_b(\tau)d\tau$$
$$+ \frac{1}{\epsilon}\int_{t_0}^{t} \Phi(t, \tau)\Delta_1(\tau)d\tau + \int_{t_0}^{t} \Phi(t, \tau)\Delta_2(\tau)d\tau \tag{4.45}$$

$$\|\phi(t)\| \le \|\Phi(t, t_0)\| \, \|\phi(t_0)\| + \frac{1}{\epsilon}\int_{t_0}^{t} \|\Phi(t, \tau)\| \, \|B_2(x(\tau), 0, \tau)u_b(\tau)\| d\tau$$
$$+ \frac{1}{\epsilon}\int_{t_0}^{t} \|\Phi(t, \tau)\| \, \|\Delta_1(\tau)\| d\tau + \int_{t_0}^{t} \|\phi(t, \tau)\| \, \|\Delta_2(\tau)\| d\tau \tag{4.46}$$

By Lipschitz property of a , A and B , and the boundedness of the solution we have

$$\|\Delta_1\| = \|\delta a + \delta Az + \delta_1 Az^0 + \delta Bu + \delta_1 Bu^0\|$$

$$\le \|\delta a\| + \|\delta A\| \, \|z\| + \|\delta_1 A\| \, \|z^0\| + \|\delta B\| \, \|u\| + \|\delta_1 B\| \, \|u^0\|$$

$$= \|a(x, \epsilon, t) - a(x^0, 0, t)\| + \|A(X, \epsilon, t) - A(x^0, 0, t)\| \, \|z\|$$

$$+ \|A(x, o, t) - A(x^0, 0, t)\| \, \|z^0\| +$$

$$\|B(x, \epsilon, t) - B(x^0, 0, t)\| \, \|u\| + \|B(x, o, t) - B(x^0, 0, t)\| \, \|u^0\|$$

$$= \| a(x, \epsilon, t) - a(x^0, \epsilon, t) + a(x^0, \epsilon, t) - a(x^0, 0, t) \| +$$

$$\| A(x, \epsilon, t) - A(x^0, \epsilon, t) + A(x^0, \epsilon, t) - A(x^0, 0, t) \| \| z \| +$$

$$\| A(x, o, t) - A(x^0, 0, t) \| \| z^0 \| + \| B(x, 0, t) - B(x^0, 0, t) \| \| u^0 \|$$

$$+ \| B(x, \epsilon, t) - B(x^0, \epsilon, t) + B(x^0, \epsilon, t) - B(x^0, 0, t) \| \| u \|$$

$$\leq C_1 \| x - x^0 \| + C_2 \epsilon \tag{4.47}$$

where the constants C_i, $i = 1, 2, 3, \ldots\ldots$ we use in (4.47), and later on, are all dependent on r.

Substitution of (4.47) and (4.29) into (4.46), yields

$$\| \phi(t) \| \leq \| \Phi(t, t_0) \| \| \phi(t_0) \| + \frac{1}{\epsilon} \int_{t_0}^{t} \| \Phi(t, \tau) \| \| B B^T (e^{H(t_f - t)/\epsilon})^T \cdot$$

$$W^{-1}(z_f - z_f^0) \| d\tau + \int_{t_0}^{t} \| \Phi(t, \tau) \| (\| \Delta_2(\tau) \| + C_2) d\tau +$$

$$\frac{1}{\epsilon} \int_{t_0}^{t} \| \Phi(t, \tau) \| C_1 \| x(\tau) - x^0(\tau) \| d\tau$$

$$\leq K' e^{-\alpha_1 (t - t_0)/\epsilon} + \frac{1}{\epsilon} \int_{t_0}^{t} K_1 e^{-\alpha_1 (t - \tau)/\epsilon} K'' e^{-\alpha_1 (t_f - \tau)/\epsilon} d\tau$$

$$+ \int_{t_0}^{t} K_1 e^{-\alpha_1 (t - \tau)/\epsilon} C_3 d\tau +$$

$$\frac{C_1}{\epsilon} \int_{t_0}^{t} K_1 e^{-\alpha_1 (t - \tau)/\epsilon} \| x(\tau) - x^0(\tau) \| d\tau$$

$$= K' e^{-\alpha_1(t - t_0)/\epsilon} + \frac{K_1 K''}{2\alpha_1}\left(e^{-\alpha_1(t_f - t)/\epsilon} - e^{-\alpha_1(t - t_0)/\epsilon} e^{-\alpha_1(t_f - t_0)/\epsilon}\right)$$

$$+ \frac{\epsilon K_1 C_3}{\alpha_1}\left(1 - e^{-\alpha_1(t - t_0)/\epsilon}\right) +$$

$$\frac{C_1}{\epsilon}\int_{t_0}^{t} K_1 e^{-\alpha_1(t - \tau)/\epsilon} \| x(\tau) - x^0(\tau) \| \, d\tau \tag{4.48}$$

where $\| \Delta_2 \| + C_2 \le C_3$

$$\| \phi(t) \| = \| z(t) - z^0(t) \| \le C_4 \epsilon + K_6 e^{-\alpha_1(t - t_0)/\epsilon} + K_7 e^{-\alpha_1(t_f - t)/\epsilon}$$

$$+ \frac{C_1 K_1}{\epsilon}\int_{t_0}^{t} e^{-\alpha_1(t - \tau)/\epsilon} \| x(\tau) - x^0(\tau) \| \, d\tau \qquad \text{for all } t \in [t_0, T] \tag{4.49}$$

We also have

$$\left\| u(t) - u^0(t) \right\| = \left\| u^0(t) + u_F(t) + u_b(t) - u^0(t) \right\| = \left\| u_F(t) + u_b(t) \right\|$$

$$\le \left\| u_F(t) \right\| + \left\| u_b(t) \right\|$$

$$= \left\| K(x, t)(z(t) - z^0(t)) \right\| + \left\| u_b(t) \right\|$$

$$\le \left\| K(x, t) \right\| \left\| z(t) - z^0(t) \right\| + \left\| u_b(t) \right\| \tag{4.50}$$

Upon substituting (4.49) into (4.50), we obtain

$$\left\|u(t) - u^{0}(t)\right\| \le C_6\epsilon + K_3 e^{-\alpha_1(t - t_0)/\epsilon} + K_4 e^{-\alpha_1(t_f - t)/\epsilon}$$

$$+ \frac{C_5}{\epsilon}\int_{t_0}^{t} e^{-\alpha_1(t - \tau)/\epsilon} \left\| x(\tau) - x^{0}(\tau)\right\| d\tau \qquad (4.51)$$

for all $t \epsilon [t_0, \ T]$

Now, let

$$\mu(t) = x(t) - x^{0}(t) \qquad (4.52)$$

using (4.35a) and (4.3a), we have

$$\dot{\mu} = \dot{x} - \dot{x}^{0} = f(x, z, u, \epsilon, t) - f(x^{0}, z^{0}, u^{0}, 0, t) \triangleq \delta f \qquad (4.53)$$

Integrating both sides of (4.53) yields

$$\int_{t_0}^{t} \frac{du(\tau)}{d\tau} = \mu(t) - \mu(t_0) = \int_{t_0}^{t} \delta f(\tau) d\tau \qquad (4.54)$$

Noting that $\mu(t_0) = x(t_0) - x^{0}(t_0) = 0$, equation (4.54) yields

$$\mu(t) = \int_{t_0}^{t} \delta f(\tau) d\tau \qquad (4.55)$$

The Lipschitz property of f in all its arguments and the boundedness of the solution for $t \epsilon [t_0, T]$ implies

$$\left\|\mu(t)\right\| \le \int_{t_0}^{t} (C_7 \left\|\mu(\tau)\right\| + C_8 \left\|\phi(\tau)\right\| + C_9 \left\|u(\tau) - u^{0}(\tau)\right\| + C_{10}\epsilon) d\tau \qquad (4.56)$$

Substituting (4.49) and (4.51) into (4.56), we obtain

$$\left\|\mu(t)\right\| \le C_7\int_{t_0}^{t}\left\|\mu(\tau)\right\| d\tau + \frac{C_{11}}{\epsilon}\int_{t_0}^{t}\int_{t_0}^{\tau} e^{-\alpha_1(\tau - \sigma)/\epsilon}\left\|\mu(\sigma)\right\| d\sigma d\tau$$

$$+ C_{12}\int_{t_0}^{t} e^{-\alpha_1(\tau - t_0)/\epsilon} d\tau + C_{13}\int_{t_0}^{t} e^{-\alpha_1(t_f - \tau)/\epsilon} d\tau + C_{14}\epsilon \tag{4.57}$$

The second term on the right-hand side of (4.57) can be written as

$$\frac{C_{11}}{\epsilon}\int_{t_0}^{t}\int_{t_0}^{\tau}(e^{-\alpha_1(\tau - \sigma)/\epsilon}\left\|\mu(\sigma)\right\| d\sigma)d\tau =$$

$$\frac{C_{11}}{\epsilon}\int_{\sigma=t_0}^{t}\int_{\tau=\sigma}^{t} e^{-\alpha_1(\tau - \sigma)/\epsilon} d\tau \left\|\mu(\sigma)\right\| d\sigma =$$

$$\frac{C_{11}}{\alpha_1}\int_{t_0}^{t}(1 - e^{-\alpha_1(t - \sigma)/\epsilon})\left\|\mu(\sigma)\right\| d\sigma \le$$

$$\frac{C_{11}}{\alpha_1}\int_{t_0}^{t}\left\|\mu(\sigma)\right\| d\sigma \tag{4.58}$$

The third and forth terms on the right-hand side of (4.57) satisfy the inequalities, respectively,

$$C_{12}\int_{t_0}^{t} e^{-\alpha_1(\tau - t_0)/\epsilon} d\tau \le \epsilon C_{12}/\alpha_1 \tag{4.59}$$

$$C_{13}\int_{t_0}^{t} e^{-\alpha_1(t_f - \tau)/\epsilon} d\tau \le 2\epsilon C_{13}/\alpha_1 \tag{4.60}$$

Substituting (4.58)-(4.60) back into (4.57), we obtain

$$||\mu(t)|| \le C_7\int_{t_0}^{t} ||\mu(\tau)||\, d\tau + \frac{C_{11}}{\alpha_1}\int_{t_0}^{t} ||\mu(\sigma)||\, d\sigma + \epsilon(C_{14} + \frac{C_{12}}{\alpha_1} + \frac{2C_{13}}{\alpha_1})$$

$$= C_{15}\epsilon + C_{16}\int_{t_0}^{t} ||\mu(\tau)||\, d\tau \tag{4.61}$$

In equation (4.61), $C_{15}\epsilon$, C_{16}, are nonnegative constants and $||\mu(\tau)||$ is a nonnegative valued continuous function. By Bellman-Gronwall inequality we obtain

$$||\mu(t)|| = ||x(t) - \overset{o}{x}(t)|| \le C_{15}\epsilon \exp\int_{t_0}^{t} C_{16} d\tau$$

$$= C_{15}\epsilon e^{C_{16}(t - t_0)} \le C_{17}\epsilon \tag{4.62}$$

Substituting (4.62) back into (4.49), yields

$$||\phi(t)|| = ||z(t) - z^{0}(t)|| \leq C_4\epsilon + K_6 e^{-\alpha_1(t - t_0)/\epsilon} + K_7 e^{-\alpha_1(t_f - t)/\epsilon} +$$

$$\frac{C_1K_1}{\epsilon}\int_{t_0}^{t} e^{-\alpha_1(t - \tau)/\epsilon} C_{17}\epsilon d\tau$$

$$= C_4\epsilon + K_6 e^{-\alpha_1(t - t_0)/\epsilon} + K_7 e^{-\alpha_1(t_f - t)/\epsilon} +$$

$$\frac{C_1K_1C_{17}\epsilon}{\alpha_1}[1 - e^{-\alpha_1(t - t_0)/\epsilon}] \qquad (4.63)$$

Rewrite (4.63) as

$$||\phi(t)|| = ||z(t) - z^{0}(t)|| \leq C_{18}\epsilon + K_6 e^{-\alpha_1(t - t_0)/\epsilon} + K_7 e^{-\alpha_1(t_f - t)/\epsilon},$$

$$\text{for all } t \in [t_0, T], \qquad (4.64)$$

Similarly, substitution of (4.62) into (4.51), yields

$$||u(t) - u^{0}(t)|| \leq C_{19}\epsilon + K_3 e^{-\alpha_1(t - t_0)/\epsilon} + K_4 e^{-\alpha_1(t_f - t)/\epsilon},$$

$$\text{for all } t \in [t_0, T], \qquad (4.65)$$

Now, let us show that x, z, u, are bounded by r. We write $||x||$ as

$$||x|| \leq ||x^{0}|| + ||x - x^{0}|| \leq K_3' + \epsilon\, C_{15} e^{C_{16}(t - t_0)} \qquad (4.66)$$

where x^0 is the reduced solution which is bounded by some constant, say K_3'. For any $r > K_3'$, and $t_1 \in [t_0, T]$ there exist $\epsilon^* > 0$ such that every $\epsilon < \epsilon^*$, $\|x\| \leq r$, for every $t \in [t_0, t_1]$. For example, for $r = 2K_3'$, ϵ^* can be taken as $\epsilon^* = K_3'/C_{15}\exp(C_{16}(t_1 - t_0))$. Similarly, z and u are bounded by r.

From the above discussions we see that r can be chosen large enough such that for sufficiently small ϵ the trajectory does not leave the compact set S for $t \in [t_0, t_f]$. This implies that $T = t_f$.

From equation (4.62), we have proved that the slow variable x satisfies

$$\|x(t) - x^0(t)\| \leq K_1\epsilon = O(\epsilon) \quad , \quad \text{for all } t \in [t_0, t_f] \tag{4.67}$$

This implies that

$$\|x(t_f) - x^0(t_f)\| = O(\epsilon) \tag{4.68}$$

where $x^0(t_f) = x_f$

Now, let us rewrite (4.35b) as

$$\begin{aligned}\epsilon\dot{z}(t) = a\,(x, \epsilon, t) + B\,(x, \epsilon, t)u^0(t) - B\,(x, \epsilon, t)K(x, t)z^0(t) \; + \\ \epsilon g_1(x, z, u, \epsilon, t) + (A\,(x, \epsilon, t) + B\,(x, \epsilon, t)K(x, t))z(t) \; + \\ B\,(x, \epsilon, t)u_b(t)\end{aligned} \tag{4.69}$$

The transition matrix of (4.69) can be written as (see Kokotovic, Khalil and O'Reilly [19], page 230)

$$\Phi(t,\tau) = e^{H(x(t))(t - \tau)/\epsilon} + \epsilon\psi_1(t, \tau) \tag{4.70}$$

where $\|\psi(t, \tau)\| \le Ke^{-\alpha(t - \tau)/\epsilon}$

Hence,

$$z(t_f) = \Phi(t_f, t_0)z(t_0) + \frac{1}{\epsilon}\int_{t_0}^{t_f} e^{H(x(t_f))(t_f - \tau)/\epsilon} g_2(\tau)d\tau +$$
$$\frac{1}{\epsilon}\int_{t_0}^{t_f} e^{H(x(t_f))(t_f - \tau)/\epsilon} B\ (x(\tau), \epsilon, \tau)u_b(\tau)d\tau +$$
$$\int_{t_0}^{t_f} \psi_1(t_f, \tau)g_2(\tau)d\tau + \int_{t_0}^{t_f} \psi_1(t_f, \tau)B\ (x(\tau), \epsilon, \tau)u_b(\tau)d\tau \tag{4.71}$$

where

$$g_2 = a + B\,u^0 - B\,Kz^0 + \epsilon g_1 = g_2(x, z, u, \epsilon, t)$$
$$H = A + B\,K \tag{4.72}$$

and

$$\Phi(t_f, t_0)z(t_0) = O(\epsilon)$$
$$\int_{t_0}^{t_f} \psi_1(t_f, \tau)g_2(\tau)d\tau = O(\epsilon) \tag{4.73}$$
$$\int_{t_0}^{t_f} \psi_1(t_f, \tau)B\ (x(\tau), \epsilon, \tau)u_b(\tau)d\tau = O(\epsilon)$$

Equation (4.71) can be rewritten as

$$
\begin{aligned}
z(t_f) = O(\epsilon) &+ \frac{1}{\epsilon}\int_{t_0}^{t_f} e^{H(x(t_f))(t_f - \tau)/\epsilon} g_2(t_f)d\tau + \\
&\frac{1}{\epsilon}\int_{t_0}^{t_f} e^{H(x(t_f))(t_f - \tau)/\epsilon} [g_2(\tau) - g_2(t_f)]d\tau + \\
&\frac{1}{\epsilon}\int_{t_0}^{t_f} e^{H(x(t_f))(t_f - \tau)/\epsilon} B_2(x(t_f), \epsilon, t)u_b(\tau)d\tau + \\
&\frac{1}{\epsilon}\int_{t_0}^{t_f} e^{H(x(t_f))(t_f - \tau)/\epsilon} \cdot \\
&[B_2[(x(\tau), \epsilon, t) - B_2(x(t_f), \epsilon, t)]u_b(\tau)d\tau
\end{aligned}
\tag{4.74}
$$

The norm of the third term on the right-hand side of (4.74) can be written as

$$
\left\| \frac{1}{\epsilon}\int_{t_0}^{t_f} e^{H(x(t_f))(t_f - \tau)/\epsilon} (g_2(\tau) - g_2(t_f))d\tau \right\| \le
$$

$$
\frac{1}{\epsilon}\int_{t_0}^{t_f} \left\| e^{H(x(t_f))(t_f - \tau)/\epsilon} \right\| \left\| g_2(\tau) - g_2(t_f) \right\| d\tau \tag{4.75}
$$

We want to show that g_2 is Lipschitzian in "t" with constant independent of "ϵ". Let us rewrite g_2 as

$$g_2 = a\ (x,\ t,\ \epsilon) + B\ (x,\ t,\ \epsilon)\overset{0}{u}(t) - B\ (x,\ t,\ \epsilon)K(x,\ t)\overset{0}{z}(t) +$$

$$\epsilon g_1(x,\ z,\ u,\ \epsilon,\ t) \tag{4.76}$$

since x, z, and u are sufficiently smooth and differentiable, we have

$$\|x(t_2) - x(t_1)\| \leq K' \|t_2 - t_1\|$$

$$\|z(t_2) - z(t_1)\| \leq \frac{K''}{\epsilon} \|t_2 - t_1\| \tag{4.77}$$

$$\|u(t_2) - u(t_1)\| \leq \frac{K'''}{\epsilon} \|t_2 - t_1\|$$

With (4.77), the first term on the right-hand side of (4.76) is Lipschitzian in "t" with constant independent of "ϵ", which is

$$\begin{aligned}\|a\ (x(t_2),\ t_2,\ \epsilon) - a\ (x(t_1),\ t_1,\ \epsilon)\| &\leq d_4\|x(t_2) - x(t_1)\| + \\ &\quad d_5\|t_2 - t_1\| \\ &= K_1'\|t_2 - t_1\|\end{aligned} \tag{4.78}$$

Similarly, the second and third terms on the right-hand side of (4.76) are Lipschian in "t" with constant independent of "ϵ". The g_1 in the fourth term can be written as

$$\left\| g_1(x(t_2),\ z(t_2),\ u(t_2),\ \epsilon,\ t_2) - g_1(x(t_1),\ z(t_1),\ u(t_1),\ \epsilon,\ t_1) \right\| \le$$

$$d_6 \left\| x(t_2) - x(t_1) \right\| + d_7 \left\| z(t_2) - z(t_1) \right\| + d_8 \left\| u(t_2) - u(t_1) \right\| +$$

$$d_9 \left\| t_2 - t_1 \right\| \tag{4.79}$$

Substituting (4.77) into (4.79), we obtain

$$\left\| g_1(x(t_2),\ z(t_2),\ u(t_2),\ \epsilon,\ t_2) - g_1(x(t_1),\ z(t_1),\ u(t_1),\ \epsilon,\ t_1) \right\| \le$$

$$\frac{L}{\epsilon} \left\| t_2 - t_1 \right\| \tag{4.80}$$

Hence, ϵg_1 is also Lipschitzian in "t" with constant independent of "ϵ". This shows that g_2 is Lipschitzian in "t" with constant independent of "ϵ". Equation (4.75) can now be written as

$$\left\| \frac{1}{\epsilon} \int_{t_0}^{t_f} e^{H(x(t_f))(t_f - \tau)/\epsilon} (g_2(\tau) - g_2(t_f)) d\tau \right\| \le$$

$$\frac{L}{\epsilon} \int_{t_0}^{t_f} \left\| e^{H(x(t_f))(t_f - \tau)/\epsilon} \right\| (t_f - \tau)\, d\tau \le$$

$$\frac{L}{\epsilon} \int_{t_0}^{t_f} K e^{-\alpha(t_f - \tau)/\epsilon} (t_f - \tau) d\tau =$$

$$\int_{t_0}^{t_f} LK e^{-\alpha(t_f - \tau)/\epsilon} ((t_f - \tau)/\epsilon) d\tau$$

$$-\int_0^{(t_f-t_0)/\epsilon} KLe^{-\alpha\lambda}\lambda d\lambda = O(\epsilon) \tag{4.81}$$

Similarly, the fifth term on the right-hand side of (4.74) can also be shown to be $O(\epsilon)$. Equation (4.74) now become

$$z(t_f) = O(\epsilon) + \frac{1}{\epsilon}\int_{t_0}^{t_f} e^{H(x(t_f))(t_f - \tau)/\epsilon} g_2(t_f)d\tau +$$

$$\frac{1}{\epsilon}\int_{t_0}^{t_f} e^{H(x(t_f))(t_f - \tau)/\epsilon} B\,(x(t_f))u_b(\tau)d\tau$$

$$= O(\epsilon) - [I - e^{H(x(t_f))(t_f - t_0)/\epsilon}]H^{-1}(x(t_f))g_2(t_f) + z_f - z^0(t_f) \tag{4.82}$$

Rewrite (4.82) as

$$z(t_f) = O(\epsilon) - H^{-1}(x(t_f))[a\,(x(t_f)) + B\,(x(t_f))u^0(t_f) + A\,(x(t_f))z^0(t_f) +$$

$$\epsilon g_1(t_f)] + H^{-1}(x(t_f))[A\,(x(t_f)) + B\,(x(t_f))K(t_f)]z^0(t_f) + z_f -$$

$$z(t_f) = O(\epsilon) + z^0(t_f) + z_f - z^0(t_f) = z_f + O(\epsilon) \tag{4.83}$$

Hence

$$\left\| z(t_f) - z_f \right\| = O(\epsilon) \tag{4.84}$$

The cost function of this nonlinear system is recalled as

$$J = \int_{t_0}^{t_f} [V_1(x, \epsilon, t) + z^T V_2(x, \epsilon, t) z + u^T R(x, \epsilon, t) u] dt$$

$$= \int_{t_0}^{t_f} L(x, z, u, \epsilon, t) dt \tag{4.85}$$

and

$$J^0 = \int_{t_0}^{t_f} L(x^0, z^0, u^0, 0, t) dt \tag{4.86}$$

since $\|x\| \le r$, $\|z\| \le r$, $\|u\| \le r$, the Lipschitz property of L implies

$$\|L(x, z, u) - L(x^0, z^0, u)\| \le K(\|x(t) - x^0(t)\| + \|u(t) - u^0(t)\| + \|z(t) - z^0(t)\| \tag{4.87}$$

Therefore,

$$\|J(u_c) - J(u^0)\| \le \int_{t_0}^{t_f} \|L(x, z, u) - L(x^0, z^0, u^0)\| dt$$

$$\le \int_{t_0}^{t_f} K(\|x(t) - x^0(t)\| + \|u(t) - u^0(t)\| + \|z(t) - z^0(t)\|) dt \tag{4.88}$$

After substituting (4.62), (4.64) and (4.65) into (4.88), we obtain

$$\|J(u_c) - J(u^0)\| \le \int_{t_0}^{t_f} (K_8 \epsilon + K_9 e^{-\alpha_1 (t - t_0)/\epsilon} + K_{10} e^{-\alpha_1 (t_f - t)/\epsilon}) dt$$

$$= O(\epsilon) \tag{4.89}$$

which proves the theorem.

IV.4 NUMERICAL EXAMPLES

In order to demonstrate the performance of the composite control, two numerical examples are presented in this section, one of them is an interception problem in the horizontal plane treated in Visser and Shinar [31], the other one is a linear example.

Example 4.1

Consider an interception problem in the horizontal plane; the nonlinear equations of motion are (see [31])

$$\frac{dR}{dt} = V_E \mathrm{COS}\gamma - V_P \mathrm{SIN}(\gamma - \chi) \quad , \qquad R(t_0) = R_0,\ R(t_f) = R_f \qquad (4.90a)$$

$$\frac{d\gamma}{dt} = -\frac{1}{R}[V_E \mathrm{SIN}\gamma - V_P \mathrm{SIN}(\gamma - \chi)] \quad , \qquad \gamma(t_0) = \gamma_0 \qquad (4.90b)$$

$$\epsilon \frac{d\chi}{dt} = u \quad , \qquad \chi(t_0) = \chi_0 \qquad (4.90c)$$

In Fig.4.1 the geometry of the pursuit is depicted, where R is range between the two airplanes, V_E and V_P the target and pursuer velocity respectively.

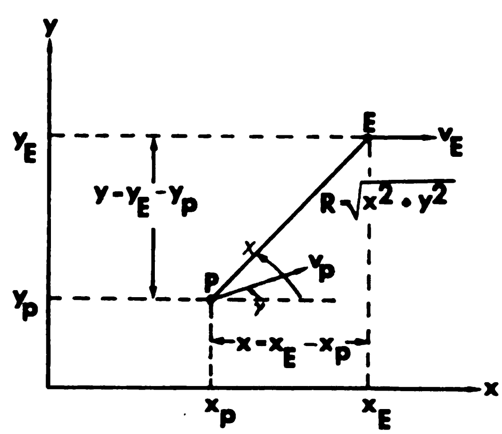

FIG.4.1 Interception geometry in the horizontal plane

The actual rate of turn of the pursuer is controlled by $-1 \le u \le 1$. Capture is determined by

$$R(t_f) = R_f \ , \qquad t_f < \infty \tag{4.91}$$

The objective of the pursuer is to minimize a performance index

$$J = \int_{t_0}^{t_f} (1 + pu^2)dt \tag{4.92}$$

It is important to notice that in [31] the constraint on the control u is taken care of by a penalization term in equation (4.92), e.g., it was not explicity considered in solving the optimal control problem.

The composite control is derived below.

<u>The reduced control</u>: The reduced problem is obtained by setting $\epsilon = 0$ in (4.90c), which yields

$$u^o = 0 \ , \quad \text{implies } [0 \quad 1] \begin{bmatrix} \chi^o \\ u^o \end{bmatrix} = 0 \tag{4.93}$$

which is not a standard singularly perturbed form, but satisfies Assumption 4.2. Hence, there is a constant permutation matrix P such that

$$[0 \quad 1] \begin{bmatrix} 0 & 1 \\ 1 & 0 \end{bmatrix} \begin{bmatrix} 0 & 1 \\ 1 & 0 \end{bmatrix} \begin{bmatrix} \chi^o \\ u^o \end{bmatrix} = [1 \quad 0] \begin{bmatrix} u^o \\ \chi^o \end{bmatrix} \tag{4.94}$$

<u>The boundary-layer stabilizing control</u>: The boundary-layer system is obtained by (left boundary-layer)

$$\frac{d\chi}{d\tau} = u \tag{4.95}$$

the boundary-layer stabilizing control is given taken as

$$u_F = -K(\chi - \overset{o}{\chi}) \quad , \qquad K > 0 \tag{4.96}$$

where K is chosen properly in order to satisfy the constraint $-1 \le u \le 1$.

In this example, the final time t_f and the terminal conditions of $\chi(t_f)$ are not specified. Hence, we do not need right boundary-layer control u_b to steer $\chi(t)$ from $\overset{o}{\chi}(t)$ to the desired state χ_f. The composite control is taken as

$$u_c = \overset{o}{u} + u_F = - K(\chi - \overset{o}{\chi}) \quad , \qquad K > 0 \tag{4.97}$$

The boundary conditions and fixed parameters are summarized in Table 4.1 [31]

Initial flight path angle	$\gamma_0 = 40^o$
Initial azimuth angle	$\chi_0 = -45^o$
Initial normalized range	$R_0 = 1.0$
Final normalized range	$R_f = .1333$
Speed ratio	$V_E/V_P = .6$
Performance index weighting parameter	$p = 2$

Table 4.1 Boundary conditions and parameters for Example 4.1

Figs.4.2 - 4.3 show the range R, the flight path angle γ and azimuth angle χ time histories for a value of $\epsilon = .1$ when the composite control (4.97) is applied to the system (4.90).
This shows that the capture time t_f obtained by using the composite control is $t_f = 2.13$ which is very close to the exact solution $t_f = 1.942$, (see [31]). The composite control u_c time histories is also shown in Fig.4.4. Table 4.2 summarized some numerical results for several values of ϵ.

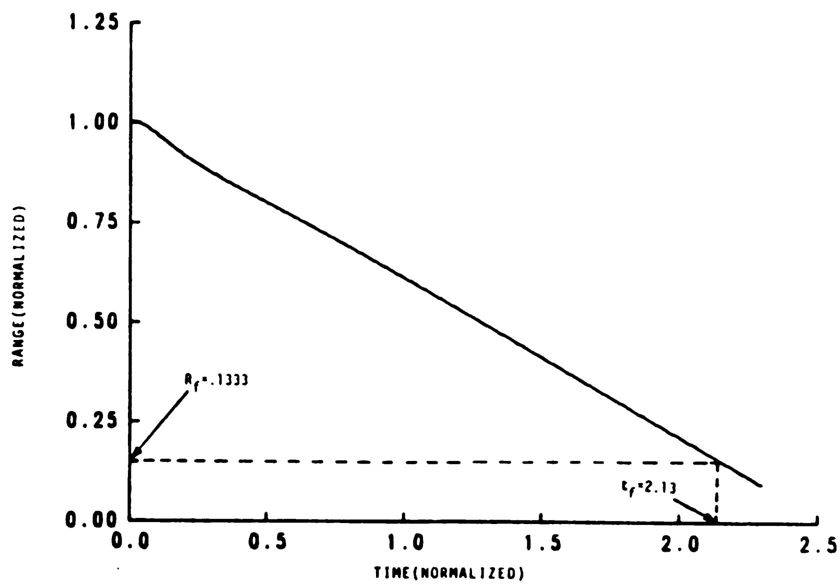

Fig.4.2 Range time histories (with composite control) for a value of $\epsilon = .1$

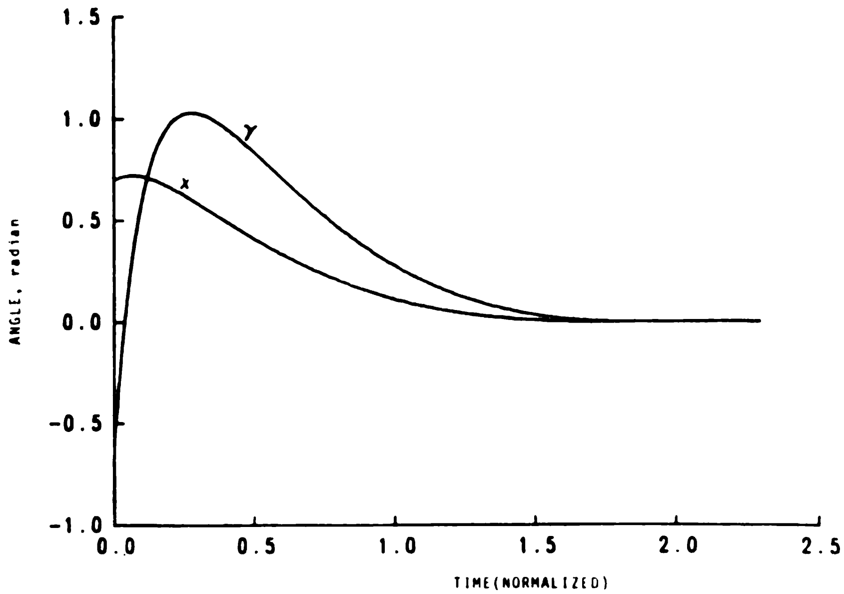

Fig.4.3 Azimuth angle and flight path angle time histories (with composite control) for a value of ϵ = .1

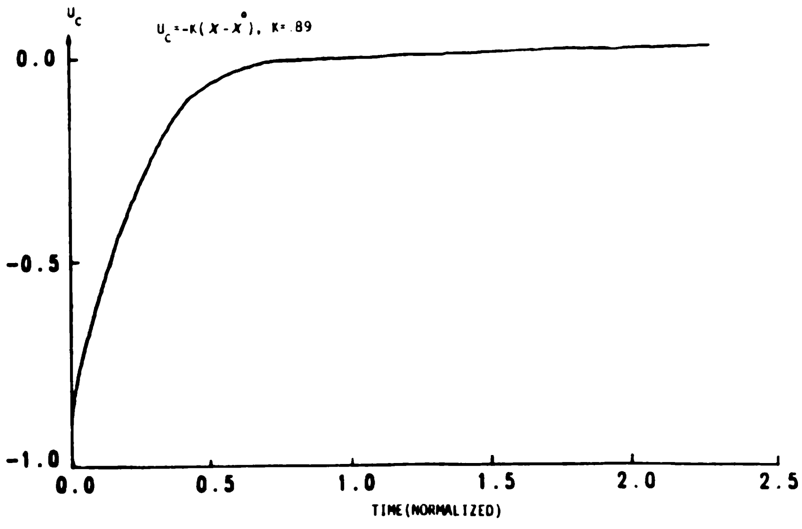

Fig.4.4 Composite control time histories

ϵ	$u(t_0)$ with composite control	$u(t_0)$ exact sol.	t_f with composite control	t_f exact sol.	J with composite control	J exact sol.
.10	-.885	.8323	2.130	1.942	2.093	2.042
.15	-.885	.8463	2.135	1.988	2.154	2.146
.20	-.885	.8596	2.200	2.033	2.285	2.255
.25	-.885	.8736	2.230	2.077	2.395	2.368
.30	-.885	.8860	2.280	2.121	2.526	2.489
.35	-.885	.8965	2.366	2.166	2.654	2.614
.40	-.885	.9078	2.378	2.208	2.805	2.747
.45	-.885	.9190	2.445	2.248	3.034	2.886
.50	-.885	.9320	2.490	2.288	3.158	3.033

Table 4.2 Comparision of exact and composite control solutions

Example 4.2

Consider the linear system

$$\dot{x} = z \tag{4.98a}$$

$$\epsilon\dot{z} = -x + z + u \tag{4.98b}$$

which is a special case of (4.1) with $A_{22} = 1$ (not Hurwitz). It is desired to steer the state from $x(0) = z(0) = 0$ to $x(1) = 1$, $z(1) = 0$.

<u>The reduced control</u>: The reduced control problem is defined by

$$\dot{x}^0 = x^0 - u^0 , \qquad x^0(0) = 0,\ x^0(1) = 1 \tag{4.99}$$

and the reduced control is given by

$$u^{o}(t) = -.313e^{(1 - t)} \tag{4.100}$$

<u>The boundary-layer stabilizing control</u>:

$$u_F = -K(z - z^{o}) = -K(z - .157e^{(-t + 1)} - .157e^{(t + 1)}) \quad , K > 0 \tag{4.101}$$

where z^{o} is obtained from reduced solution

<u>Right boundary-layer control</u>: The right boundary-layer model is given by

$$\frac{dz}{d\sigma} = -x^{o} + z + u = -x^{o} + z + [u^{o} - K(z - z^{o}) + u_b] \tag{4.102}$$

Defining $z_b = z - z^{o}$, we obtain

$$\frac{dz_b}{d\sigma} = (1 - K)z_b + u_b \tag{4.103}$$

By using the minimum energy control (see(4.23)) and the controllability Grammian W (see(4.28)), the right boundary-layer control u_b is given by

$$u_b = e^{(t - 1)/\epsilon} W^{-1}[z_f - z^{o}(t_f)] = e^{(t - 1)/\epsilon} 2(0 - 1.317)$$

$$= -2.634e^{(t - 1)/\epsilon} \tag{4.104}$$

The composite control is taken as

$$u_c = u^o + u_F + u_b = -.313e^{(1 - t)} - K(z - .157e^{(-t + 1)} - e^{(t + 1)}) -$$
$$2.634e^{(t - 1)/\epsilon} \qquad (4.105)$$

Application of the control (4.105) to the system brings $(x(t), z(t))$ to within $O(\epsilon)$ from the target point (1, 0), for sufficiently small ϵ. To get a better feeling for the deviation from the target point we calculate $(x(1), z(1))$ for $\epsilon = .1$, .05, and .01 (see Table 4.3). Fig.4.5 shows the trajectory of $x(t)$ and $z(t)$ for a value of $\epsilon = .01$. The results confirm that the final point is within an $O(\epsilon)$ neighborhood of the target. If 10 % error is tolerable, then $\epsilon = .05$ is small enough for the control to be successful. If 2 % error is tolerable then $\epsilon = .01$ is small enough. The results also show that in this example, for $\epsilon = .1$ the error might not be tolerable.

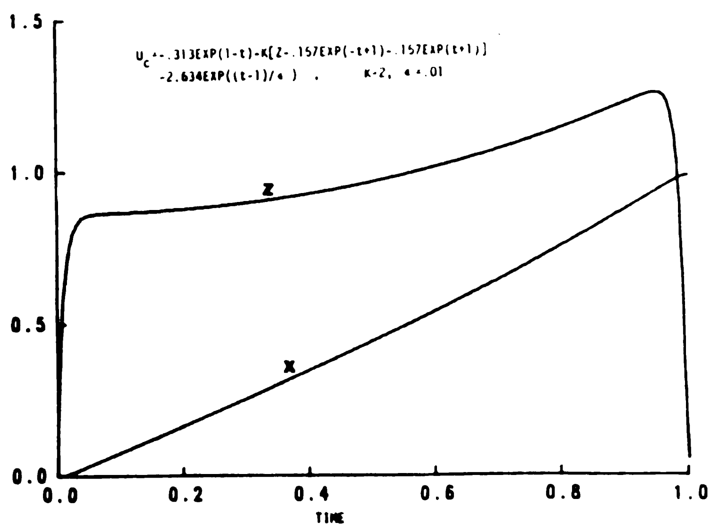

Fig.4.5 State trajectory (with composite control) for a value of $\epsilon = .01$

	$\epsilon = .1$	$\epsilon = .05$	$\epsilon = .01$
x(1)	.7500	.9120	.9730
z(1)	.1520	.0200	.0036

Table 4.3 The target point (x(1), z(1)) for ϵ = .1, .05 and .01

V. APPLICATION OF THE COMPOSITE CONTROL TO MANEUVERS IN A VERTICAL PLANE

In this chapter, we apply the composite control strategy to the optimal maneuvers of an aircraft in a vertical plane. The system model will be represented in the singularly perturbed form (4.1) of Chapter IV via a change of variables and state feedback. One of the examples of interest is the minimum time-to-climb problem which is treated in Section III.1.2.

V.1 COMPOSITE CONTROL

The equations of motion for flight in a vertical plane are given by (see (2.44) of Chapter II or (3.12) of Chapter III)

$$\frac{dE}{dt} = \frac{V}{m}[T(E, V) - \frac{1}{2}\rho V^2 s(C_{D_0}(V) + \eta(V)C_{L\alpha}(V)\alpha^2)]$$

$$= f(E, V, \gamma, \alpha, \epsilon, t) \tag{5.1a}$$

$$\epsilon\frac{dV}{dt} = \frac{\epsilon g}{W}[T(E, V) - \frac{1}{2}\rho V^2 s(C_{D_0}(V) + \eta(V)C_{L\alpha}(V)\alpha^2)] - gSIN\gamma$$

$$= -gSIN\gamma + \epsilon g_1(E, V, \gamma, \alpha, \epsilon, t) \tag{5.1b}$$

$$\epsilon\frac{d\gamma}{dt} = \frac{g}{2W}\rho V s C_{L\alpha}(V)\alpha - \frac{g}{V}COS\gamma \tag{5.1c}$$

A control $\alpha(t)$ is sought to steer the state $E(t_0) = E_0$, $V(t_0) = V_0$, $\gamma(t_0) = \gamma_0$ to a terminal state $E(t_f) = E_f$, $V(t_f) = V_f$, $\gamma(t_f) = \gamma_f$; while minimizing the cost functional

$$J = \int_{t_0}^{t_f} \ell(E,\ V,\ \gamma,\ \alpha,\ \epsilon,\ t)dt \tag{5.2}$$

The model (5.1) is in the singularly perturbed form but it is not in the form (4.1) of Chapter IV since (5.1b) and (5.1c) are nonlinear in the fast variables V and γ. Our first task is to use state transformations and feedback to bring the model (5.1) into the form (4.1). In other words, we want to linearize the boundary-layer system. We introduce the new variable

$$Z = -gSIN\gamma \tag{5.3}$$

instead of the variable γ. Taking the derivative of Z, we obtain

$$\epsilon\dot{Z} = -g\,COS\gamma \cdot \epsilon\dot{\gamma} \tag{5.4}$$

substitution of (5.1c) into (5.4) yields

$$\epsilon\dot{Z} = -\frac{1}{2}\ \frac{g^2}{W}\ \rho VsC_{L\alpha}(V)COS\gamma\ .\ \alpha + \frac{g^2}{V}\ COS^2\gamma \tag{5.5}$$

Furthermore, assuming that $COS\gamma\ .\ VC_{L\alpha}(V) > 0$, we set

$$\alpha(t) = \frac{1}{\frac{1}{2}\ \frac{g^2}{W}\rho VsC_{L\alpha}(V)COS\gamma}\ [\frac{g^2}{V}\ COS^2\gamma - u] \tag{5.6}$$

After substituting (5.6) back into (5.1a), (5.1b) and (5.5), the system (5.1) becomes

$$\frac{dE}{dt} = \frac{V}{m}\{T(E, V) - \frac{1}{2}\rho V^2 s[C_{D_0}(V) + \eta(V)C_{L\alpha}(V) \cdot \alpha^2]\}$$

$$= f(E, V, Z, u, \epsilon, t) \tag{5.7a}$$

$$\epsilon\frac{dV}{dt} = \frac{\epsilon g}{W}\{T(E, V) - \frac{1}{2}\rho V^2 s[C_{D_0}(V) + \eta(V)C_{L\alpha}(V) \cdot \alpha^2]\} + Z$$

$$= Z + \epsilon g_1(E, V, Z, u, \epsilon, t) \tag{5.7b}$$

$$\epsilon\frac{dZ}{dt} = u \tag{5.7c}$$

which is of the form (4.1) and

$$J = \int_{t_0}^{t_f} \ell(E, V, Z, u, \epsilon, t)dt \tag{5.8}$$

We suppose that the cost (5.2) is such that (5.8) is of the form (4.2), i.e., quadratic in V, Z and u. The composite control can now be derived as in Chapter IV.

<u>The reduced control</u>: The reduced problem is given by

$$\dot{E}^o = f(E^o, V^o, 0, 0, 0, t) \tag{5.9a}$$

$$0 = Z^o \tag{5.9b}$$

$$0 = u^o \tag{5.9c}$$

with boundary conditions $E^o(t_0) = E_0$, $E^o(t_f) = E_f$ and

$$J^o = \int_{t_0}^{t_f} \ell(E^o, V^o, 0, 0, 0, t)dt \tag{5.10}$$

The algebraic equations (5.9b) and (5.9c) can be written as

$$\begin{bmatrix} 0 & 1 & 0 \\ 0 & 0 & 1 \end{bmatrix} \begin{bmatrix} V^{o} \\ Z^{o} \\ u^{o} \end{bmatrix} = \begin{bmatrix} 0 \\ 0 \end{bmatrix} \tag{5.11}$$

which is not a standard singularly perturbed form since (5.11) does not have a unique root in Z^{o} and V^{o}, but it satisfies Assumption 4.2. Hence, there is a constant permutation matrix P such that

$$\begin{bmatrix} 0 & 1 & 0 \\ 0 & 0 & 1 \end{bmatrix} \begin{bmatrix} 0 & 0 & 1 \\ 0 & 1 & 0 \\ 1 & 0 & 0 \end{bmatrix} \begin{bmatrix} 0 & 0 & 1 \\ 0 & 1 & 0 \\ 1 & 0 & 0 \end{bmatrix} \begin{bmatrix} V^{o} \\ Z^{o} \\ u^{o} \end{bmatrix} =$$

$$\begin{bmatrix} 0 & 1 & 0 \\ 1 & 0 & 0 \end{bmatrix} \begin{bmatrix} u^{o} \\ Z^{o} \\ V^{o} \end{bmatrix} = 0 \tag{5.12}$$

This permutation has the meaning of using the velocity V^{o} as the control variable in the reduced problem.

<u>The boundary-layer stabilizing control</u>: The left boundary-layer system is

$$\frac{dV}{d\tau} = Z = G_1 \tag{5.13a}$$

$$\frac{dZ}{d\tau} = u_F = G_2 \tag{5.13b}$$

The Jacobian matrix of (5.13) is

$$J = \begin{bmatrix} \frac{\partial G_1}{\partial V} & \frac{\partial G_1}{\partial Z} \\ \frac{\partial G_2}{\partial V} & \frac{\partial G_2}{\partial Z} \end{bmatrix} = \begin{bmatrix} 0 & 1 \\ 0 & 0 \end{bmatrix} \tag{5.14}$$

whose characteristic equation is

$$s^2 = 0 \tag{5.15}$$

The two roots are zero, so, this system does not satisfies the requirement $Re\lambda(J)<0$. In order to stabilize the boundary-layer, u_F is chosen as

$$u_F = -b_1(V - V^0) - b_2 Z \ , \qquad b_1>0,\ b_2>0 \tag{5.16}$$

This control is not active on the slow manifold (e.g., at $V = V^0$ and $\gamma = 0$).

<u>The right boundary-layer control</u>: The right boundary-layer system is given by

$$\frac{dV}{d\sigma} = Z \tag{5.17a}$$

$$\frac{dZ}{d\sigma} = -b_1(V - V^0) - b_2 Z + u_b \tag{5.17b}$$

where u_b is only effective during the right boundary-layer. Equation (5.17) can be rewritten by setting $\tilde{V} = V - V^0$ as

$$\frac{d\tilde{V}}{d\sigma} = Z \tag{5.18a}$$

$$\frac{dZ}{d\sigma} = -b_1\tilde{V} - b_2 Z + u_b \tag{5.18b}$$

The right boundary-layer problem is to move $\tilde{V}$ and Z from $\tilde{V} = 0$, $Z = 0$ at $\sigma = -\Delta/\epsilon$ to $\tilde{V} = V_f - V^o(t_f)$, $Z = Z_f - Z^o(t_f) = Z_f$ at $\sigma = 0$. The solution of this steering control u_b is

$$u_b = B^T(e^{H(t_f - t)/\epsilon})^T W^{-1}(\infty)\left[\begin{bmatrix} Z_f \\ V_f \end{bmatrix} - \begin{bmatrix} 0 \\ V^o(t_f) \end{bmatrix}\right] \tag{5.19}$$

where $H = \begin{bmatrix} 0 & 0 \\ -b_1 & -b_2 \end{bmatrix}$, $B = \begin{bmatrix} 0 \\ 1 \end{bmatrix}$, and $W(\infty) = \int_0^\infty e^{\lambda H} B B^T (e^{\lambda H})^T d\lambda$

The composite control $\alpha_c(t)$ is taken as

$$\alpha_c = \frac{1}{\frac{g^2}{2W}\rho V s C_{L\alpha}(V)\cos\gamma}\left[\frac{g^2}{V}\cos^2\gamma - (u^o + u_F + u_b)\right] \tag{5.20}$$

After substituting $u^o = 0$, u_F and u_b into (5.20), the composite control α_c is rewritten as

$$\alpha_c = \frac{1}{\frac{g^2}{2W}\rho V s C_{L\alpha}(V)\cos\gamma}\left\{\frac{g^2}{V}\cos^2\gamma + b_1(V - V^o) + b_2 Z - B^T(e^{H(t_f - t)/\epsilon})^T \cdot\right.$$

$$\left. W^{-1}(\infty)\left[\begin{bmatrix} Z_f \\ V_f \end{bmatrix} - \begin{bmatrix} 0 \\ V^o(t_f) \end{bmatrix}\right]\right\} \tag{5.21}$$

V.2 APPLICATION OF THE COMPOSITE CONTROL TO THE MINIMUM TIME-TO-CLIMB PROBLEM

One of the interesting problems of optimal maneuvers of an aircraft in a vertical plane is the minimum time-to-climb (MTC) problem. This problem has been extensively studied in the literature because of the obvious interest in performance and climbing techniques of modern fighter aircrafts. For example, Bryson, Desai and Hoffman [16] used energy-state approximation in performance optimization of supersonic aircraft. Kelley [45] proposed optimum zoom climb techniques in 1959, and Kelley and Edelbaum [1] proposed energy climb, energy turn and asymptotic expansion in 1970. Ardema [4] solved the minimum time-to-climb problem by singular perturbations and matched asymptotic expansions.

In this section, we apply the composite control α_c, which has been obtained in the previous section, to this specific maneuver problem in a vertical plane. In order to illustrate the solution, two numerical examples are now considered. The first example is "airplane 2" of [16] which is the same model treated in Section III.1.2. The second example is "airplane 1" which is also considered in [16]. The model is given by the nonlinear singularly perturbed system equation (5.1).

Example 5.1

Given the nonlinear singularly perturbed system equation (5.1) for "airplane 2", and all the areodynamic parameters data are given in [16], it is desired to steer the state of the system from the initial state $E(t_0) = 1500000$, $V(t_0) = .5$ Mach and $\gamma(t_0) = 0^0$ to the final state $E(t_f) = 5000000$, $V(t_f) = 2.00$ Mach and $\gamma(t_f) =$ free, while minimizing t_f

It is important to mention here again that for this minimum time-to-climb problem, t_f is unknown (to be determined). In order to obtain the right boundary-layer control u_b (see equation (5.17)), we need to estimate t_f apriori. This problem can be circumvented by solving (i.e., integrating) the right boundary-layer solution in reverse direction off-line until it matches the slow manifold, then t_f can be determined. In this particular example $t_f = 170$sec.

The composite control α_c is applied to the system equation (5.22), and the resulting energy E, Velocity V, flight path angle γ and flight trajectory (path) are shown in Figs.5.1-5.4, respectively. In Fig.5.2, it is seen that this composite control steers the state of the aircraft to a final stste (2.06 Mach and altitude 79733 FT) which is about 3% error relative to the given final velocity (2.00 Mach), and about .333% error relative to the given final altitude (80000 FT). The total error is about 3.333% which is $O(\epsilon)$ close to the desired state. The comparison of the composite control α_c with the approximate control α_{app} which is obtained by off-line singular perturbation approximation of the optimal trajectories (see Section III.1.1) is also shown in Fig.5.5.

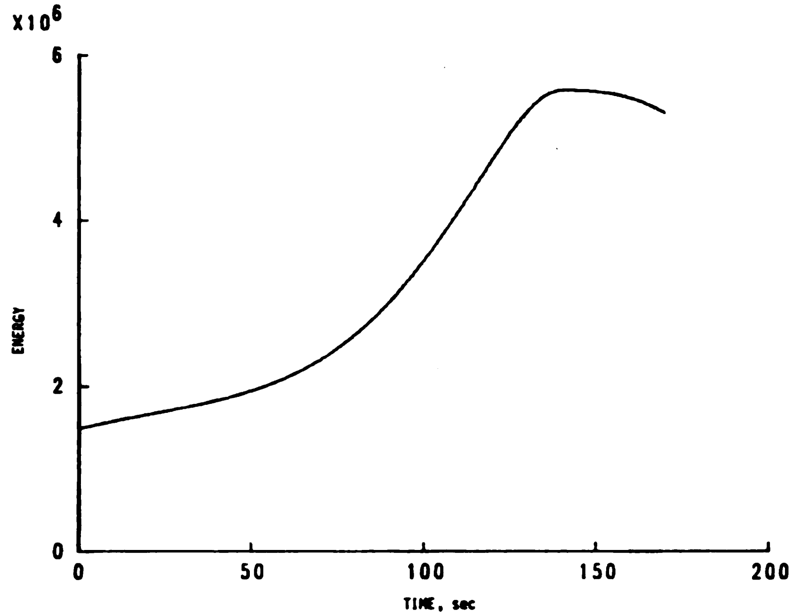

Fig.5.1 Energy time history for airplane 2 with composite control

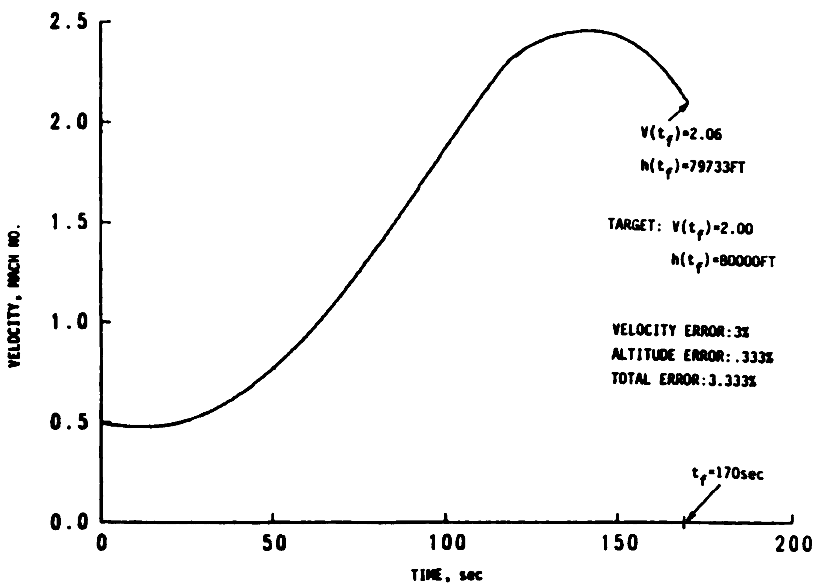

Fig.5.2 Velocity time history for airplane 2 with composite control

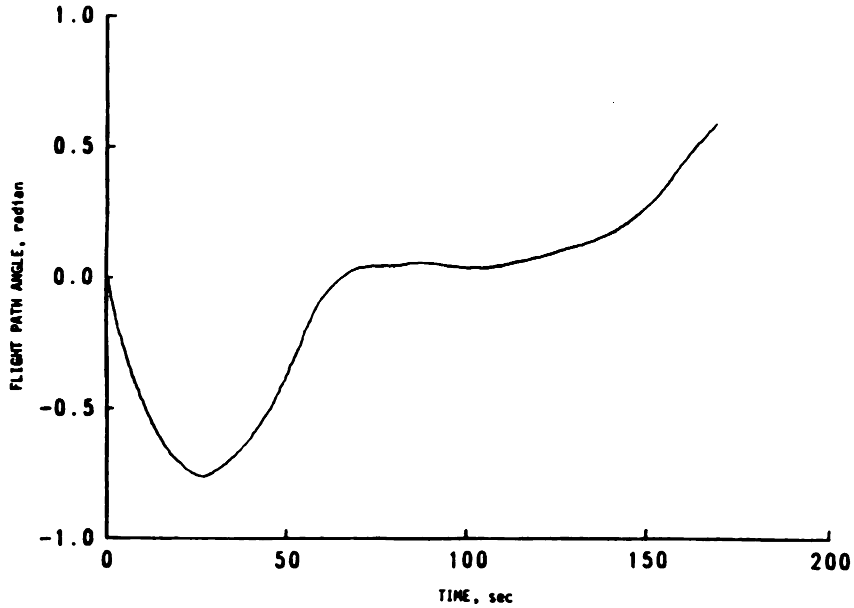

Fig.5.3 Flight path angle time history for airplane 2 with composite control

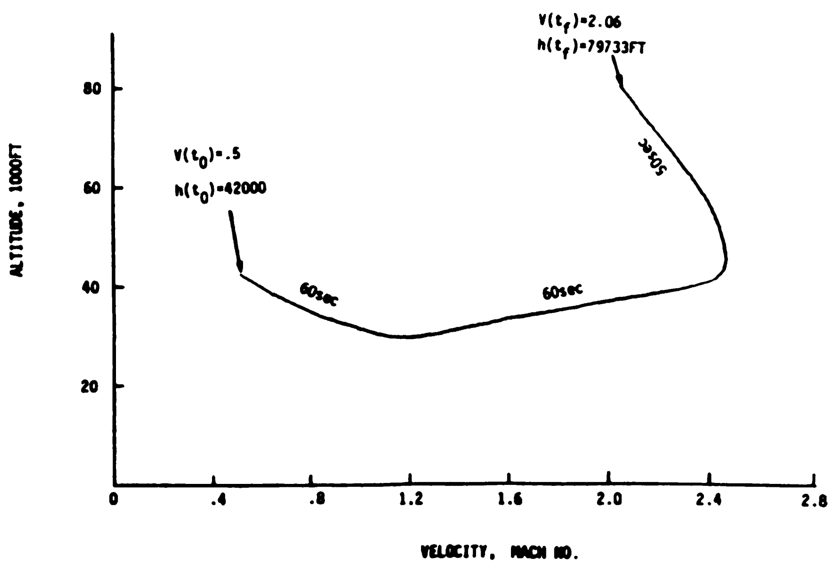

Fig.5.4 Flight trajectory for airplane 2 with composite control

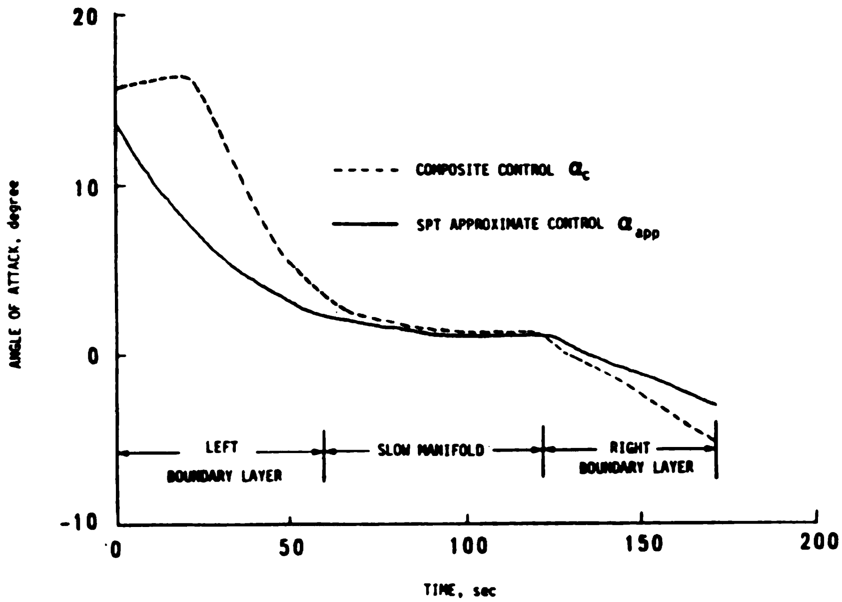

Fig.5.5 Comparison of the approximate control and composite control

In order to demonstrate the composite control strategy, we choose twelve different boundary conditions (the values are chosen such that no saturation occurs), and we use the same airplane 2 as an example. The simulation results are summarized in Table 5.1, which shows that this composite control indeed steers the system from the initial state to a final state which is $O(\epsilon)$ close to the desired final state.

CASE	INITIAL POINT	TERMINAL POINT (DESIRED)	FINAL POINT (ACTUAL)	ERROR	t_f (sec)
1	h=42000FT V=.5M E=1500000sec^2	h=100000FT V=2.4M E=6800000sec^2	h=99590FT V=2.56M E=7288000sec^2	h=.41% V=6.7% TOTAL:7.11%	190
2	h=42000FT V=.5M E=1500000sec^2	h=60000FT V=1.0M E=2560000sec^2	h=60822FT V=1.058M E=2655000sec^2	h=1.37% V=5.8% TOTAL:7.17%	103
3	h=60000FT V=1.0M E=2560000sec^2	h=80000FT V=2.0M E=5000000sec^2	h=79100FT V=2.11M E=5320000sec^2	h=1.125% V=5.5% TOTAL:6.625%	145
4	h=80000FT V=2.0M E=5000000sec^2	h=100000FT V=2.4M E=6800000sec^2	h=100876FT V=2.412M E=6871000sec^2	h=.876% V=5% TOTAL:5.876%	100
5	h=42000FT V=.5M E=1500000sec^2	h=80000 V=2.0M E=5000000sec^2	h=79733FT V=2.06M E=5210000sec^2	h=.333% V=3% TOTAL:3.333%	170
6	h=60000FT V=1.0M E=2560000sec^2	h=100000FT V=2.4M E=6800000sec^2	h=99950FT V=2.46M E=6986800sec^2	h=.05% V=2.5% TOTAL:2.55%	160
7	h=100000FT V=2.4M E=6800000sec^2	h=42000FT V=.5M E=1500000sec^2	h=43000FT V=.53M E=1560000sec^2	h=2.38% V=6% TOTAL:8.38%	185
8	h=80000FT V=2.0M E=5000000sec^2	h=42000FT V=.5M E=1500000sec^2	h=41800FT V=.52M E=1520000sec^2	h=.48% V=4% TOTAL:4.48%	160
9	h=60000FT V=1.0M E=2560000sec^2	h=42000FT V=.5M E=1500000sec^2	h=41700FT V=.528M E=1516000sec^2	h=.71% V=5.6% TOTAL:6.31%	95
10	h=100000FT V=2.4M E=6800000sec^2	h=60000FT V=1.0M E=2560000sec^2	h=59900FT V=1.06M E=2628000sec^2	h=.17% V=6% TOTAL:6.17%	154
11	h=80000FFT V=2.0M E=5000000sec^2	h=60000FT V=1.0M E=2560000sec^2	h=61400FT V=1.05M E=2663600sec^2	h=2.33% V=5% TOTAL:7.33%	140
12	h=100000FT V=2.4M E=6800000sec^2	h=80000FT V=2.0M E=5000000sec^2	h=80100FT V=2.15M E=5458000sec^2	h=.125% V=7.5% TOTAL:7.625%	89

Table 5.1 The simulation results of minimum time-to-climb with composite control for airplane 2 under various boundary conditions

A characteristic phenomenon of singularly perturbed systems is that, in general, the reduced solution does not satisfy all boundary conditions. It satisfies only a projection of the boundary conditions on the slow manifold, i.e., boundary conditions on the slow variables. Changes in boundary conditions of the fast variables that do not change the boundary conditions of the slow variables will not effect the reduced solution. In order to demonstrate this phenomenon, let us take cases 5 and 8 as examples. First, we keep the same initial conditions and change the terminal conditions of the fast variables to V_f = 2.65 Mach and h_f = 20000 FT in Case 5. Second, we change the initial conditions of the fast variables to V_0 = 2.65 Mach and h_0 = 20000 FT and keep the same terminal conditions as in Case 8. In both cases the boundary conditions on energy are unaltered. Simulation results are shown in Fig.5.6 and Fig.5.7, respectively. The results show different behaviors of boundary-layers but the slow manifolds remain the same.

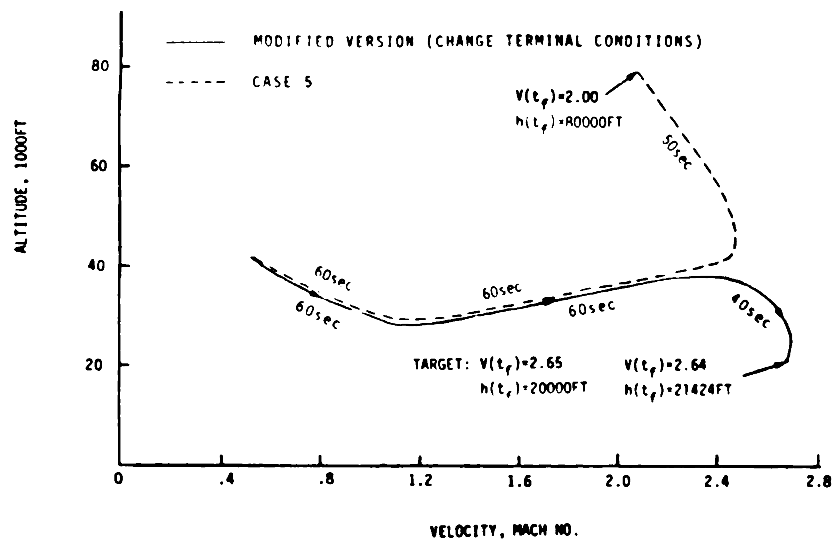

Fig.5.6 Flight trajectory of Case 5 under modified version (change terminal boundary conditions) for airplane 2 with composite control

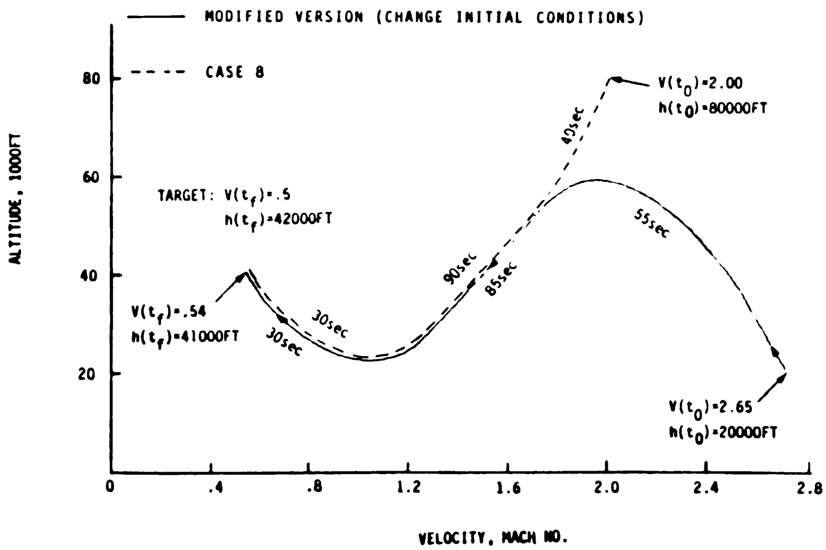

Fig.5.7 Flight trajectory of Case 8 under modified version (change initial boundary conditions) for airplane 2 with composite control

Example 5.2

Consider the same nonlinear singularly perturbed system (5.1) for "airplane 1". It is desired to steer the state of the system from

$V(t_0) = .38$ Mach, $E(t_0) = 89921\ \sec^2$, $h(t_0) = 0$, $\gamma(t_0) = 0$

to the final state $V(t_f) = 1.00$ Mach, $E(t_f) = 2576000\ \sec^2$, $h(t_f) = 65600$ FT, $\gamma(t_f) =$ free, while minimizing t_f. This example is different from the previous one in two aspects. First, the path for "airplane 1" exhibits a discontinuity in velocity (a zoom dive), which is not present in "airplane 2". Second, for this take off example, it is necessary to consider the constraint

$$V \le (2E)^{1/2} \tag{5.23}$$

where $V \le (2E)^{1/2}$ insures $h \ge 0$. In general, we have to consider this constraint all the time during the entire trajectory except when the trajectory is far away from $h = 0$ (see previous example 5.1).

The composite control α_c is applied to this "airplane 1" system equation (5.1) and all the aerodynamic parameters data are given in [16]. The resulting flight path trajectory is shown in Fig.5.8. It is seen that this composite control steers the state of the aircraft to a final state (1.03 Mach and altitude 63177 FT) which is about 3% error relative to the given final velocity (1.00 Mach), and about 3.7% error relative to the given final altitude (65600 FT). The total error is about 6.7% which is $O(\epsilon)$ close to the desired state. The time estimate on this composite control path is 260 sec from $h = 0$, $V = .38$ plus 40 sec dive and 55 sec zoom, the total time is 355 sec. Use of the energy-state approximation (see [16]) gives the total time 377 sec. The time computed by using steepest descent is 332 sec (see [16]). The flight trajectory which was obtained by Bryson ,et al. [16] using energy-state approximation for this "airplane 1" exhibits a discontinuity in velocity (a zoom dive) near Mach number 1, 1.2, 1.8 which may cause considerable errors.

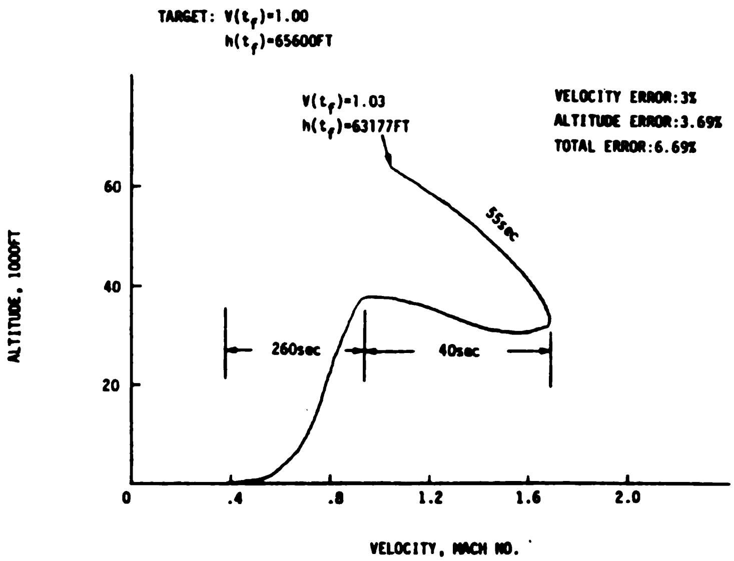

Fig.5.8 Flight trajectory for airplane 1 with composite control

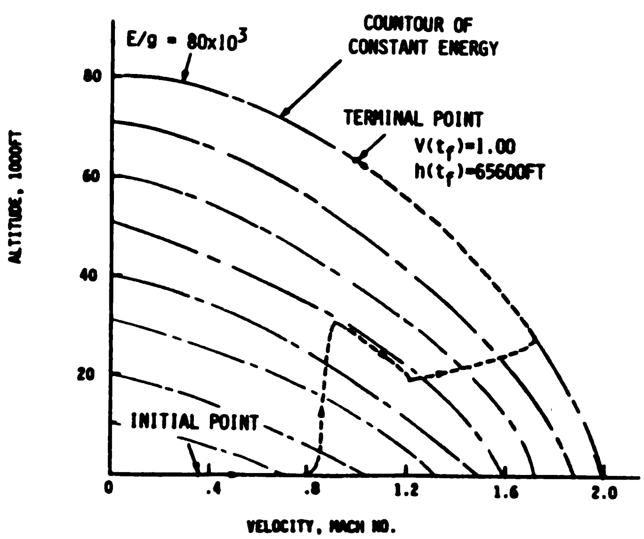

Fig.5.9 Flight trajectory for airplane 1 by Bryson's energy-state approximation

VI. CONCLUSIONS

In this thesis three topics related to nonlinear singularly perturbed optimal control problems were discussed. The results of the analysis were illustrated by the optimal maneuvers of an aircraft in a vertical plane which is based on a minimum time intercept problem. The contributions of the thesis are:

(1). A normalization scheme for the time-scale modeling of dynamic systems arising in flight mechanics has been proposed. This scheme is based on the dynamic state equations and the normalizing reference data. It is relatively easy to apply, and is an improvement over the ad hoc methods currently in use. This scheme has been applied to a typical class of aircraft flight dynamics problems. Numerical examples showed that the time-scale separations as computed by this scheme generally agree with previous practice and assumptions.

(2). Application of singular perturbation techniques to trajectory optimization problems in flight mechanics has been studied. It has been demonstrated that for auto-pilot implementation, the open loop control results in a boundary-layer instability. This instability problem has been circumvented by using feedback stabilization schemes.

(3). A composite control approach has been proposed to steer the state of a singularly perturbed system from a given initial state to a given final state, while minimizing a cost functional. Asymptotic validity has been proved by showing that its application to the singularly perturbed system results in a final state which is $O(\epsilon)$ close to the desired stste and the cost under the composite control is $O(\epsilon)$

close to the optimal cost of the reduced control problem. Our analysis does not involve asymptotic analysis of the full optimal control, therefore our assumptions are weaker than earlier assumptions. Application of the composite control strategy to maneuvers of an aircraft in a vertical plane has also been discussed. The attractiveness of the composite control approach has been demonstrated on the minimum time-to-climb problem.

Further work should address the following points. First, the multiple-time-scale modeling procedure of Chapter II should be validated using real data of high-performance aircrafts. Second, for relatively large value of ϵ, the composite control will have to be corrected to account for $O(\epsilon)$ terms that have been neglected throughout the derivations. To account for $O(\epsilon)$ terms the slow and fast models will have to be corrected by including higher-order terms and the effect of boundary conditions will be corrected by including higher-order terms. Also the effect of the fast control on the slow subsystem will have to be taken into consideration. Another possible extension of the results of this thesis is the application the composite control strategy to minimum fuel climb, minimum time turn and maximum range glide problems. Until now it has been applied only to minimum time-to-climb problem. These seem to be challenging problems and are left for future research.

LIST OF REFERENCES

LIST OF REFERENCES

[1] H. J. Kelley, and T. N. Edelbaum, "Energy Climb, Energy Turn, and Asymptotic Expansions," Journal of Aircraft, Vol. 7, No.1, 1970.

[2] H. J. Kelley, "Reduce-Order Modeling in Aircraft Mission Analysis," AIAA Journal, Vol. 9, No. 2, Feb., 1971.

[3] H. J. Kelley, "Flight Path Optimization with Multiple Time-Scales," Journal of Aircraft, Vol. 8, Apr. 1971.

[4] M. D. Ardema, "Solution of the Minimum Time-to-Climb Problem by Matched Asymptotic Expansions," AIAA Journal, Vol. 14, 1976.

[5] A. J. Calise, "Singular Perturbation Method for Variational Problems in Aircraft Flight," IEEE Trans. Aut. Control, Vol. AC-21, Jun. 1976.

[6] A. J. Calise, "A Singular Perturbation Analysis of Optimal Aerodynamic and Thrust Magnitude Control," IEEE Trans. Aut. Control, Vol. AC-24, No. 5, Oct. 1979.

[7] R. B. Washburn, R. K. Mehra and S. Sajan, "Application of Singular Perturbation Techniques (SPT) and Continuation Methods for On-line Aircraft Trajectory Optimization," Proceedings of the Conference on Decision and Control, San Diego, Calif. Jan. 1979, PP. 983-990.

[8] J. H. Chow, and P. V. Kokotovic, "Eigenvalue Placement in Two Time -Scale System," Proceedings of the IFAC Workshop, 1976.

[9] G. P. Syrcos, and P. Sannuti, "Singular Perturbation Modeling of Continuous and Discrete Physical Systems," IFAC Workshop on Singular Perturbations and Robustness in Control Systems, July, 1982.

[10] J. Shinar, "Remark on Singular Perturbation Technique Applied in Nonlinear Optimal Control," Proceedings of the 2^{nd} IFAC Workshop on Control Applications on Nonlinear Programming and Optimization, 1980.

[11] M. D. Ardema, and N. Rajan, "Separation of Time-Scales in Aircraft Trajectory Optimization," AIAA Atmosopheric Flight Mechanics Conference, Aug. 1983, Gatlinburg, Tennessee.

[12] N. X. Vinh, "Optimal Trajectories in Atmospheric Flight," Chapter 3, 1980.

[13] A. Miele, "Flight Mechanics," Vol.1, Addison-Wesley Company, Inc. 1962.

[14] B. Atkin, "Dynamics of Atmospheric Flight," John Wiley & Sons,inc. 1972.

[15] E. S. Rutowski, "Energy Approach to the General Performance Problem," J. Aeronautical Science, 1954.

[16] A. E. Bryson, M. N. Desai, and W. C. Hoffman, "Energy-State Approximation in Performance Optimization of Supersonic Aircraft," Journal of Aircraft, Vol.6, 1969.

[17] H. J. Kelley, "Aircraft Manueuver Optimization by Reduced-Order Approximation," Control and Dynamic System, Vol. 10, C. T. Leondes, Ed., Academic Press, 1973.

[18] A, J. Calise, "Singular Perturbation Techniques for On-Line Optimal Flight-Path Control," AIAA Journal, Vol. 4, PP. 398-405, 1981.

[19] P. V. Kokotovic, H. K. Khalil, and J. O'Reilly, "Singular Perturbation Methods in Control Analysis and Design," Academic Press, 1986.

[20] J. D. Cole, "Perturbation Methods in Applied Mechanics," Blaisdll, Waltham, MA., 1986.

[21] A. N. Tihonov, "Systems of Differential Equations Containing Small Parameter in the Derivatives," Math. Sbor., 31, PP. 575, 1952.

[22] W. Wasow, "Asymptotic Expansions for Ordinary Differential Equations," Interscience, New York, 1965.

[23] J. H. Chow, "A Class of Singularly Perturbed Nonlinear Fixed-End Point Control Problems," J. Optimiz. Theory and Appl., 29, PP. 231-281, 1979.

[24] M. I. Freeman, and b. Granoff, "Formal Asymptotic Solution of A Singularly Perturbed Nonlinear Optimal Control Problem," J. Optimiz. Theory and Appl. 19, pp. 301, 1976.

[25] A. B. Vasileva, "Asymptotic Solution of Two-Point Boundary Value Problems for Singularly Perturbed Conditionally Stable System," In Singular Perturbation, Order Reduction in Control System Design. ASME, New York, PP. 57-62, 1972.

[26] R. R. Wilde, and P. V. Kokotovic, "Optimal Open and Closed Open Control of Singularly Perturbed Linear Systems," IEEE Trans. Aut. Control, AC-18. PP. 616, 1973.

[27] M. D. Ardema, "Nonlinear Singularly Perturbed Optimal Control Problems with Singular Arcs, " Automatica, 16, PP. 99, 1980.

[28] A. J. Calise, "Entended Energy Management Methods for Flight Performance Optimization," AIAA Journal, 15, PP.314, 1977.

[29] J. Shinar, et. al, "Analysis of Optimal Turning Maneuvers in the Vertical Plane," J. Guidance and Control, 3, PP. 69, 1980.

[30] J. Shinar, and A. Merari, "Aircraft Performance Optimization by Forced Singular Perturbation," 12th Congress of ICAS, Munich, Germany.

[31] H. G. Visser, and J. Shinar, "First-Order Corrections in Optimal Feedback Control of Singularly Perturbed Nonlinear Systems," IEEE Trans. Aut. Control, Vol. AC-31, 1986.

[32] A. Weston, G. Cliff, and H. J. Kelley, "Onboard Near-Optimal Climb-Dash Energy Management," J. of Guidanec, Vol. 8, No. 3,1985.

[33] P. V. Kokotovic and P. Sannuti, "Singular Perturbation Method for Reducing the Model Order in Optimal Control Design," IEEE Trans. Aut. Control, Vol. AC-13, PP. 377-384, 1968.

[34] M. Vidyasagar, "Nonlinear Systems Analysis," Prentice-Hall, Inc. 1978.

[35] H. K. Khalil, "Feedback Control of Implicity Singularly Perturbed Systems," The 23rd IEEE Conference on Decision and Control, Vol. 2 of 3, PP. 1054, 1984. Las Vegas.

[36] R. E. O'Malley, Jr. "Introduction to Singular Perturbations," Academic Press, New York, 1974.

[37] P. Sannuti, "A Note on Obtaining Reduced Order Optimal Control Problems by Singular Perturbations," IEEE Trans. Aut. Control, AC-19, PP. 256, 1974.

[38] J. H. Chow and P. V. Kokotovic, "A Decomposition of Near-optimal Regulators for Systems with Slow and Fast Modes," IEEE Trans. Aut. Control, Vol. AC-21, PP. 701-705, 1976.

[39] J. H. Chow and P. V. Kokotovic, "Two-time Scale Feedback Design of A Class of Nonlinear Systems," IEEE Trans, Aut. Control, Vol. AC-16, PP. 756-770, 1978.

[40] M. Suzuki, "Composite Control for Singularly Perturbed Systems," IEEE Trans. Aut. Control, Vol. AC-26, PP. 505-507, 1981.

[41] A. Saberi and H. K. Khalil, "Stabilization and Regulation of Nonlinear Singularly Perturbed Systems: Composite Control," IEEE Trans. Aut. Control, Vol. AC-30, August, 1985.

[42] C. T. Chen, "Linear System Theory and Design," Holt, Rinehart and Winston, 1984.

[43] J. Shinar, D. Yair and Y. Rotman, "Analysis of Optimal Loop and Split-S by Energy-state Modeling," Iseral J. of Technology, Vol. 16, PP. 70-82, 1978.

[44] R. Aggarwal, A. J. Calise and E. Goldstein, "Singular Perturbation Analysis of Optimal Flight Profiles for Transport Aircraft," Proc. JACC, PP. 1261-1269, 1977.

[45] H. J. Kelley, "An Investigation of Optimum Zoom Climb Techniques," J. of Aerospace Science, 26, PP. 794-802, 1959.

[46] A. Chakravarty, "Four-dimensional Fuel-Optimal Guidance in the Presence of Winds," J. of Guidance, Control, and Dynamics, January/February, 1985.